The Dissertation Committee for Xian Zhang Certifies that this is the approved version of the following dissertation:

NEURODEGENERATION CAUSED BY MITOCHONDRIAL COMPLEX I DYSFUNCTION IN THE MOUSE RETINA

Committee:

Francisco Gonzalez-Lima, Supervisor

Theresa Jones

Juan Salinas

Christine Schmidt

Creed Abell

NEURODEGENERATION CAUSED BY MITOCHONDRIAL COMPLEX I DYSFUNCTION IN THE MOUSE RETINA

by

Xian Zhang, MD

Dissertation

Presented to the Faculty of the Graduate School of

The University of Texas at Austin

in Partial Fulfillment

of the Requirements

for the Degree of

Doctor of Philosophy

The University of Texas at Austin

May, 2005

Dedication

To

My loving husband, Yongchao, my daughter, Austine

and

My parents, Renmin Zhang and Pei Shen,

for their love and support

Acknowledgements

First and foremost, I would like to thank my mentor, Dr. Gonzalez-Lima, for all the guidance, support, and encouragement he provided in the past five years. I greatly benefited from his knowledge and experience. Without his help, I would not have achieved this accomplishment.

I am deeply grateful to the members of my dissertation committee, Dr. Theresa Jones, Dr. Juan Salinas, Dr. Christine Schmidt, Dr. Creed Abell for advice and guidance in their areas of expertise, and for reviewing my dissertation. I also appreciate the advice from Dr. Abell (as the director of the Institute for Neuroscience) that made it possible for me to pursue the Ph.D. in Neuroscience at UT Austin.

Special thanks go to Ms. Alison Crane Tannenbaum, for the technical education and advice she provided to my project, proofreading of my dissertation, and consistent help and support during my graduate study at UT Austin.

I wish to thank former and current members of the "FGL" group for their assistance and friendship. Especially, I would like to thank Dr. Dirk Jones, for his technical help, Dr. Julio Rojas, for his being interested in this project and his help with the last phase of this project, and other members of the group who are also my best friends: Penny Riha, Kati Wrubel, Aleksandra Bruchey, Jason Shumake, Douglas Barrett, Rene Colorado, Jaclyn Spivey, Frank Puga, and former member, Monica Maldonado.

I would like to express my sincere gratitude to my parents, Pei Shen and Renmin Zhang, for always being supportive and encouraging, and for their help in every possible way in my life. I would also like to thank my parents-in-law, Suqin Tao and Xiangzhong Zhang, for taking good care of my newborn daughter so I could concentrate on my dissertation work. Thanks also go to my sister, Hong Zhang, for her continuous support.

Finally, special thanks to my husband, Yongchao Zhang, for being such a wonderful partner, friend, and father to our lovely daughter. I am deeply appreciative of his love, encouragement, and support along the way. I could not have made it here without his support.

NEURODEGENERATION CAUSED BY MITOCHONDRIAL COMPLEX I DYSFUNCTION IN THE MOUSE RETINA

Publication No._____

Xian Zhang, Ph.D.

The University of Texas at Austin, 2005

Supervisor: Francisco Gonzalez-Lima

Neurodegenerative diseases have been closely linked to dysfunction of mitochondria. For example, Leber's hereditary optic neuropathy is associated with mutations in mitochondrial complex I. To create an *in vivo* animal model of neurodegeneration for studying the mechanisms and treatments of neurodegenerative diseases, the mouse eye was injected with the pesticide rotenone, a specific mitochondrial complex I inhibitor. Then, the neurotoxicity of rotenone on the retina was characterized at the cellular level. Finally, a therapeutic intervention was tested using the model. A dose of methylene blue was found to effectively prevent the neurodegeneration caused by rotenone.

Following intravitreal injection of rotenone, the retinal ganglion cell layer (GCL) and the retinal nerve fiber layer (RNFL) showed degeneration as indicated by

the reduction of their thicknesses. The maximum reduction in the GCL and RNFL thickness in complex I staining was around 40% and 89% respectively at 24 h. The GCL thickness reduction was also verified with cresyl violet staining. The number of GCL cells was reduced by 21% (cell profile counts) and 23% (unbiased stereological cell counts) in rotenone-treated eyes. There was a preferential reduction in the proportion of larger cells, while no overall cellular morphometric changes (soma area, perimeter, and diameter) were observed. Therefore, the reduction in GCL thickness 24 h after rotenone microinjection could be accounted for by cell loss and nerve fiber shrinkage, but not by overall soma size change.

This optic neuropathy model was used to test the hypothesis that methylene blue, a reduction–oxidation agent that can act as a powerful antioxidant, may be protective against rotenone. Rotenone-induced neurodegeneration in the retinal ganglion cell layer 24 h after injection was completely prevented by the injection of methylene blue along with rotenone, as indicated by both the GCL thickness and cell numbers.

This is the first animal model of optic neuropathy resulting from mitochondrial dysfunction, and our studies suggest that it could be used as a convenient means to test new treatments to prevent neurodegeneration. It was concluded that methylene blue may be a promising therapeutic agent in optic neuropathy and perhaps other neurodegenerative diseases caused by mitochondrial dysfunction.

Table of Contents

List of Tables

List of Figures

Chapter 1: Introduction

1.1 MITOCHONDRIA AND MITOCHONDRIAL DISEASES

Mitochondria are cytoplasmic organelles and the site of cellular respiration (aerobic metabolism) in almost all eukaryotes (the organisms composed of one or more cells containing visibly evident nuclei and organelles). The most important function of mitochondria is to convert energy from nutrient molecules (substrates) and to store it in the form of adenosine triphosphate (ATP). ATP is the universal energy source for performing a wide range of cellular functions. We cannot survive, even for a moment, without a sufficient supply of ATP. In order to carry out energy conversion, mitochondria reduce oxygen to water using some of the energy provided by substrates. The ATP-generating process in which oxygen serves as the ultimate electron acceptor in mitochondria is called cellular respiration (Stryer, 1999). The primary purpose of our respiratory and circulatory systems is to deliver oxygen to the tissues for use by mitochondria, and to eliminate carbon dioxide.

1.1.1 Structure and function of mitochondria

Each mitochondrion has an outer membrane that is permeable to large molecules, and an inner membrane that is relatively impermeable and contains the

electron transport enzyme complexes. The inner compartment of the mitochondrion, enclosed by the inner membrane, is the matrix where the Krebs cycle takes place (Figure 1.1).

The electron transport complexes are transport enzymes embedded in the inner mitochondrial membrane, designated complexes I through V (Figure 1.1). They can use molecular oxygen to oxidize both NADH and $FADH_2$, which are the electron donors from nutrient molecules that are produced by the Krebs cycle. Complexes I and II collect electrons and transfer them to ubiquinone (coenzyme Q_{10}). The electrons then move sequentially to complex III, cytochrome c, complex IV, and finally, to oxygen, which is the terminal electron acceptor (Figure 1.1). The energy of electron transport can then be used by the complexes to pump hydrogen protons into the intermembrane space, producing an electrochemical proton gradient that stores potential energy. The flow of protons from the intermembrane space back into the inner matrix through Complex V (ATP synthase) allows the complex to use the energy stored in the proton gradient to condense ADP with inorganic phosphate into ATP, a process called oxidative phosphorylation (Voet and Voet, 1995). A very important metabolic role of mitochondria is their role in energy metabolism through oxidative phosphorylation because the vast majority of cellular ATP is provided by mitochondria through oxidative phosphorylation.

Figure 1.1: Illustration of mitochondrial complexes and place of action and functional organization of oxidative phosphorylation system. Coenzyme Q, also called ubiquinone, shuttles electrons from complexes I and II to complex III. Complexes I, III, and IV create an electrochemical gradient, used by ATP synthase for ATP generation.

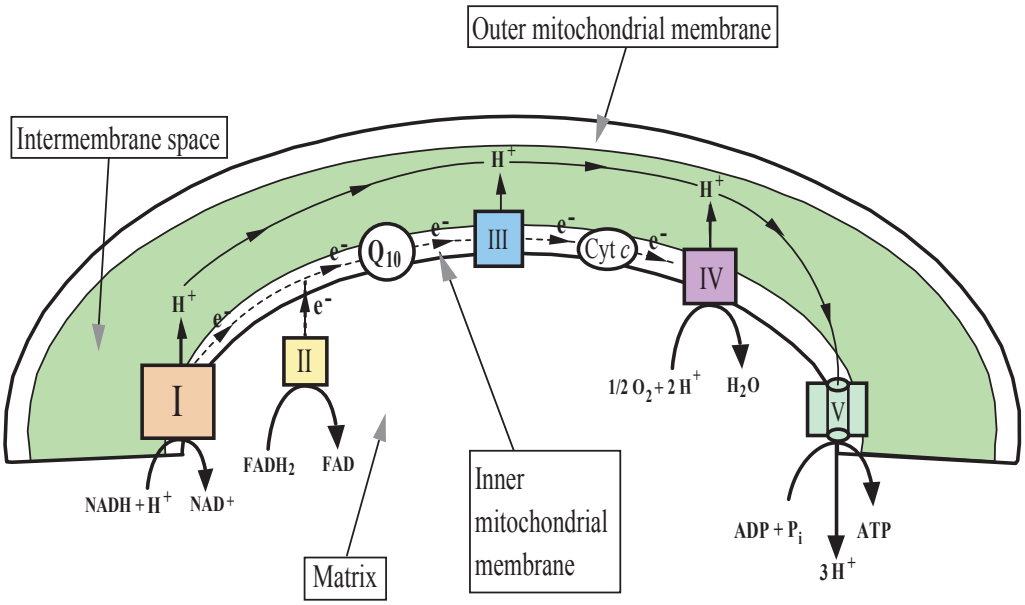

1.1.2 Mitochondrial dysfunction is associated with neurodegenerative disorders

The role of mitochondria in human disease was overlooked until the discovery of Luft's disease (a hypermetablic disorder of striated muscle caused by an abnormal quantity and type of mitochondria and characterized by progressive weakness and an abnormally increased basal metabolic rate) in 1958 (Luft et al., 1962). Since then, over 120 human mitochondrial diseases have been discovered in which there are functional

disturbances and structural alterations in the mitochondria (Luft, 1994). Most of these diseases involve highly energy-dependent cells, such as those in the central nervous system, retina, or skeletal muscle system. Many of these diseases are associated with specific or inherited mitochondrial DNA point mutations and DNA rearrangement mutations (deletions and insertions) accompanying electron transport chain deficiencies (Beal, 1998; DiMauro, 2001; Wallace et al., 1999). A critical role for mitochondrial dysfunction in neurodegenerative diseases is gaining increasing acceptance.

Human mitochondrial DNA (mtDNA) is a 16569 base pair circular and highly compact double-stranded DNA. It has only 37 genes, of which 13 encode subunits of mitochondrial complexes required for oxidative phosphorylation, two genes encode ribosomal RNAs (rRNAs), and 22 genes encode transfer RNAs (tRNAs) required for their translation (DiMauro, 2001). Of the 13 subunits encoded by mtDNA, seven subunits belong to complex I, one to complex III, three to complex IV, and two to ATP synthase (Genova et al., 2004).

The integrity of mtDNA is required for normal mitochondrial function. Many types of mutations and deletions in mtDNA have been reported to cause diseases due to the dysfunction of mitochondria (DiMauro, 2001). The decline of mitochondrial respiratory function is also observed in idiopathic neurodegenerative diseases. Mitochondrial dysfunction has widely been accepted to be a major event that contributes to the degeneration process in neurodegenerative diseases (Beal, 1998; Brown and Wallace, 1994; Valla et al., 2001).

Some of the neurodegenerative diseases, their corresponding deficient mitochondrial electron transport chain enzymes, and the correspondent common enzyme inhibitors (of natural or synthetic origin) are listed in Table 1.1.

Table 1.1: Mitochondrial complex deficiencies, their associated neurodegenerative diseases, and common inhibitors corresponding to the complexes. Abbreviations: HD - Huntington's disease (complex II/III deficiency); FA - Friedreich's ataxia (complex I – III deficiency); PD - Parkinson's disease (complex I deficiency), and AD - Alzheimer's disease (complex IV deficiency); ALS - Amyotrophic lateral sclerosis.

Deficient enzymes	Diseases	Enzyme Inhibitors
Complex I (NADH-cytochrome c reductase; or NADH dehydrogenase)	PD; LHON; Focal dystonia (Schapira, 1998); ALS (Luft, 1994)	• Rotenone (Degli Esposti, 1998) • MPP^+, the active metabolite of MPTP and a selective inhibitor (Storey et al., 1992) • Amytal (Ernster et al., 1963; Storey, 1980)
Complex II (succinate dehydrogenase).	HD; FA (Beal, 1998)	• Malonate, reversible inhibitor (Beal et al., 1993b) • 3-nitropropionic acid (3-NP), irreversible inhibitor (Beal et al., 1993a)
Complex III (ubiquinone–cytochrome *c* oxidoreductase),	HD; FA (Beal, 1998)	• Antimycin (Bailey et al., 1999)
Complex IV (cytochrome c oxidase)	AD (Valla et al., 2001)	• Azide; cyanide; sulfide; nitric oxide

A dysfunctional mitochondrial electron transport chain decreases ATP production and accelerates the generation of free radicals. Radicals are species containing one or more unpaired electrons, such as nitric oxide. Free radicals are an unavoidable byproduct of cellular respiration, because some electrons can leak away from the main path, especially as they pass through ubiquinone, and go directly to reduce oxygen molecules to the superoxide anion. In fact, up to 4-5% of oxygen in mitochondria is not converted to water by the action of complex IV, but is reduced by a single electron leaking from the complexes located up stream of the electron transfer chain, therefore becoming superoxide radical (Richter, 1992). Excessive free radicals, or more particularly, reactive oxygen species (ROS), can directly lead to oxidative stress. Oxidative stress refers to the imbalance between the cellular production of ROS and the antioxidant mechanisms that remove them. It has the potential to trigger a variety of cellular damage, including lipid peroxidation, DNA fragmentation, and modification of proteins. Therefore ROS are a major factor in oxidative cell injury. The mitochondrial electron transport chain is the major intracellular source of ROS, for example, the superoxide anion and hydrogen peroxide (Genova et al., 2004).

The central nervous system, including the retina, and the skeletal muscle system are particularly vulnerable to oxidative stress because they have (1) very high energy and oxygen demands, (2) a limited capacity to use substrates other than glucose for ATP synthesis, (3) abundant lipid content, and (4) relatively lower antioxidant levels compared to other organs. Neurons, in particular, are extremely dependent on mitochondria; they derive more than 90% of their ATP from mitochondrial respiration. The human brain comprises only about 2% of human body

weight but it accounts for about 20% of the body's total energy consumption (Raichle and Gusnard, 2002; Shulman et al., 2003). About 40% of all oxygen consumption in the brain is used to maintain the sodium-potassium gradient across the cell membrane. The energy reserves of the CNS are small, and irreversible cellular damage occurs after a brief deprivation of either glucose or oxygen, which may trigger a cascade of further damage, eventually leading to neuronal cell death, namely neurodegeneration. Thus, these tissues have special vulnerability to mitochondrial dysfunction. Oxidative stress, the cytotoxic consequences of ROS generation as byproducts of normal oxidative metabolism in mitochondria, has been implicated in mitochondrial neurodegenerative diseases (Coyle and Puttfarcken, 1993).

1.2 THE RETINA: A MODEL SYSTEM FOR STUDYING THE CENTRAL NERVOUS SYSTEM

The eye (see Figure 1.2 and 1.3) is a fluid-filled sphere enclosed by three layers of tissue (Bear et al., 2005). The outmost layer is composed of two types of tissue: a tough opaque white fibrous tissue called the sclera, and the cornea, a specialized transparent tissue that allows light to enter the eye. The middle layer includes three different but continuous structures: the iris, the ciliary body, and the choroid. The iris is the colored portion of the eye that can be seen through the cornea with the opening in its center, called the pupil. The size of the pupil can be adjusted under neural control with the apposing actions of the two sets of muscles in the iris. The ciliary body is a ring of tissue that encircles the lens. It includes a muscular component that is important for adjusting the refractive power of the lens, and a vascular component (the so-called ciliary processes) that produces the fluid to fill the

front of the eye. The choroid is composed of a rich capillary bed that serves as the main source of blood supply for the photoreceptors of the retina. The innermost layer of the eye is the retina, which will be discussed in more detail later on.

Figure 1.2: Illustration of the cross-section of a human eye. (Adapted and modified from http://vision-training.com/Eye%20Anatomy/Eye%20anatomy.html)

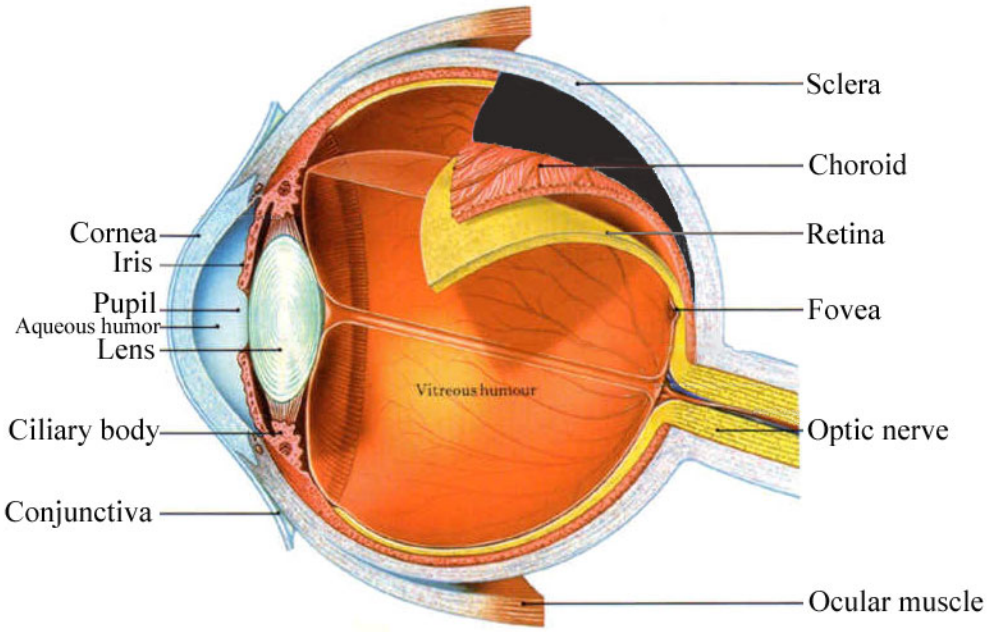

Figure 1.3: A) Cross-section of mouse eye, Nissl stained, 20 μm. B) Cross-section of mouse retina at higher magnification, Nissl stained, 30 μm.

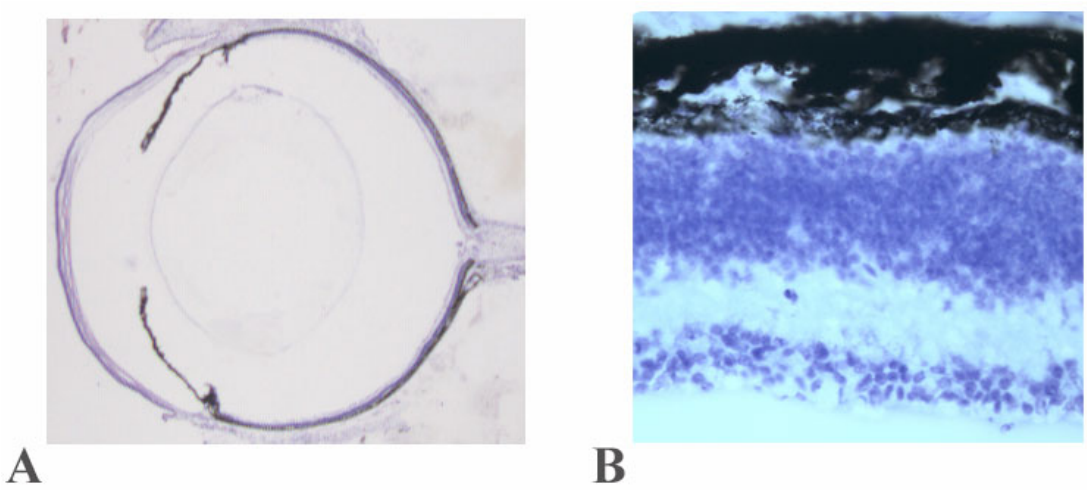

The space between the cornea and the front of the lens is filled with aqueous humor, which is a clear, watery liquid that supplies nutrients to the structures with which it makes contact. The aqueous humor is produced by the ciliary processes in the posterior chamber (the region between the lens and the iris) and flows into the anterior chamber through the pupil. A specialized meshwork of cells that lies at the junction of the iris and the cornea is responsible for its uptake. Under normal conditions, the rates of aqueous humor production and uptake are in equilibrium, maintaining a constant intraocular pressure. Abnormally high levels of intraocular pressure, which occur in glaucoma, can reduce the blood supply to the eye and eventually damage retinal neurons.

The space between the back of the lens and the surface of the retina is filled with a thick, gelatinous substance called the vitreous humor, which accounts for about 80% of the volume of the eye in humans. In addition to maintaining the shape of the eye, the vitreous humor contains phagocytic cells that remove blood and other debris that might otherwise interfere with light transmission. However, the housekeeping abilities of the vitreous humor are limited, as seen in many middle-aged and elderly individuals with vitreal “floaters”. Floaters are collections of debris that are too large for phagocytic consumption; they remain in the vitreous humor and cast annoying shadows on the retina.

Consistent with its status as a part of the central nervous system, the retina is the only structure in the eye that contains neurons connected to photoreceptors capable of converting light into electric signals. These signals are transmitted through the optic nerve to other higher centers in the brain for further processing necessary for visual perception. Besides photoreceptors, there are four types of neurons in the retina: bipolar cells, ganglion cells, horizontal cells, and amacrine cells. The cell bodies and processes of these cells are located in five alternating layers within the retina, with the cell bodies in the inner nuclear, outer nuclear, and ganglion cell layers, and the processes and synaptic contacts in the inner plexiform and outer plexiform layers. A two-synapse pathway - photoreceptor cell to bipolar cell to ganglion cell - is the major path of information flow from the photoreceptors to the optic nerve. The two other types of neurons in the retina, horizontal cells and amacrine cells, are interneurons that have their cell bodies in the inner nuclear layer and are primarily responsible for lateral interactions within the retina (Reid, 1999).

The innermost layer of the retina is the retinal nerve fiber layer (RNFL), containing the axons of the ganglion cells. The ganglion cell layer (GCL) contains mainly the cell bodies of the ganglion cells and some displaced amacrine cells. The inner plexiform layer (IPL) consists of the dendrites of the ganglion cells and the neurites (dendrites and axons) of the bipolar cells and the amacrine cells (Figure 1.4). The visual information processing of the retina starts when the light hits the photoreceptor cells located in the outer surface of the retina, after coming through the cornea, the lens, the vitreous body, and the inner layers of the retina including the RNFL, GCL, IPL, and INL. However the information flows in the opposite direction from the photoreceptors to the ganglion cells, and through their axons to the optic nerve, and up to the brain.

Figure 1.4: A section of human retina with its corresponding diagram of cells. (Adapted and modified from http://thalamus.wustl.edu/course/eyeret.html)

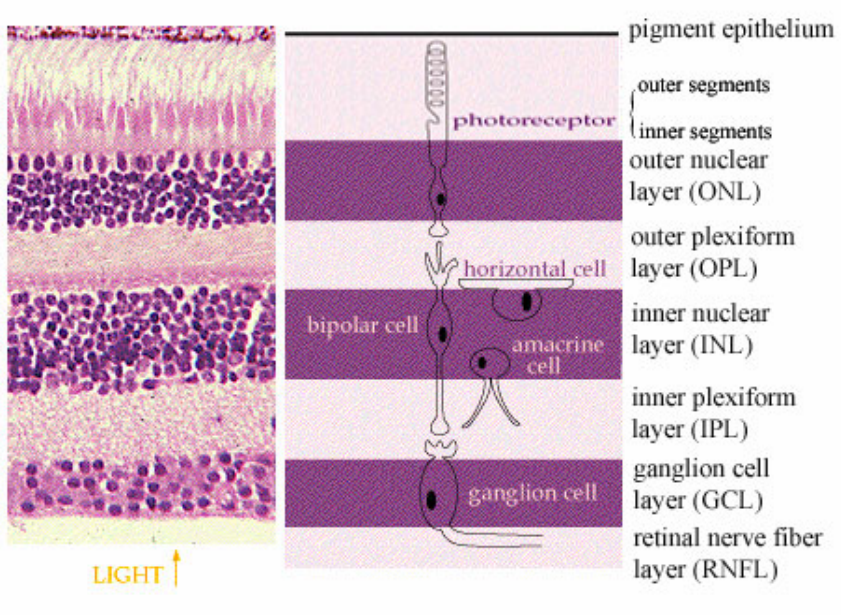

The retina is a well-characterized system that provides unique opportunities to investigate a range of neuroscience-related issues in health and disease, from the molecular to the systems levels. Its unique features have made it a classic model for understanding brain function. The retina has been called an “approachable part of the brain” (Dowling, 1987) for the following reasons.

First of all, despite their peripheral locations, the retina and the optic nerve are legitimate parts of the central nervous system. They are derived embryonically from the brain region called the “diencephalon”. During development, an outpocketing of

the diencephalon is formed, then undergoes invagination to form the optic cup. The inner wall of the optic cup gives rise to the retina, while the outer wall gives rise to the pigment epithelium.

Second, the retina is a relatively simple but well-organized neural circuit system. It is comprised of only a few classes of neurons, but it has the same types of functional elements and neurotransmitters found in other parts of the central nervous system (Wassle and Boycott, 1991). The circuit of the retina and the optic nerve is arranged in a manner that has been less difficult to unravel than the circuits in other areas of the brain.

Third, the retina allows easy access. In fact, it is the only part of the central nervous system that can be visualized without any invasive administration.

Last, the small size of the retina has even become an advantage in certain histological, ultrastructural, and morphometric studies. For instance, tissue processing requires less time, and also a great proportion of the eye can be represented in a microscopic field.

The retina is an ideal model system for studies in neuroscience. Developmental studies of the retina and the central visual pathways have had a substantial impact on other fields of neuroscience, and exploration of retinal circuitry has led to a sophisticated understanding of how neural cells communicate and process information.

1.3 LEBER'S HEREDITARY OPTIC NEUROPATHY IS LINKED TO MITOCHONDRIAL COMPLEX I DYSFUNCTION

1.3.1 Leber's hereditary optic neuropathy (LHON)

LHON, a model disease for mitochondrial neurodegenerative diseases (Brown et al., 1992), was first described by Theodor Leber in 1871. It is an inherited form of bilateral optic atrophy. It classically manifests as acute or subacute onset with bilateral central vision loss associated with the degeneration of the retinal ganglion cell layer and the optic nerve. The initial symptom typically is a blurring of vision bilaterally. Over weeks or months, the blindspots are progressively enlarged to an absolute central scotoma which is a blind or dark spot in the visual field. Typically, the onset and progression of blindness is relatively rapid, with both eyes developing vision loss within a year. Although the onset age ranges from 10 to 70 or so, the mean age of onset is in the mid-20's for both genders. LHON is one of the neurodegenerative diseases (degeneration of the retinal ganglion cells) that are caused by dysfunction of mitochondria, especially complex I of the electron transport chain of the mitochondria. LHON is the most common cause of blindness in otherwise healthy young men (Schapira, 1998).

It has been agreed broadly that there are three types of mtDNA complex I gene mutations that account for the vast majority of LHON cases (Howell, 1998). About 90-95% of LHON cases are the result of one of the three mtDNA point mutations at nucleotide positions 3460/ND1, 11778/ND4 and 14484/ND6, all of which affect complex I (Besch et al., 1999; Brown et al., 1992; Beal, 1998). These three mutations are called "primary mutations" in the sense that no additional mtDNA mutations are

required to cause the disease, and they are not seen in controls. The 11778 mutation in ND4 is found in 50% of LHON families (Schapira, 1998). Sixteen other mutations associated with LHON are “secondary mutations” because either the mutations must occur in some combination or they can be found in controls.

The peripapillary microangiopathy feature of LHON is tortuous vessels in the central retina (Beal et al., 1997). However, in some LHON cases, other more severe neurological abnormalities are also observed, the most common of which is early-onset dystonia associated with basal ganglia degeneration (Wallace et al., 1999). Electrophysiological studies of LHON patients have shown desynchronized visual evoked potentials (VEPs) during the acute phase and extinguished VEPs during the atrophic stage, both indicating retinal ganglion cell dysfunction. However, the patients have normal electroretinograms (ERG) and electrooculograms (EOG), which indicate the functional integrity of photoreceptors, bipolar cells, and retinal pigment epithelium (Sherman and Kleiner, 1994).

Maternal inheritance shows in some of the LHON families, which led to an intensive mtDNA analysis on this disorder, since one unique property of mtDNA is that it is passed exclusively through the mother. The few sperm mitochondrial DNA copies that may enter the ovum have little effect on the genotype since it is a very small portion of several hundreds to thousands of mitochondrial DNA copies (Gyllensten et al., 1991).

1.3.2 Mitochondrial complex I

Mitochondrial complex I is also called nicotinamide adenine dinucleotide (NADH)-quinone oxidoreductase, NADH-cytochrome c reductase, or NADH dehydrogenase. Complex I is the first and the largest complex of the mitochondrial respiratory chain. It catalyzes the following reaction: $NADH + CoQ + H^+ \rightarrow NAD^+ + CoQH_2$, transferring electrons from NADH to co-enzyme Q and beginning the electron transport chain (ETC). It is a multienzyme, integral membrane protein complex of 43 distinct proteins encoded by both nuclear and mitochondrial genomes (Greenamyre et al., 2001; Hatefi, 1985). The mtDNA-encoded subunits are all part of the membrane arm which is associated with the inner mitochondrial membrane; the other arm of this elbow-shaped complex faces the matrix. There are 13 mtDNA-encoded subunits in mitochondrial complexes, and more than half of them are the subunits of complex I (ND1, ND2, ND3, ND4, ND4L, ND5 and ND6). Among these subunits, the ND1 subunit is the binding site for quinone, the electron acceptor of complex I in the electron transport chain, and rotenone, a specific exogenous complex I inhibitor (Hatefi, 1985; Schapira, 1998; Genova et al., 2004).

1.4 ROTENONE – A COMPLEX I INHIBITOR

There is a compelling need for animal models of neurodegenerative diseases. LHON attracted our attention because it stimulates the idea of creating an *in vivo* neurodegeneration model using the retina and the optic nerve, the "approachable part of the brain" (Dowling, 1987), by impairing the function of mitochondrial complex I. Therefore, the first objective of this dissertation was to model mitochondrial toxicity using defective complex I. This model has the potential to be used as a means of exploring the *in vivo* mechanism of neuronal cell death as well as treatment, not only for LHON or other optic neuropathies, but, more importantly, for neurodegenerative diseases in general.

There are over sixty different types of complex I inhibitors (Degli Esposti, 1998). They can be classified into two general categories: compounds of natural or of commercial origin. However, only a few of them are commonly used.

Since the reports in early 1960s (e.g. Lindahl and Oberg, 1961) , rotenone has become the classic inhibitor of complex I. Over the past few years, it has been widely used in studies involving neurodegeneration, especially in Parkinson's disease (PD) (Betarbet et al., 2000; Ferrante et al., 1997), because the brains of PD patients showed decreased activity of complex I. Rotenone is the most potent and most abundant member of a family called rotenoids, which are of natural origin and are organic chemical compounds extracted from the roots of certain species of the bean family genera *Lonchocarpus* and *Derris*, and often referred to as Cube Root. It is widely used as a fish poison in management of fish populations, for example, to remove some or

all of the fish from a pond as part of a renovation plan. It is also widely used by gardeners because it is especially effective for eliminating the most troublesome of pests, such as leaf-eating caterpillars, beetles, and squash bugs. Rotenone is a potent and specific inhibitor of mitochondrial complex I, binding to subunit ND1 of complex I firmly and irreversibly (Ernster et al., 1963; Singer and Ramsay, 1994).

Figure 1.5: Structure of rotenone (CASRN 83-79-4; Molecular formula: C23H24O6)

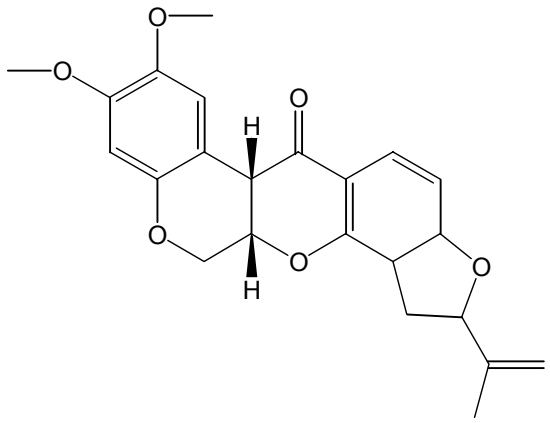

Other classic complex I inhibitors include 1-methyl-4-phenyl-1,2,3,6-tetrahydropyridine (MPTP) and amytal, which are both synthetic inhibitors of complex I. MPTP can cross the blood–brain barrier because it is lipophilic. It is oxidized to its neurotoxic form, 1-methyl-4-phenylpyridinium ion (MPP^+) by monoamine oxidase B in glial cells (Singer and Ramsay, 1990). MPP^+ is selectively accumulated in the mitochondrial matrix of dopaminergic neurons by the dopamine re-uptake system

(Javitch et al., 1985) due to its positive charge. MPP^+ was reported to cause the specific toxicity in dopaminergic neurons resulting in Parkinsonism (Greenamyre et al., 2001). MPP^+ inhibits complex I in the mitochondrial respiratory chain by binding at the same site as rotenone (Ramsay et al., 1991). The inhibition of complex I by MPP^+ in dopaminergic cells is considered to cause the MPTP-induced Parkinsonism.

Amytal (5-ethyl-5-isoamylbarbituric acid) was also used as one of the first inhibitors of complex I (Ernster et al., 1955). However, its inhibition is neither strong nor specific. A high concentration of amytal is required for maximal inhibition, and it also inhibits other enzymes, for example, choline oxidation (Storey, 1980). Thus, it is not the agent of choice for the current study.

Rotenone was chosen as a complex I inhibitor for our study due to its specific features. It is a sensitive and irreversible inhibitor of mitochondrial complex I and it has features not found in two other common complex I inhibitors, MPTP and amytal. Unlike MPTP, which is selective for dopaminergic neurons and depends on the dopamine transporters to gain access to the neurons, rotenone is extremely lipophilic and can easily penetrate biological membranes (Ernster et al., 1963) while the highly charged 1-methyl-4-phenylpyridinium ion (MPP^+, the main metabolite of MPTP) would have much more difficulty to pass through. Rotenone is also more potent than MPP^+ (Heikkila et al., 1986). Rotenone may be a more appropriate model candidate than amytal, as rotenone binds to the electron transfer system firmly and irreversibly (Ernster et al., 1963). In addition, a study using rotenone includes environmental significance. It is a pesticide of natural origin (derived from plants) and found in a variety of commercial garden and animal-care products. It is widely used on home-

grown fruits and vegetables and also commonly used in fishery management in lakes. Because rotenone is a naturally occurring and widely used pesticide, studies with rotenone may provide clues to an environmental role of pesticides in neurodegenerative diseases. Therefore, rotenone is likely to offer a more widely applicable model of environmental toxin exposure than MPTP or amytal.

1.5 METHYLENE BLUE - A THERAPEUTIC INTERVENTION

The purpose of creating a neurodegeneration model is not only to aid the study of the mechanisms of neurodegeneration, but more importantly, to meet the need of therapeutic interventions. An early study by Lindahl and Oberg (1961) attracted our attention because they demonstrated that exposure of intact and excised gill filaments to rotenone induced a decreased oxygen consumption, and addition of methylene blue (MB), an oxidation-reduction (redox) dye, reduced the inhibition of oxygen uptake caused by rotenone and restored up to 83% of the normal respiration (Lindahl and Oberg, 1961). This suggested that MB might be effective in reversing the effects of rotenone.

MB is one of the reducible dyes that are “autoxidizable”. Its characteristic redox couple feature (Figure 1.5) allows it to be an electron mediator between enzymes and substrates, which has attracted considerable interest. In its oxidized form, methylene blue retains its blue color, but becomes colorless in its reduced form, leucomethylene blue.

Figure 1.6 Reduction of MB to colorless Leucomethylene blue.

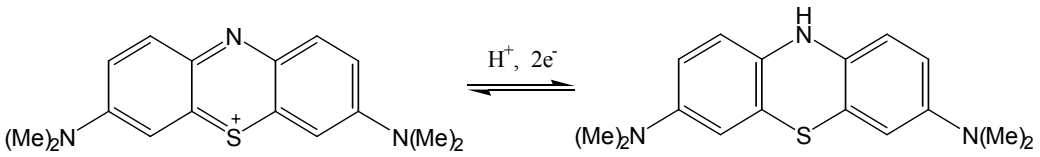

Methylene Blue (blue) Leucomethylene Blue (colorless)

MB is not only a redox dye but also an FDA-approved drug that has been used in clinical medicine for nearly 100 years. The history of safe MB use in humans for many years in various treatments makes it additionally attractive. Its traditional uses in histological techniques, diagnosis, as well as in disease treatments are based on its tissue-staining properties and its oxidative-reductive capacity. Administered locally or systemically, it has been used for the detection of anatomic and pathologic structures during surgical operations, for example, to mark the blood vessel by applying to the adventitia of blood vessels during coronary artery bypass and other vascular procedures (Barber et al., 1995); to identify a fistula (a tiny channel or tract that develops in the presence of inflammation and infection) and ruptured amniotic membranes, or diseased pelvic peritoneum in obstetrics (Manhes et al., 2004); to detect glandular tissues, such as on parathyroid glands or pancreatic (Derom et al., 1993); and to inactivate viruses in fresh frozen plasma and blood products (Floyd et al., 2004; Wieding et al., 1993). Therapeutically, methylene blue has long been recognized as an effective antidote when administrated systemically in low doses in man and in domestic animals due to its reducing action for drug-induced, and some

forms of idiopathic, methemoglobinemia (Bodansky and Gutmann, 1947; Clifton and Leikin, 2003; Bradberry, 2003; Etteldorf, 1951), and for drug-related encephalopathy in cancer chemotherapy with ifosfamide (Kupfer et al., 1994; Kupfer et al., 1996). In addition, MB has also been used to treat dementia and manic-depressive psychosis (Naylor et al., 1986; Wainwright and Crossley, 2002).

MB is a suitable treatment candidate for neurodegenerative diseases caused by mitochondrial dysfunction because it can enter the nervous tissue as well as its mitochondria (Peter et al., 2000; Hassan and Fridovich, 1979; O'Leary et al., 2005; Richardson, 2005). O'Leary et al. (2005) have shown that MB was able to cross the blood-brain barrier when administered intraperitoneally to rats. The stained brain tissue was visible after dissection when deoxidized because MB regained its blue color. Pharmacokinetics studies have shown that intravenous administration resulted in higher concentration of MB in both blood and brain than oral administration did, while MB concentration is much higher in the brain than in the blood after 1 hr following intraperitoneal administration (Peter et al., 2000). Hassan and Fridovich (1979) have demonstrated that MB is capable of entering the mitochondria and diverting a portion of the electron flow to molecular oxygen. Behaviorally, it has been shown that methylene blue improved memory retention in inhibitory avoidance responses when given immediately after training in rats (Martinez et al., 1978). Studies in our laboratory have also found MB enhances spatial memory retention impaired by sodium azide (an inhibitor for mitochondrial complex IV) (Callaway et al., 2002) or in normal rats (Callaway et al., 2004).

Two major pharmacological mechanisms for MB's protective metabolic function have been documented. One mechanism involves improving oxygen consumption. MB acts as a redox agent that increases mitochondrial respiration by shuttling electrons to oxygen in the electron transport chain, resulting in elevated cellular oxygen consumption (Callaway et al., 2004; Lindahl and Oberg, 1961; Visarius et al., 1997). Therefore, it is possible that MB may increase oxygen consumption and compensate for decreased activity of mitochondrial complexes.

The other mechanism is related to its powerful antioxidant effects. For example, it inhibits superoxide, the most abundant oxygen radical generated in vivo, by accepting electrons from tissue oxidases (Kelner et al., 1988; Salaris et al., 1991). Another antioxidant action of MB is its inhibition of nitric oxide (Mayer et al., 1993). Nitric oxide can form the damaging peroxynitrite after reacting with superoxide. Therefore, MB administration could be very effective in preventing mitochondrial oxidative damage leading to neurodegeneration (Gonzalez-Lima et al., 1998).

Therefore, we hypothesize that administration of MB in our optic neuropathy model may be of therapeutic value and effectively prevent the degeneration characterized by inhibition of mitochondrial function.

1.6 EXPERIMENTAL GOALS

In the first experiment (Chapter 2), a modified tetrazolium salt method was developed to demonstrate complex I enzymatic activity on brain homogenates and rat retina. This method relies on the reduction of tetrazolium salts by hydrogen ions released during oxidation to produce a colored formazan deposit on the tissue.

Quantitative analysis was done on the intensity of formazan deposited in the incubated sections. A strong linear relationship existed between the optical density and incubation time within the first 30 min for all section thicknesses. Therefore, this tetrazolium salt method is one way to demonstrate complex I activity quantitatively in our animal model.

In the second experiment (Chapter 3), rotenone, a specific complex I inhibitor, was administered intravitreally in CBA/J mice to generate an animal model of optic neuropathy caused by defective complex I. The degeneration of the retina was demonstrated by a significant thickness reduction in the ganglion cell layer (GCL) with the rest of the retina layers relatively spared. This could be an effective *in vivo* animal model for exploring the mechanisms and treatment of neurodegenerative diseases as well as a model to study environmental involvement in neurodegenerative diseases.

The third experiment (Chapter 4) investigated in detail the disease model at the cellular level. The maximal reduction of the retinal GCL thickness that occurred as a consequence of rotenone administration could be seen 24 hours later. Retinal nerve fiber layer thickness was reduced by 89% and the number of GCL cells was reduced by 21%. Cellular morphometric data (soma area, perimeter, and diameter) did not show overall differences, but there was a relative reduction in the proportion of larger cells. Therefore, the reduction in GCL thickness after 24 hours following rotenone microinjection could be accounted for by cell loss and nerve fiber shrinkage, but not by overall soma size change.

The fourth experiment (Chapter 5) explored a therapeutic intervention in the experimental model of optic neuropathy by intravitreal injection of MB along with rotenone. The rotenone-induced neurodegeneration, indicated in Experiment 3 by significant reductions in both the thickness and cell numbers (stereology measurements) of the retinal ganglion cell layer, was completely prevented by the injection of methylene blue along with rotenone. Possible mechanisms of MB were examined. The findings suggest that methylene blue may be a promising therapeutic agent in optic neuropathy as well as neurodegenerative diseases in general.

1.7 REFERENCES

Bailey SM, Pietsch EC, Cunningham CC (1999) Ethanol stimulates the production of reactive oxygen species at mitochondrial complexes I and III. *Free Radical Biology and Medicine* 27: 891-900.

Barber DA, Rubin JW, Zumbro GL, and Tackett RL. (1995) The use of methylene blue as an extravascular surgical marker impairs vascular responses of human saphenous veins. *Journal of thoracic and cardiovascular surgery* 109: 21-29.

Beal MF, Brouillet E, Jenkins BG, Ferrante RJ, Kowall NQ, Miller JM, Storey E, Srivastava R, Rosen BR, and Hyman BT. (1993a) Neurochemical and histologic characterization of excitotoxic lesions produced by the mitochondrial toxin 3-nitropropionic acid. *J.Neurosci.* 13: 4192.

Beal MF, Brouillet E, Jenkins BG, Henshaw R, Rosen B, and Hyman BT. (1993b) Age-dependent striatal excitotoxic lesions produced by the endogenous mitochondrial inhibitor malonate. *J.Neurochem.* 61: 1147-1150.

Beal MF, Howell N, Bodis-Wollner I (1997) Mitochondria and free radicals in neurodegenerative diseases. New York: Wiley-Liss.

Beal MF (1998) Mitochondrial dysfunction in neurodegenerative diseases. *Biochimi et Biophys Acta (BBA) - Bioenergetics* 1366: 211-223.

Bear MF, Connors BW, Pardiso MA (2005) The eye. In: Neuroscience: Exploring the Brain, 2nd Edition pp 281-312. Lippincott Williams & Wilkins.

Besch D, Leo-Kottler B, Zrenner E, Wissinger B (1999) Leber's hereditary optic neuropathy: Clinical and molecular genetic findings in a patient with a new mutation in the ND6 gene. *Graefe's Archive for Clinical and Experimental Ophthalmology* 237: 745-752.

Betarbet R, Sherer TB, MacKenzie G, Garcia-Osuna M, Panov AV, Greenamyre JT (2000) Chronic systemic pesticide exposure reproduces features of Parkinson's disease. *Nat Neurosci* 3: 1301-1306.

Bodansky O, Gutmann H (1947) Treatment of methemoglobinemia. *J Pharmacol* 46-56.

Bradberry SM (2003) Occupational methaemoglobinaemia. Mechanisms of production, features, diagnosis and management including the use of methylene blue. *Toxicol Rev* 22: 13-27.

Brown MD, Voljavec AS, Lott MT, MacDonald I, Wallace DC (1992) Leber's hereditary optic neuropathy: A model for mitochondrial neurodegenerative diseases. *FASEB J* 6: 2791-2799.

Brown MD, Wallace DC (1994) Spectrum of mitochondrial DNA mutations in Leber's hereditary optic neuropathy. *Clin Neurosci* 138-145.

Callaway NL, Riha PD, Bruchey AK, Munshi Z, Gonzalez-Lima F (2004) Methylene blue improves brain oxidative metabolism and memory retention in rats. *Pharmacol Biochem and Behav* 77: 175-181.

Callaway NL, Riha PD, Wrubel KM, McCollum D, Gonzalez-Lima F (2002) Methylene blue restores spatial memory retention impaired by an inhibitor of cytochrome oxidase in rats. *Neurosci Lett* 332: 83-86.

Clifton J, Leikin JB (2003) Methylene blue. *Am J Ther* 10: 289-291.

Coyle JT, Puttfarcken P (1993) Oxidative stress, glutamate, and neurodegenerative disorders. *Science* 262: 689-695.

Degli Esposti M (1998) Inhibitors of NADH-ubiquinone reductase: an overview. *Biochimi et Biophys Acta (BBA) - Bioenergetics* 1364: 222-235.

Derom AF, Wallaert PC, Janzing HM, Derom FE (1993) Intraoperative identification of parathyroid glands with methylene blue infusion. *Am J Surg* 165: 380-382.

DiMauro S. (2001) Lessons from mitochondrial DNA mutations. *Cell & Developmental Biology* 9: 397-405.

Dowling JE (1987) The retina: an approachable part of the brain. Belknap Press.

Ernster L, Dallner G, Azzone GG (1963) Differential effects of rotenone and amytal on mitochondrial electron and energy transfer. *J Biol Chem* 238: 1124-1131.

Ernster L, Jalling O, Low H, Lindberg O (1955) Alternative pathways of mitochondrial DPNH oxidation, studied with amytal. *Exptl Cell Res Suppl* 3: 124-132.

Etteldorf JN (1951) Methylene blue in the treatment of methemoglobinemia in premature infants caused by marking ink; a report of eight cases. *J Pediatr* 38: 24-27.

Ferrante RJ, Schulz JB, Kowall NW, Beal MF (1997) Systemic administration of rotenone produces selective damage in the striatum and globus pallidus, but not in the substantia nigra. *Brain Res* 753: 157-162.

Floyd RA, Schneider J, Dittmer DP (2004) Methylene blue photoinactivation of RNA viruses. *Antiviral Research* 61: 141-151.

Genova ML, Pich MM, Bernacchia A, Bianchi C, Biondi A, Bovina C, Falasca AI, Formiggini G, Castelli GP, Lenaz G (2004) The Mitochondrial Production of Reactive Oxygen Species in Relation to Aging and Pathology. *Ann NY Acad Sci* 1011: 86-100.

Gonzalez-Lima F, Valla J, Jorandby L (1998) Cytochrome oxidase inhibition in Alzheimer's disease. In: Cytochrome oxidase in neuronal metabolism and Alzheimer's disease (Gonzalez-Lima F, ed), pp 171-200. New York: Plenum Press.

Greenamyre JT, Sherer TB, Betarbet R, Panov AV (2001) Complex I and Parkinson's disease. *IUBMB Life* 52: 135-141.

Gyllensten U, Wharton D, Josefsson A, and Wilson AC. (1991) Paternal inheritance of mitochondrial DNA in mice. *Nature* 352: 255-257.

Hassan HM, Fridovich I (1979) Intracellular production of superoxide radical and of hydrogen peroxide by redox active compounds. *Archives of Biochemistry and Biophysics* 196: 385-395.

Hatefi Y (1985) The mitochondrial electron transport and oxidative phosphorylation system. *Annual Review of Biochemistry* 54: 1015-1069.

Heikkila RE, Nicklas WN, Vyas I, Duvoisin RC (1986) Dopaminergic toxicity of rotenone and the 1-methyl-4-phenylpyridinium ion after their stereotaxic administration to rats: implication for the mechanism of 1-methyl-4-phenyl-1,2,3,6,-tetrahydropyridine toxicity. *Neurosci Lett* **62**: 389-394.

Howell N (1998) Leber hereditary optic neuropathy: Respiratory chain dysfunction and degeneration of the optic nerve. *Vision Res* 38: 1495-1504.

Javitch JA, D'Amato RJ, Strittmatter SM, Snyder SH (1985) Parkinsonism-inducing neurotoxin, N-methyl-4-phenyl-1,2,3,6 -tetrahydropyridine: uptake of the metabolite N-methyl-4-phenylpyridine by dopamine neurons explains selective toxicity. *Proc Natl Acad Sci U S A* 82: 2173-2177.

Kelner MJ, Bagnell R, Hale B, Alexander NM (1988) Potential of methylene blue to block oxygen radical generation in reperfusion injury. *Basic Life Sci* 49: 895-898.

Kupfer A, Aeschlimann C, Cerny T (1996) Methylene blue and the neurotoxic mechanisms of ifosfamide encephalopathy. *Eur J Clin Pharmacol* 50: 249-252.

Kupfer A, Aeschlimann C, Wermuth B, Cerny T (1994) Prophylaxis and reversal of ifosfamide encephalopathy with methylene-blue. *Lancet* 343: 763-764.

Lindahl PE, Oberg KE (1961) The effect of rotenone on respiration and its point of attack. *Exptl Cell Research* 23: 228.

Luft R (1994) The development of mitochondrial medicine. *Proc Natl Acad Sci* 91: 8731-8738.

Luft R, Ikkos D, Paknueru G, Ernster L, Afzelius B (1962) A case of severe hypermetabolism of nonthyroid origin with a defect in the maintenance of mitochondrial respiratory control: a correlated clinical, biochemical, and morphological study. *J Clin Invest* 41: 1776--1804.

Manhes H, Shulman A, Haag T, Canis M, Demontmarin JL (2004) Infertility due to diseased pelvic peritoneum: laparoscopic treatment. *Gynecol Obstet Invest* 37: 191-195.

Martinez JLJr, Jensen RA, Vasquez BJ, McGuinness T, McGaugh JL (1978) Methylene blue alters retention of inhibitory avoidance responses. *Physiol Psychol* 6: 387-390.

Mayer B, Brunner F, Schmidt K (1993) Inhibition of nitric oxide synthesis by methylene blue. *Biochem Pharmacol* 45: 367-374.

Naylor GJ, Maton B, Hopwood SE, Watson Y (1986) A two-year double-blind crossover trial of the prophylactic effect of methylene blue in manic-depressive psychosis. *Biol Psychiatry* 21: 915-920.

O'Leary JL, Petty J, Harris AB, Inukai J (2005) Supravital staining of mammalian brain with intra-arterial methylene blue followed by pressurized oxygen. *Stain Technology* 43: 197-201.

Peter C, Hongwan D, Kupfer A, Lauterburg BH (2000) Pharmacokinetics and organ distribution of intravenous and oral methylene blue. *Eur J Clin Pharmacol* 56: 247-250.

Raichle ME, Gusnard DA (2002) Appraising the brain's energy budget. *Proc Natl Acad Sci USA* 10237-10239.

Ramsay RR, Krueger MJ, Youngster SK, Gluck MR, Casida JE, Singer TP (1991) Interaction of 1-methyl-4-phenylpyridinium ion (MPP+) and its analogs with the rotenone/piericidin binding site of NADH dehydrogenase. *J Neurochem* 56: 1184-1190.

Reid CR (1999) Vision. In: Fundamental Neuroscience (Michael J.Zigmond, Floyd E.Bloom, Story C.Landis, James L.Roberts, Larry R.Squire, eds), pp 821-851. San Diego: Academic Press.

Richardson KC (2005) The fine structure of autonomic nerves after vital staining with methylene blue. *Anatomical Record* 164: 359-377.

Richter C (1992) Reactive oxygen and DNA damage in mitochondria. *Mutat Res* 249-255.

Salaris SC, Babbs CF, Voorhees III (1991) Methylene blue as an inhibitor of superoxide generation by xanthine oxidase: A potential new drug for the attenuation of ischemia/reperfusion injury. *Biochem Pharmacol* 42: 499-506.

Schapira AHV (1998) Human complex I defects in neurodegenerative diseases. *Biochimi et Biophys Acta (BBA) - Bioenergetics* 1364: 261-270.

Sherman J and Kleiner L. (1994) Visual system dysfunction in Leber's hereditary optic neuropathy. *Clinical Neuroscience* 2: 121-129.

Shulman RG, Hyder F, Rothman DL (2003) Cerebral metabolism and consciousness. *Crit Rev Biol* 326: 253-273.

Singer TP, Ramsay RR (1990) Mechanism of the neurotoxicity of MPTP. An update. *FEBS Lett* 274: 1-8.

Singer TP, Ramsay RR (1994) The reaction sites of rotenone and ubiquinone with mitochondrial NADH dehydrogenase. *Biochimi et Biophys Acta (BBA) - Bioenergetics* 1187: 198-202.

Storey BT. (1980) Inhibitors of energy-coupling site 1 of the mitochondrial respiratory chain. *Pharmac.Ther.* 10: 399-406.

Storey E, Hyman BT, Jenkins BT, Brouillet E, Miller JM, Rosen BR, and Beal MF. (1992) MPP produces excitotoxic lesions in rat striatum due to impairment of oxidative metabolism. *J.Neurochem.* 58: 1975-1978.

Stryer L (1999) Biochemistry. New York: W. H. Freeman and Company.

Valla J, Berndt JD, Gonzalez-Lima F (2001) Energy hypometabolism in posterior cingulate cortex of Alzheimer's patients: Superficial laminar cytochrome oxidase associated with disease duration. *J Neurosci* 21: 4923-4930.

Visarius TM, Stucki JW, Bernhard H (1997) Stimulation of respiration by methylene blue in rat liver mitochondria. *FEBS Letters* 412: 157-160.

Voet D, Voet JG (1995) Biochemistry. John Wiley & Sons, Inc.

Wainwright M, Crossley KB (2002) Methylene Blue--a therapeutic dye for all seasons? *J Chemother* 14: 431-443.

Wallace DC, Brown MD, and Lott MT. (1999) Mitochondrial DNA variation in human evolution and disease. *Gene* 238: 211-230.

Wassle H, Boycott BB (1991) Functional architecture of the mammalian retina. *Physiol Rev* 71: 447-480.

Wieding JU, Hellstern P, and Kohler M. (1993) Inactivation of viruses in fresh-frozen plasma. *Ann Hematol* 67: 259-266.

Chapter 2: Histochemistry of mitochondrial complex I activity

2.1 ABSTRACT

Mitochondrial dysfunction is associated with neurodegenerative diseases. Mitochondrial complex I (NADH dehydrogenase) is the first complex in the electron transfer chain of mitochondria. Complex I deficiency has been identified in Leber's hereditary optic neuropathy, Parkinson's disease, and dystonia. We propose to use rotenone, a specific complex I inhibitor, to generate an animal model of optic neuropathy that is known to be caused by defective complex I. The objective of this study is to develop a reliable histochemical measurement of complex I activity to assess the neurodegeneration of the retina and the optic nerve, as well as other tissues of the central nervous system. A modified tetrazolium salt method was used to demonstrate complex I enzymatic activity on rat brain homogenates and rat retina. This method relies on the reduction of tetrazolium salts by hydrogen ions released during oxidation to produce a colored formazan deposit on the tissue. Quantitative analysis was done on the intensity of formazan deposited on the incubated sections. A linear relationship existed between the optical density and incubation time within the first 30 min for all of the section thicknesses. The brain homogenate standards incubated for 25 min showed an almost perfect linear relationship between the optical density and the tissue thickness ($R^2 = 0.99$). The intensity of the two darkest layers in the retina is within the optical density range of the standards. This tetrazolium salt method is a way to demonstrate complex I activity quantitatively in our animal model.

2.2 INTRODUCTION

Mitochondria are cytoplasmic organelles and the site of cellular respiration (aerobic metabolism) in almost all eukaryotes. Mitochondrial complexes are a number of proteins and protein complexes that are located in the inner membrane and involved in the process called electron transport. The major role of the electron transport chain (ETC) system is to take energy from nicotine adenine dinucleotide (NADH) and flavin adenine dinucleotide ($FADH_2$) in the matrix and convert energy to a form that can be used to phosphorylate ADP, producing ATP. Complexes I and II collect electrons and transfer them to ubiquinone (coenzyme Q_{10}). The electrons then move sequentially to complex III, cytochrome c, complex IV, and finally, to oxygen, which is the terminal electron acceptor. The hydrogen proton, which is transported together with the electron through the inner mitochondrial membrane, produces an electrochemical proton gradient that stores potential energy. Complex V uses energy stored in the proton gradient to condense ADP with inorganic phosphate into ATP, a process called oxidative phosphorylation (Voet and Voet, 1995).

A dysfunctional mitochondrial electron transport chain decreases ATP production and accelerates the generation of free radicals. Mitochondrial dysfunction is associated with neurodegenerative diseases. For example, the electron transport Complex I deficiency, either specific or associated with other respiratory chain defects, has been identified in Leber's hereditary optic neuropathy, Parkinson's disease, and dystonia (Schapira, 1998). Reliable methods for measuring the function of mitochondrial complexes in the nervous system are essential and of great use in investigating mitochondrial involvement in these neurodegenerative diseases.

Inhibitors of mitochondrial complexes are used to generate animal models of neurodegenerative diseases. For example, sodium azide, a complex IV inhibitor, is used in an animal model of Alzheimer's disease, because these patients have a systemic inhibition of complex IV (Bennett and Rose, 1992). Systemic administration of rotenone, a specific complex I inhibitor, has been used to model Parkinson's disease, because nigrostriatal neurons exhibit an enhanced toxicity following a chronic administration of large systemic doses of rotenone (Betarbet et al., 2000). We propose to use rotenone, a specific complex I inhibitor, injected in the eye, to generate an optic neuropathy model that is known to be caused by defective complex I. Therefore, the objective of this study is to develop a reliable measurement of complex I activity to assess the neurodegeneration of the retina and the optic nerve, as well as tissues of other central nervous system components.

Mitochondrial complex I (NADH dehydrogenase) is the first complex in the electron transfer chain of mitochondria and catalyzes the transfer of electrons from NADH to coenzyme Q (CoQ):

$$NADH + CoQ + H^+ \rightarrow NAD^+ + CoQH_2 \qquad \text{(Scheme 2.1)}$$

In addition to transferring electrons to reduce coenzyme Q, this complex also translocates protons, helping to provide the electrochemical potential used to produce ATP. It is the largest complex in the ETC; the mammalian enzyme contains 43 separate protein subunits (Greenamyre et al., 2001; Robinson, 1998; Schapira, 1998; Voet and Voet, 1995).

Complex I enzymatic activity can be measured quantitatively and reliably by using histochemical and imaging techniques (Barry et al., 1993; Murray et al., 1988; Sims et al., 1974; Van Noorden and Frederiks, 1992). Tetrazolium salt methods are the most frequently used methods in the enzyme histochemical techniques for the demonstration of the activity of dehydrogenases, reductases, and oxidases (Van Noorden and Frederiks, 1992). Tetrazolium salts are colorless or yellow and water-soluble; they can be reduced metabolically to the highly colored water-insoluble microcrystalline deposits called formazans by accepting hydrogen released from the substrate through enzyme action.

The mechanism of the tetrazolium salt reaction chain consists of several electron transfers. The first step is the enzyme-mediated electron transfer from one substrate to the other. Then, the reduced coenzyme NAD^+ or flavoprotein reduces the tetrazolium salt to its formazan deposit which is colored, and finely granular (see Scheme 2.2).

Nitro BT (Oxidized) + NADH → Formazan (Reduced) + NAD (Scheme 2.2)

The general formula of tetrazolium compounds is

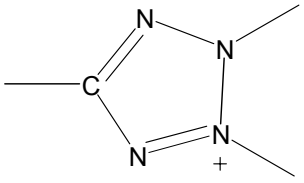

After they are reduced by accepting hydrogen they become an insoluble colored formazan whose general formula is

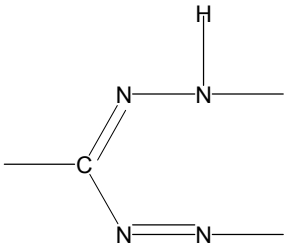

The intensity of the formazan color can be measured quantitatively, providing a measure of the activity of complex I.

2.3 METHOD

2.3.1 Materials

All materials were purchased from Sigma-Aldrich, St. Louis, MO.

2.3.2 Sample preparation

All experimental procedures were performed in accordance with NIH guidelines and were approved by the Institutional Animal Care and Use Committee (IACUC) of the University of Texas at Austin. Brain tissue standards were prepared based on the procedure of Gonzalez-Lima et al. (1998). Briefly, the brains of male Sprague-Dawley rats that had not been perfused or exposed to anesthetics were used. After decapitation the unfixed brains were quickly harvested and stored at 4°C in sodium phosphate buffer (pH, 7.4) until all brains were collected. Then the tissue was transferred to chilled clear glass homogenizer tubes kept on ice and homogenized by hand for about 2-3 min or until uniform. Aliquots of the brain tissue were transferred to microtubes and then centrifuged at low speed (1000 rmp, 5-10 sec). The brain

homogenate, along with the microtubes, was then frozen in isopentane and stored at -40 °C.

2.3.3 Histochemical reactions

In order to prepare tissue standards, brain tissue homogenate was frozen inside plastic tubes. Then the tissue was removed, mounted, and sectioned at 10, 20, 40, 60, and 80 μm on a cryostat on the same day they were to be used in histochemical procedures. Sections of rat eyes that were previously cut at 40 μm anterior-posteriorly were also prepared. Slides with fresh-frozen sections were put into three consecutive baths of 0.1 M sodium phosphate buffer solution (PBS) with 10% (w/v) sucrose for 5 min each to increase adherence of the tissue to the slide. The three baths were filled at the same time so they were warmed up gradually to room temperature. After rinsing in 0.1M PBS, slides were incubated at 37^{o}C in the dark for 15, 25, 35, and 45 min with agitation in 0.1M PBS containing NADH (Sigma, 1 mg/ml), nitroblue tetrazolium (Sigma, 1.33 mg/ml), and sodium azide (Sigma, 0.065 mg/ml). Sodium azide was used to inhibit cytochrome oxidase (complex IV) (Gonzalez-Lima and Cada, 1998). A detailed protocol of complex I staining appears in Appendix.

2.3.4 Microscopic imaging analysis

Optical densitometry measurements were used to quantify complex I histochemistry. A high resolution video camera (Javelin JE-7442) was mounted on an Olympus light microscope (model BX40) to capture the images which were then transmitted to a frame grabber in a computer where the image was digitized. Image

analysis was completed using JAVA (Jandel Scientific) imaging software. The same microscope lamp intensity level was maintained throughout the study.

The gray levels of a standard calibration strip with a range of known optical densities were measured, and a best-fit mathematical equation (optical density as a function of gray levels) was created based on the gray levels and the optical density measurements. The equation was then applied on all the gray levels measured from the imaging processing system to convert them into values of optical density which is proportional to brightness. All experimental values were within the range of optical densities covered by the standards.

2.4 RESULT

The presence of complex I in the histochemical preparation appeared as a shade of purple. The cross section of the rat retina showed distinctive laminar structure in the staining (Figure 2.1). The inner segment layer and the ganglion cell layer were fairly dark purple, indicating the overwhelming complex I activity, while the inner plexiform layer was lighter. The inner and outer nuclear layers, which are mostly composed of cell bodies, showed pinkish color.

Figure 2.1 A) Cross-section of rat eye. B) Cross-section of rat retina at higher magnification. Complex I staining, 40 μm sections.

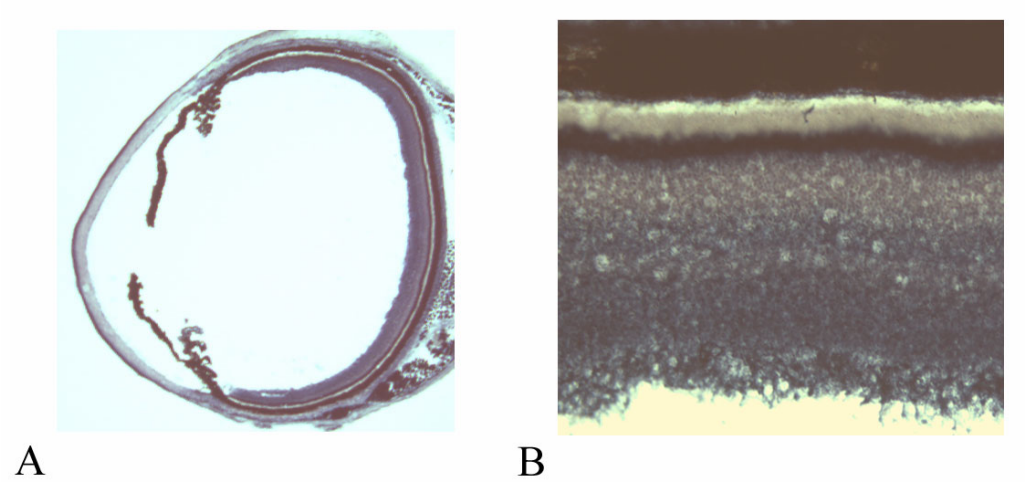

A linear relationship existed between the optical density and incubation time within the first 30 min for all section thicknesses. The darkness of the stain on the brain homogenate increased with the section thickness (Figure 2.2). Since all sections with different thicknesses reached their saturation of staining around 35 min, a 25 min incubation time was optimal because it was just below the saturation level. The values of optical density for the brain homogenate standards, incubated for 25 min, were plotted as shown in Figure 2.3, and resulted in an almost perfect linear relationship between the optical density and the tissue thickness ($R^2 = 0.99$).

Figure 2.2 Effect of incubation time on optical density of rat brain homogenates of 10, 20, 40, 60, and 80 μm thickness.

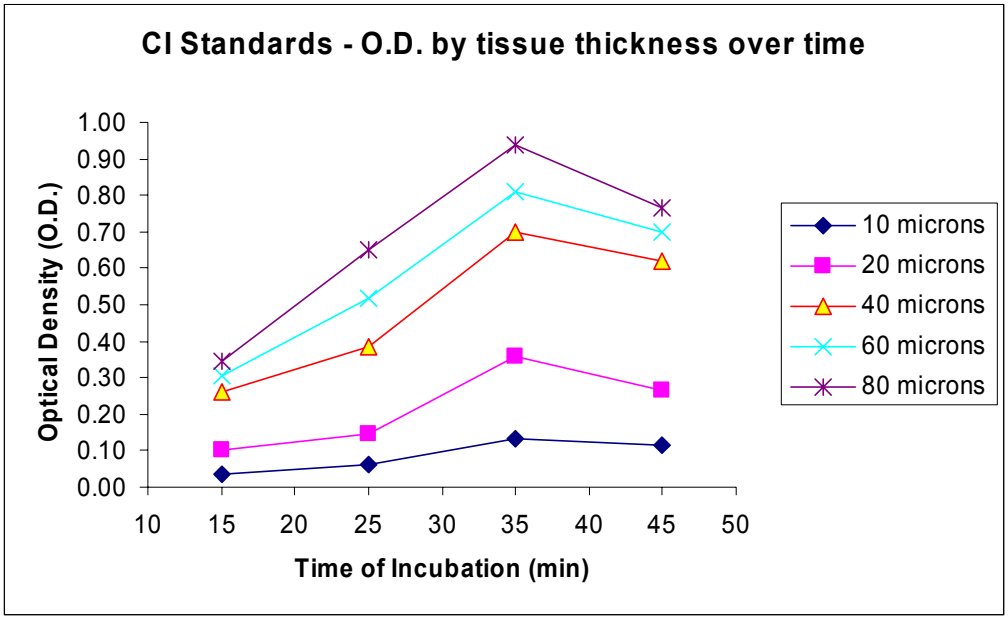

Figure 2.3 Effect of section thickness on optical density of standard rat brain homogenate sections incubated for 25 min at 37°C. The optical density increases linearly with increased thickness of the standards.

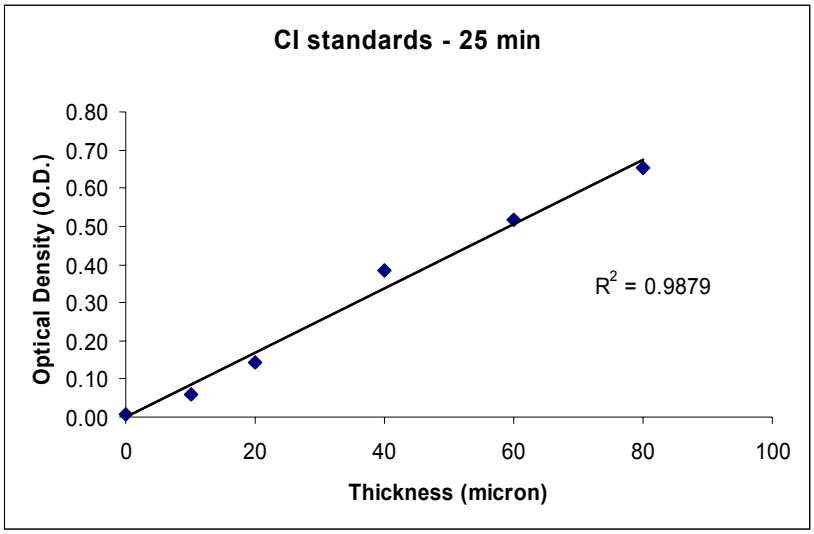

To estimate the range of optical density in the retina, data were taken from the 40 μm inner segment layer and the ganglion cell layer, which appeared to be the two darkest layers in the retina (Figure 2.4). The optical density values were below 0.68, well within the optical density range of the standards (Figure 2.2).

Figure 2.4 Effect of incubation time on optical density of the inner segment layer and the ganglion cell layer of the rat retina.

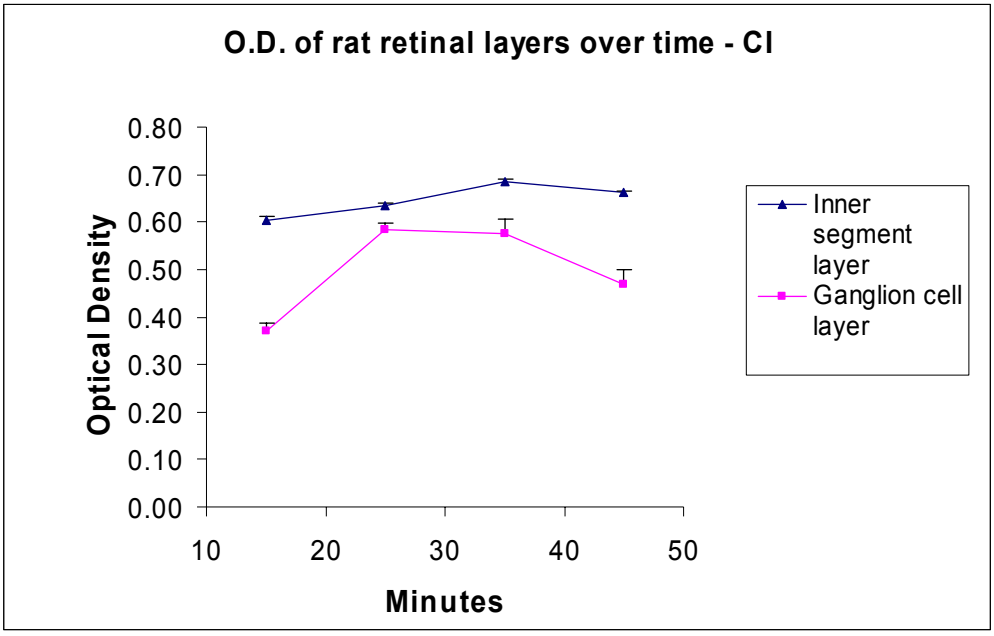

2.5 DISCUSSION

Mitochondrial complex I activity was revealed histochemically using a modified procedure based mainly on the techniques of Murray et al. (1988) and Barry et al. (1993). The enzymatic activity was assessed quantitatively from the intensity of formazan deposited on the incubated tissue sections. There was a linear relationship between the optical density and the incubation time within 35 min, and a strong linear

relationship between the optical density and various thicknesses of standards after incubation for 25 min.

We do not know why the retinal sections stained both pink and blue by this procedure, but it has been reported that most tetrazolium salts give red formazans in normal tissue, whereas blue formazans occur in ischemic tissues (Hoyer and Lyon, 1991). One type of monotetrazolium salt always gives blue formazans, but it is not commercially available (Hoyer and Lyon, 1991). It appeared from our slides that the cell bodies were mostly pink and the neuropil were mostly blue.

An exogenous electron carrier such as menadione or (1-methoxy) phenazine methosulfate can be added to the incubation medium in order to speed up the electron transfer to the tetrazolium salt, because the redox potential of coenzyme and tetrazolium salt do not have a fast electron flow from coenzyme to tetrazolium salt. The choice of these intermediate electron carriers depends on the localization of the dehydrogenase of interest (Van Noorden and Frederiks, 1992). For mitochondrial enzymes, phenazine methosulfate should be chosen because 1-methoxyphenazine methosulfate cannot pass the mitochondrial membrane (Kugler, 1982). In our study, the stain appeared sufficient without the use of any exogenous electron carrier, therefore it was not included in the protocol.

An autoradiographic assay has been developed to study complex I using the binding of [^{3}H]dihydrorotenone (Talpade et al., 2000). One of the limitations of this autoradiographic method is that it only assesses the enzyme availability for binding the chemical and not the enzymatic activity or function of complex I. Non-specific binding is another problem with this method.

The histochemical assay of complex I activity can be specifically inhibited by rotenone. Rotenone is an irreversible and specific complex I inhibitor (Lindahl and Oberg, 1961) that we propose to use in our animal model. Jung et al., (2002) used similar reagents and concentrations of incubation solution to those in our protocol, and tested the specificity of complex I in the presence of rotenone. The enzyme activity decreased significantly after a highly saturating concentration of rotenone (60 μM) was added. The activity did not decrease in the presence of the inhibitors of other complexes of the ETC.

In summary, the tetrazolium salt method is the most commonly used method to evaluate complex I enzymatic activity. The demonstration of complex I relies on the reduction of tetrazolium salts by hydrogen ions released during oxidation through enzyme activity to produce colored formazan deposit on the tissue. This enables the quantitative assay of complex I activity using densitometric analysis on the intensity of formazan deposited on the incubated sections of any tissue.

Acknowledgement

The author thanks Jason Berndt for his technical help.

2.6 REFERENCE

Barry MA, Halsell CB, Whitehead MC (1993) Organization of the nucleus of the solitary tract in the hamster: acetylcholinesterase, NADH dehydrogenase, and cytochrome oxidase histochemistry. *Microscopy research and technique* 26: 231-244.

Bennett MC, Rose GM (1992) Chronic sodium azide treatment impairs learning of the Morris water maze task. *Behav Neural Biol* 58: 72-75.

Betarbet R, Sherer TB, MacKenzie G, Garcia-Osuna M, Panov AV, Greenamyre JT (2000) Chronic systemic pesticide exposure reproduces features of Parkinson's disease. *Nat Neurosci* 3: 1301-1306.

Gonzalez-Lima F, Cada A (1998) Quantitative histochemistry of cytochrome oxidase activity. In: Cytochrome oxidase in neuronal metabolism and Alzheimer's disease (Gonzalez-Lima F, ed), pp 55-90. New York: Plenum Press.

Gonzalez-Lima F, Valla J, Jorandby L (1998) Cytochrome oxidase inhibition in Alzheimer's disease. In: Cytochrome oxidase in neuronal metabolism and Alzheimer's disease (Gonzalez-Lima F, ed), pp 171-200. New York: Plenum Press.

Greenamyre JT, Sherer TB, Betarbet R, Panov AV (2001) Complex I and Parkinson's disease. *IUBMB Life* 52: 135-141.

Hoyer PE, Lyon H (1991) Enzyme Histochemistry III: Oxidoreductases. In: Theory and Strategy in Histochemistry (Lyon H, ed), pp 337-364. Germany: Springer Verlag.

Jung C, Higgins CMJ, Xu Z (2002) A quantitative histochemical assay for activities of mitochondrial electron transport chain complexes in mouse spinal cord sections. *J Neurosci Methods* 114: 165-172.

Kugler P (1982) Quantitative dehydrogenase histochemistry with exogenous electron carriers (PNS, MPMS, MB). *Histochemistry* 93: 537-540.

Lindahl PE, Oberg KE (1961) The effect of rotenone on respiration and its point of attack. *Exptl Cell Research* 23: 228.

Murray GI, Burke MD, Ewen SWB (1988) Enzyme histochemical demonstration of NADH dehydrogenase on resin-embedded tissue. *The Journal of Histochemistry and Cytochemistry* 36: 815-819.

Robinson BH (1998) Human Complex I deficiency: Clinical spectrum and involvement of oxygen free radicals in the pathogenicity of the defect. *Biochimi et Biophys Acta (BBA) - Bioenergetics* 1364: 271-286.

Schapira AHV (1998) Human complex I defects in neurodegenerative diseases. *Biochimi et Biophys Acta (BBA) - Bioenergetics* 1364: 261-270.

Sims KL, Kauffman FC, Johnson EC, Pickel VM (1974) Cytochemical localization of brain nicotinamide adenine dinucleotide phosphate (oxidized)-dependent dehydrogenases qualitative and quantitative distributions. *The Journal of Histochemistry and Cytochemistry* 22: 7-19.

Talpade DJ, Greene JG, Higgins DSJr, Greenamyre JT (2000) In vivo labeling of mitochondrial complex I (NADH:ubiquinone oxidoreductase) in rat brain using [3H] dihydrorotenone. *J Neurochem* 75: 2611-2621.

Van Noorden CJF, Frederiks WM (1992) Microscopy handbooks 26. New York: Oxford University Press.

Voet D, Voet JG (1995) Biochemistry. John Wiley & Sons, Inc.

Chapter 3: Effects of Pesticide Rotenone in the Mouse Retina: A Potential Model to Investigate Environmental Contributions to Neurodegenerative Diseases

3.1 ABSTRACT

To help fulfill the need for developing effective *in vivo* animal models for exploring the mechanisms and treatment of neurodegenerative diseases, we developed a mouse model of optic neuropathy caused by mitochondrial complex I dysfunction by intravitreal administration of rotenone, a complex I inhibitor, in CBA/J mice. Retinal thickness was measured in sections stained histochemically for complex I enzymatic activity. The retinal ganglion cell layer of eyes injected with rotenone was significantly thinner than that of the control eyes injected with the vehicle, dimethyl sulfoxide, at 1, 24, and 48 h survival times. The largest reduction in thickness was 41% at 24 h post-injection. This effect is consistent with the degeneration of retinal ganglion cells in Leber's hereditary optic neuropathy. This is the first animal model of optic neuropathy resulting from mitochondrial dysfunction, and it could be used as an efficient and convenient way to test new treatments for mitochondrial neurodegenerative diseases. This model could also be used to study environmental involvement in neurodegenerative diseases.

3.2 INTRODUCTION

There is a compelling need to develop effective animal models for exploring the mechanisms and treatment of neurodegenerative diseases. The objective of this study was to create a mouse model of optic neuropathy caused by mitochondrial dysfunction using rotenone, a naturally occurring pesticide that inhibits mitochondrial complex I (Degli Esposti, 1998; Ernster et al., 1963; Lindahl and Oberg, 1961). Mitochondrial dysfunction has been identified in neurodegenerative disorders, including Parkinson's disease, Huntington's disease, and Alzheimer's disease (Valla et al., 2001; Brown and Wallace, 1994; Betarbet et al., 2000), and a role for the mitochondrial electron transport chain and oxidative phosphorylation is gathering increasing experimental support. For example, increasing evidence shows that Leber's hereditary optic neuropathy (LHON) is a neurodegenerative disease linked to mitochondrial complex I dysfunction (Brown and Wallace, 1994; Howell and Mackey, 1998). LHON has come to be regarded as a model disease for mitochondrial neurodegenerative diseases because "LHON can now be understood as a cooperative interplay of genetic, environmental, and physiological factors" (Brown et al., 1992).

Complex I is an integral membrane protein complex composed of 43 separate protein subunits in mammals (Greenamyre et al., 2001; Robinson, 1998; Schapira, 1998), seven of which (ND1, ND2, ND3, ND4, ND4L, ND5 and ND6) are encoded by mitochondrial DNA (mtDNA) (Walker et al., 1992). Three primary mtDNA point mutations have been linked to LHON and account for 90-95% of the occurrence of the disorder (Brown and Wallace, 1994; Besch et al., 1999). The three primary mutations are at nucleotide positions 11778/ND4, 3460/ND1 and 14484/ND6, all of which affect

complex I. In addition, at least 16 different secondary mtDNA mutations have been found (Brown and Wallace, 1994; Brown, 1999). LHON is the most common cause of blindness in otherwise healthy young men (Schapira, 1998). It is a maternally inherited disease which classically manifests as acute or subacute onset with bilateral central vision loss associated with the degeneration of the retinal ganglion cell layer and the optic nerve (Howell and Mackey, 1998; Brown et al., 1992).

To date, no effective treatment is available for mitochondrial neurodegenerative diseases, including LHON, and to our knowledge, there were no *in vivo* animal models for optic neuropathy caused by mitochondrial dysfunction. Thus, there was a great need to develop an animal model to test candidate treatments.

Inhibition of complex I activity in retinal neurons should lead to dysfunctional mitochondria, which could be potentially a good model of complex I-related optic neuropathy. Since the retina is part of the central nervous system, this could also be an *in vivo* model for neurodegenerative diseases in general. One of the complex I inhibitors is rotenone, a natural substance found in the stems and roots of certain tropical plants. It is a very commonly used compound for treating lakes and has been used in numerous lakes and reservoirs to remove unwanted fish species and restore traditional fisheries. In addition, it is used as a garden insecticide to control chewing insects. Rotenone is a specific and irreversible inhibitor of complex I through its firm binding to complex I (Ernster et al., 1963). To create a neurodegenerative animal model using rotenone administration in the eye is not only important for optic neuropathic processes but also can be of environmental significance.

3.3 MATERIALS AND METHODS

3.3.1 Subjects and anesthetics

Male CBA/J mice (25-44 g, N = 32) were used in this study. The mice were anesthetized by an intraperitoneal injection of a mixture of ketamine hydrochloride (45 mg/kg), xylazine hydrochloride (9 mg/kg), and acepromazine (1.5 mg/kg).

3.3.2 Intravitreal injection

Rotenone was administered into one eye of each mouse via intravitreal injection, while the vehicle, dimethyl sulfoxide (DMSO), was injected into the other eye of each mouse as a within-subject control. In a pilot study with 7 mice, several doses of rotenone were tested (0.065 to 0.2 mg/kg). The largest dose (0.2 mg/kg) appeared more effective in reducing retinal thickness and it was thus selected for subsequent study. One eye of each mouse was intravitreally injected with 0.5 μl rotenone (31.18 mM) in dimethyl sulfoxide (DMSO) over 2 min using a microinjection pump (CMA microdialysis AB, North Chelmsford, MA). The intravitreal injection point was just behind the limbus of the cornea in the superior and temporal quadrant of the eye to give access to the vitreous body without damaging the retina. A small sclerotomy was first performed using a fine needle (30 gauge). Then the injections were administered via 30-G blunt-ended dental injection needles (Monoject®, Sherwood Medical Company, Norfolk, NE) connected via polyethylene tubing to 10-μl Hamilton microsyringes (Hamilton Company, Reno, NV) powered by the microinjection pump. After the injections were completed, the needles were left in place for an additional 40 sec to allow for diffusion away from the needle tip and to

avoid any efflux of fluid through the injection site (Salinas et al., 1997). The other eye received the same volume and rate of injection of the vehicle DMSO only. Mice (N = 25) were randomly divided into 3 survival time groups following the injection (1 h, 24 h, and 48 h following injection); an additional control group received no injection. At the end of each survival time, the animals were decapitated and the eyeballs were rapidly removed, frozen in isopentane, and sectioned at 20 μm in a cryostat (Reichert-Jung) at –18^{o}C.

3.3.3 Complex I histochemistry

Sections were stained for complex I activity following a well-documented method using tetrazolium, which has been well-documented in brain and spinal cord (Barry et al., 1993; Murray et al., 1988; Jung et al., 2002), and we validated it for the retina (Chapter 2). Tetrazolium salts are colorless or yellow and water-soluble; they can be reduced metabolically to the highly colored water-insoluble microcrystalline deposits called formazans by accepting hydrogen released from the substrate (NADH) through enzyme action which is, in this case, complex I (see Chapter 2). Using the optimal conditions explained in Chapter 2, fresh-frozen sections were incubated at 37^{o}C for about 20 min with agitation in phosphate buffer containing NADH (Sigma, 1 mg/ml), nitroblue tetrazolium (Sigma, 1.33 mg/ml), and sodium azide (Sigma, 0.065 mg/ml) for inhibiting complex IV activity (Gonzalez-Lima and Cada, 1998). Sections were then dehydrated in graded ethanols and coverslipped from xylene, with Permount.

3.3.4 Image analysis

Using a microscopic image-processing system which included an Olympus BX40 microscope (Olympus America; Lake Success, NY), a CCD camera (Javelin Electronics; Torrance, CA), a Targa M8 image capture board and JAVA imaging software (Jandel Scientific; Corte Madera, CA), thickness was measured in the GCL, the inner plexiform layer (IPL), and the whole retina, from eye sections stained for complex I activity. To avoid the possible confound of retinal thickness differences by location, data were always taken from the same position, the center of the retina at about twice the diameter of the optic disc away from the center of the optic nerve. About 20 measurements were taken with equal intervals in distance along the cross-section of the retina within the screen of the monitor, and from both sides of the optic nerve.

3.3.5 Statistical analysis

A repeated measures analysis of variance followed by multiple comparisons and tests for simple effects was used to evaluate group differences at $p < 0.05$. Statistical differences in thickness of the GCL, IPL and the whole retina in rotenone treated eyes vs. the vehicle DMSO treated eyes in different survival times were evaluated. A two-tailed t-test at $p < 0.05$ was used with paired samples from both eyes in each subject from the 24 h group, to further test the significance of differences in IPL thickness between the rotenone-treated eye of each subject and its vehicle DMSO-treated control eye. The “n” equals number of mice with pairs of rotenone treated and control eyes, and pairs of eyes of the control subjects that received no injection.

3.4 RESULTS

The complex I staining of the cross-sectional mouse retina at 24 h following rotenone injection is shown in Figure 3.1. The neuropil (dendrites and axons) could be distinguished from the cell bodies by the color of the stain, blue for neuropil and pink for cell bodies. The different patterns of each retinal layer allowed its delineation from other layers. However, the retinal nerve fiber layer (RNFL) is too thin to be distinguished from the ganglion cell layer, and it was included in the GCL for the thickness measurement. It appears clearly that the GCL thickness of the rotenone treated eyes (Figure 3.1 A) is thinner than that of the DMSO treated control eyes (Figure 3.1 B).

Figure 3.1 Cross section of the retina with complex I staining in rotenone treated (A) and DMSO treated control (B) of 24 h post-injection group. The thickness of the ganglion cell layer (GCL) is indicated by the distance between two arrows. The inner plexiform layer (IPL) was delineated based on the blue stain. Complex I histochemistry resulted in blue staining of the IPL, which delineated this layer from other retinal layers (not shown in black and white photo). The entire unit bar length represents one tenth of a millimeter.

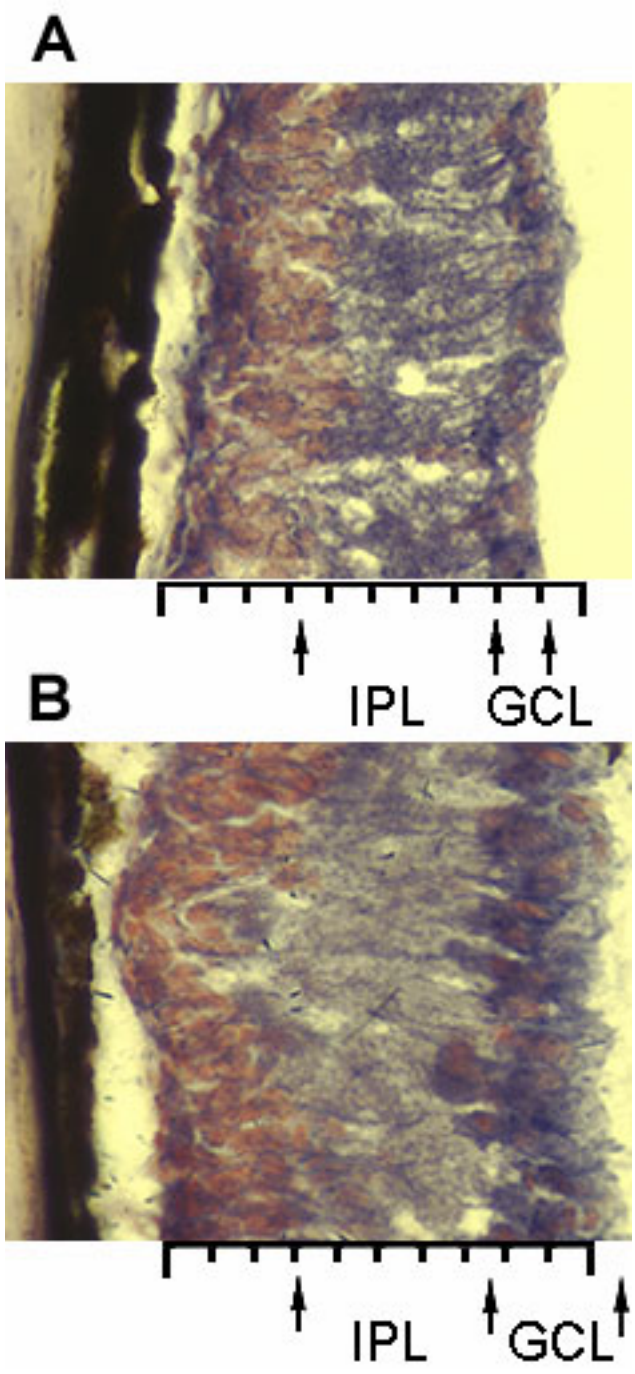
A
IPL
GCL
B
IPL
GCL

Results (Table 3.1) on the GCL thickness showed that the thickness of the retinal ganglion cell layer (GCL) of the rotenone treated eyes was significantly reduced compared to that of the DMSO control eyes at 1 h ($n = 8$, $p < 0.001$), 24 h ($n = 10$, $p < 0.001$), and 48 h survival times ($n = 5$, $p = 0.02$). Among the three groups the largest reduction of the GCL thickness was 41% at 24 h post-injection (Figure 3.1 and 3.2). Using multiple comparisons followed by Bonferroni correction, no difference in the thickness of retinal GCL was found between non-injected and DMSO treated control eyes across different post-injection time groups. However, within the rotenone treated groups, the GCL of the 1 h and 24 h post-injection groups was significantly thinner in comparison to the non-injected group ($p = 0.028$ and 0.002 respectively).

Table 3.1 Retinal thickness (mean ± standard error, microns) of different post-injection groups: non-injection (NI) control group, 1 h, 24 h, 48 h. GCL= ganglion cell layer, IPL= inner plexiform layer, WH= whole retina. * Significant (P<0.05) difference between rotenone and control groups.

		Control			Rotenone		
Group	N	GCL	IPL	WH	GCL	IPL	WH
NI	3	26.25±5.63	32.93±8.01	87.89±13.3	25.79±6.04	33.28±6.45	91.74±10.93
1 h	8	23.92±2.37	37.58±2.33	100.01±8.5	**17.05±0.9***	38.75±2.31	97.54±6.24
24 h	9	23.83±1.97	36.25±2.52	95.66±7.20	**13.57±1.0***	**30.86±1.6***	**76.53±3.59***
48 h	5	23.71±1.79	31.95±1.55	89.26±4.63	**19.16±1.7***	31.64±1.56	84.83±5.55

For retinal layers other than the GCL, the rotenone treated eyes also showed significantly reduced thickness compared to the DMSO treated control eyes in the 24 h post-injection group in both the inner-plexiform layer (IPL, $p = 0.042$) and the whole retina ($p = 0.025$) when using the global error terms pooled from all the time groups. For testing the effect of rotenone on retinal layers other than the GCL and IPL, the thickness of the GCL and IPL was subtracted from that of the whole retina to provide a measure of retinal thickness without the effect of the GCL and IPL. No significant statistical differences were found in the rest of the retina.

Figure 3.2 Percent of reduction (mean ± standard error bars) in the ganglion cell layer (GCL) thickness of rotenone vs. DMSO (control) treated eyes in different post-injection time groups: non-injection (NI), 1 h, 24 h and 48 h groups.

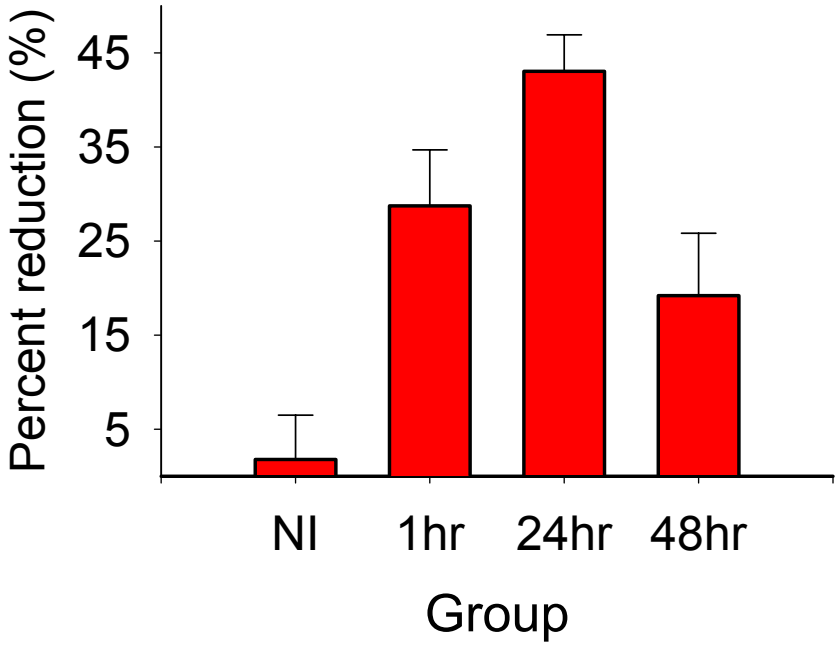

3.5 DISCUSSION

The first animal model of optic neuropathy caused by mitochondrial dysfunction was established through intravitreal injection of rotenone, a specific inhibitor of mitochondrial complex I. The retinal ganglion cell layer was significantly reduced at 1, 24, and 48 h following injection, with the largest reduction of 41% at 24 h post-injection. This effect is consistent with the degeneration of retinal ganglion cells in Leber's hereditary optic neuropathy. The retina is derived from the diencephalons; therefore, it is a part of the central nervous system. A neurodegenerative animal model developed in the eye not only provides a relatively independent simple *in vivo* central nervous system that does not rely on the function of other CNS regions, but also permits easy access for various research techniques and for drug delivery.

Since neurons (e.g., retinal ganglion cells) have very limited capacity for regeneration, the "recovery" phenomenon that appeared at 48 h in GCL thickness reduction may be explained by the regeneration of the neurites (dendrites and axons) of the ganglion cells and displaced amacrine cells, and/or the generation or regeneration of glial cells in this layer. Only about 60% (Drager and Olsen, 1981) or 41% (Jeon et al., 1998) of total cells in the mouse GCL are ganglion cells (Jeon et al., 1998); the rest of the cells are displaced amacrine cells and glial cells. The displaced amacrine cells can comprise up to 50% in rats (Perry, 1981), and 60% in mouse (Jeon et al., 1998), of the total cells in the GCL. It has been demonstrated that retinal ganglion cells in the retinas of adult mammals have the capacity to regenerate neurites after they are injured *in vivo* (So and Aguayo, 1985) and *in vitro* (Takano et al., 2002;

Thanos and Thiel, 1990). However the “recovery” phenomenon that appeared here needs further evaluation with an increased number of subjects (n = 5, here).

A tetrazolium salt histochemical method was used in this study to demonstrate complex I activity in the retina. However, because tissue shrinkage occurred profoundly in the GCL and to a less degree in the IPL at 24 h post-injection, the phenomenon of the darker staining intensity that appeared in the two layers of most rotenone-treated sections compared to the control may not simply indicate elevated level of complex I activity. In fact, the intended use of the complex I histochemistry technique here was to delineate the complete boundary of the retinal ganglion cell layer and the nerve fiber layer, rather than to provide quantitation of complex I activity.

Mitochondrial complex I staining is more suitable than other common histological methods, such as Nissl staining, for two reasons. First, rotenone is a selective complex I inhibitor, and complex I staining is specific to the effect of rotenone. Second, the neuropil surrounding the cell bodies in the retinal ganglion cell layer (GCL), especially the retinal nerve fibers at the inner surface of the GCL, is visible only in complex I stained tissues. Therefore, it provides information not shown with other techniques.

The results of this study showed that rotenone administration to the eye caused a loss of tissue (most likely neurons and their processes) in both the GCL and the IPL. The GCL contains optic nerve fibers and the retinal ganglion cell bodies, while the IPL contains dendrites of retinal ganglion cells and neurites of bipolar cells and amacrine cells. In the rodent retina, just like the human retina, small and medium-

sized ganglion cells predominate in the central retina, and large cells locate mostly in the peripheral regions (Kageyama and Wong-Riley, 1984). Data were taken from the center of the retina due to the vulnerability of small ganglion cells in optic neuropathies (Kageyama and Wong-Riley, 1984). The damage of the retinal ganglion cells in the central retina of this model is consistent with the retinal pathological manifestation seen in LHON patients (Beal et al., 1997; Brown et al., 1992; Howell, 1998).

The etiology of LHON is complex, which is indicated by its remarkable features. For example, there is a highly variable penetrance (the proportion of individuals of a particular genotype that express its phenotypic effect in a given environment), even within the same family with the same pathogenic homoplasmic mutation (all mtDNA copies are mutated) (Howell, 1998). Transmission of a LHON mutation from one generation to another does not always correlate with transmission of the disease; many family members of LHON patients harbor the same mutation, but they are visually asymptomatic (Riordan and Harding, 1995). The primary mtDNA mutation is not sufficient for the manifestation of the optic neuropathy (Howell and Mackey, 1998). The disparity between the phenotypic expression and the genotype suggests that the genetic factor is not the sole factor; thus the etiology of the disease may not be simply one of genetic defects but may be exacerbated by or caused by environmental toxic agents inhibiting mitochondrial respiration (Berndt et al., 2001). This is supported by the work of Carelli et al. (2002) who have shown that environmental factors are needed to express the neuropathy. This idea is also supported by recent toxicological studies of Parkinson's disease, which indicate links

to rotenone (Betarbet et al., 2000). More attention should be given to the contribution of exposure to environmental toxins, including pesticides, to the incidence of mitochondrial neurodegenerative diseases.

Rotenone was chosen as a complex I inhibitor for this study due to specific features. It is a naturally occurring pesticide (derived from plants) widely used on home-grown fruits and vegetables and also used as a fish toxin, so it is found in a variety of commercial garden and animal-care products. Rotenone is a potent and specific inhibitor of mitochondrial complex I, binding to subunit ND1 of complex I (Singer and Ramsay, 1994). It has features not found in two other common complex I inhibitors, 1-methyl-4-phenyl-1,2,3,6,-tetrahydropyridine (MPTP) and amytal (Degli Esposti, 1998). Unlike MPTP, which is selective for dopaminergic neurons and depends on the dopamine transporters to gain access to the neurons, rotenone is extremely lipophilic and can easily penetrate biological membranes (Ernster et al., 1963), while the highly charged 1-methyl-4-phenylpyridinium ion (MPP^+, the main metabolite of MPTP) would have much more difficulty passing through. Rotenone has also been found to be more potent than MPP^+ (Heikkila et al., 1986). Amytal is also a complex I inhibitor that had been used earlier (Ernster et al., 1955). However, a high concentration of amytal is required for maximal inhibition, and it inhibits enzymes other than complex I as well (Storey, 1980); therefore, it is neither a strong nor a specific inhibitor for complex I. Thus, rotenone may be a more appropriate model candidate than amytal as rotenone binds to the electron transfer system firmly and irreversibly (Ernster et al., 1963). In addition, rotenone may also offer a more widely applicable model of environmental toxin exposure than MPTP or amytal.

The neuronal toxicity of rotenone has been attributed to several aspects of defective cell metabolism. It blocks the oxidation of NADH to ubiquinone by binding to complex I, greatly reducing mitochondrial proton motive force necessary to generate the mitochondrial transmembrane potential, resulting in reduced production of ATP (Pastorino et al., 1995). Apoptosis has been induced by rotenone after 20 min in a liver cell line, and it was not reversed with the removal of rotenone (Isenberg and Klaunig, 2000). This indicates that mitochondrial dysfunction induced by acute rotenone administration may trigger a cascade of further damage, even in the absence of rotenone, eventually leading to cell death.

The simplicity of our animal model may serve as a convenient way *in vivo* to study mitochondrial dysfunction in neurodegeneration. While animal models of Parkinson's disease require chronic exposure to toxins over a period of weeks or months (Betarbet et al., 2000), the present model can be rapidly performed – it takes only about a day for robust damage to occur. Therefore, this animal model may provide an efficient and convenient way to screen new candidate treatments.

Acknowledgement

We thank Dr. Juan Salinas and Dr. Yvon Delville for use of their equipment. Supported by NIEHS grant ES07784.

3.6 REFERENCE

Barry MA, Halsell CB, Whitehead MC (1993) Organization of the nucleus of the solitary tract in the hamster: acetylcholinesterase, NADH dehydrogenase, and cytochrome oxidase histochemistry. Microscopy research and technique 26: 231-244.

Beal MF, Howell N, Bodis-Wollner I (1997) Mitochondria and free radicals in neurodegenerative diseases. New York: Wiley-Liss.

Berndt JD, Callaway NL, Gonzalez-Lima F (2001) Effects of chronic sodium azide on brain and muscle cytochrome oxidase activity: A potential model to investigate environmental contributions to neurodegenerative diseases. Journal of Toxicology and Environmental Health - Part A 63: 67-77.

Besch D, Leo-Kottler B, Zrenner E, Wissinger B (1999) Leber's hereditary optic neuropathy: Clinical and molecular genetic findings in a patient with a new mutation in the ND6 gene. Graefe's Archive for Clinical and Experimental Ophthalmology 237: 745-752.

Betarbet R, Sherer TB, MacKenzie G, Garcia-Osuna M, Panov AV, Greenamyre JT (2000) Chronic systemic pesticide exposure reproduces features of Parkinson's disease. Nat Neurosci 3: 1301-1306.

Brown MD, Voljavec AS, Lott MT, MacDonald I, Wallace DC (1992) Leber's hereditary optic neuropathy: A model for mitochondrial neurodegenerative diseases. FASEB J 6: 2791-2799.

Brown MD, Wallace DC (1994) Spectrum of mitochondrial DNA mutations in Leber's hereditary optic neuropathy. Clin Neurosci 138-145.

Brown MD (1999) The enigmatic relationship between mitochondrial dysfunction and Leber's hereditary optic neuropathy. Journal of the Neurological Sciences 165: 1-5.

Carelli V, Ross-Cisneros FN, Sadun AA (2002) Optic nerve degeneration and mitochondrial dysfunction: genetic and acquired optic neuropathies. Neurochemistry International 40: 573-584.

Degli Esposti M (1998) Inhibitors of NADH-ubiquinone reductase: an overview. Biochimi et Biophys Acta (BBA) - Bioenergetics 1364: 222-235.

Drager UC, Olsen JF (1981) Ganglion cell distribution in the retina of the mouse. Invest Ophthalmol Vis Sci 20: 285-293.

Ernster L, Dallner G, Azzone GG (1963) Differential effects of rotenone and amytal on mitochondrial electron and energy transfer. J Biol Chem 238: 1124-1131.

Ernster L, Jalling O, Low H, Lindberg O (1955) Alternative pathways of mitochondrial DPNH oxidation, studied with amytal. Exptl Cell Res Suppl 3: 124-132.

Gonzalez-Lima F, Cada A (1998) Quantitative histochemistry of cytochrome oxidase activity. In: Cytochrome oxidase in neuronal metabolism and Alzheimer's disease (Gonzalez-Lima F, ed), pp 55-90. New York: Plenum Press.

Greenamyre JT, Sherer TB, Betarbet R, Panov AV (2001) Complex I and Parkinson's disease. IUBMB Life 52: 135-141.

Heikkila RE, Nicklas WN, Vyas I, Duvoisin RC (1986) Dopaminergic toxicity of rotenone and the 1-methyl-4-phenylpyridinium ion after their stereotaxic administration to rats: implication for the mechanism of 1-methyl-4-phenyl-1,2,3,6,-tetrahydropyridine toxicity. Neurosci Lett 62: 389-394.

Howell N, Mackey DA (1998) Low-penetrance branches in matrilineal pedigrees with leber hereditary optic neuropathy [2]. American Journal of Human Genetics 63: 1220-1224.

Howell N (1998) Leber hereditary optic neuropathy: Respiratory chain dysfunction and degeneration of the optic nerve. Vision Res 38: 1495-1504.

Isenberg JS, Klaunig JE (2000) Role of the mitochondrial membrane permeability transition (MPT) in rotenone-induced apoptosis in liver cells. Toxicol Sci 53: 340-351.

Jeon C-J, Strettoi E, Masland RH (1998) The major cell populations of the mouse retina. The Journal of Neuroscience 18: 8936-8946.

Jung C, Higgins CMJ, Xu Z (2002) A quantitative histochemical assay for activities of mitochondrial electron transport chain complexes in mouse spinal cord sections. J Neurosci Methods 114: 165-172.

Kageyama GH, Wong-Riley MTT (1984) The histochemical localization of cytochrome oxidase in the retina and lateral geniculate nucleus of the ferret, cat, and monkey, with particular reference to retinal mosaics and on/off-center visual channels. J Neurosci 4: 2445-2459.

Lindahl PE, Oberg KE (1961) The effect of rotenone on respiration and its point of attack. Exptl Cell Research 23: 228.

Murray GI, Burke MD, Ewen SWB (1988) Enzyme histochemical demonstration of NADH dehydrogenase on resin-embedded tissue. The Journal of Histochemistry and Cytochemistry 36: 815-819.

Pastorino JG, Snyder JW, Hoek JB, Farber JL (1995) Ca depletion prevents anoxic death of hepatocytes by inhibiting mitochondrial permeability transition. American Journal of Physiology - Cell Physiology 268: C676-C685.

Perry VH (1981) Evidence for an amacrine cell system in the ganglion cell layer of the rat retina. Neuroscience 6: 931-934.

Riordan E, Harding A (1995) Leber's hereditary optic neuropathy: the clinical relevance of different mitochondrial DNA mutations. J Med Genet 32: 81-87.

Robinson BH (1998) Human Complex I deficiency: Clinical spectrum and involvement of oxygen free radicals in the pathogenicity of the defect. Biochimi et Biophys Acta (BBA) - Bioenergetics 1364: 271-286.

Salinas JA, Introini-Collison IB, Dalmaz C, McGaugh JL (1997) Posttraining intraamygdala infusions of oxotremorine and propranolol modulate storage of memory for reductions in reward magnitude. Neurobiol Learn Mem 68: 51-59.

Schapira AHV (1998) Human complex I defects in neurodegenerative diseases. Biochimi et Biophys Acta (BBA) - Bioenergetics 1364: 261-270.

Singer TP, Ramsay RR (1994) The reaction sites of rotenone and ubiquinone with mitochondrial NADH dehydrogenase. Biochimica et Biophysica Acta - Bioenergetics 1187: 198-202.

So K-F, Aguayo AJ (1985) Lengthy regrowth of cut axons from ganglion cells after peripheral nerve transplantation into the retina of adult rats. Brain Res 328: 349-354.

Storey BT. (1980) Inhibitors of energy-coupling site 1 of the mitochondrial respiratory chain. Pharmac.Ther. 10: 399-406.

Takano M, Horie H, Iijima Y, Dezawa M, Sawada H, Ishikawa Y (2002) Brain-derived Neurotrophic Factor Enhances Neurite Regeneration from Retinal Ganglion Cells in Aged Human Retina in vitro. Experimental Eye Research 74: 319-323.

Thanos S, Thiel HJ (1990) Regenerative and proliferative capacity of adult human retinal cells in vitro. Graefes Arch Clin Exp Ophthalmol 228: 369-376.

Valla J, Berndt JD, Gonzalez-Lima F (2001) Energy hypometabolism in posterior cingulate cortex of Alzheimer's patients: Superficial laminar cytochrome oxidase associated with disease duration. J Neurosci 21: 4923-4930.

Walker JE, Arizmendi JM, Dupuis A, Fearnley IM, Finel M, Medd SM, Pilkington SJ, Runswick MJ, Skehel JM (1992) Sequences of 20 subunits of NADH:ubiquinone oxidoreductase from bovine heart mitochondria. Application of a novel strategy for sequencing proteins using the polymerase chain reaction. Journal of Molecular Biology 226: 1051-1072.

Chapter 4: Neurodegeneration Caused by Rotenone in the Mouse Retina: A Cellular Morphometric study

4.1 ABSTRACT

Rotenone is a widely used pesticide that inhibits complex I of the mitochondrial respiratory chain. Complex I dysfunction is linked to the degeneration of retinal ganglion cells in Leber's hereditary optic neuropathy. The neurodegeneration of the retina was investigated in mice with intravitreal microinjection of rotenone in one eye and the vehicle dimethyl sulfoxide in the contralateral control eye, as a within-subject control. The retinal ganglion cell layer (GCL) of eyes injected with rotenone became significantly thinner than that of the control eyes after 24 h, but not as early as after 0.5 h. This reduction was observed with complex I histochemistry and with Nissl staining of cell bodies. After 24 h, retinal nerve fiber layer thickness was reduced by 89% and the number of GCL cells was reduced by 21% in rotenone-treated eyes. Cellular morphometric data (soma area, perimeter, and diameter) did not show overall differences, but there was a preferential reduction in the proportion of larger cells. Therefore, the reduction in GCL thickness after 24 h of rotenone microinjection could be accounted for by cell loss and nerve fiber shrinkage, but not by overall soma size change. Rotenone-induced degeneration of the ganglion cell layer could be used as a convenient way to evaluate mechanisms and treatments for the neurodegeneration caused by mitochondrial dysfunction.

4.2 INTRODUCTION

There is a compelling need to understand the mechanisms of neurodegeneration that may be caused or exacerbated by environmental toxins (Betarbet et al., 2000; Berndt et al., 2001; Sherer et al., 2003). Rotenone is a naturally occurring and widely used pesticide (Nagatsu, 2002), thus studies with rotenone may provide clues to an environmental role of pesticides in neurodegenerative diseases. Mitochondrial dysfunction is associated with neurodegenerative disorders such as Leber's hereditary optic neuropathy, Parkinson's disease, Huntington's disease, and Alzheimer's disease (Beal, 1998; Betarbet et al., 2000; Gonzalez-Lima and Cada, 1998; Howell, 1998; Valla et al., 2001). A dysfunctional mitochondrial electron transport chain decreases ATP production and accelerates the generation of free radicals (Beal, 1998). Leber's hereditary optic neuropathy (LHON) is regarded as a model disease for mitochondrial neurodegenerative diseases (Brown et al., 1992), and is the most common cause of blindness in otherwise healthy young men (Schapira, 1998). It is also the most common disease associated with mutations of the mitochondrial DNA (mtDNA) (Manfredi and Beal, 2005). LHON is a maternally inherited disease which classically presents as acute or subacute onset with bilateral central vision loss associated with the degeneration of the retinal ganglion cell layer and the optic nerve (Howell, 1998).

LHON is linked to mitochondrial complex I dysfunction (Brown et al., 1992). Complex I, nicotinamide adenine dinucleotide (NADH)-quinone oxidoreductase, is the first and the largest complex of the mitochondrial respiratory chain. It catalyzes the reduction of NADH to ubiquinone. Complex I is an integral membrane protein

complex composed of about 43 subunits, seven of which (ND1, ND2, ND3, ND4, ND4L, ND5 and ND6) are encoded by mitochondrial DNA (mtDNA) (Hatefi, 1985; Walker et al., 1992). About 90-95% of LHON cases are the result of one of three primary mitochondrial DNA (mtDNA) point mutations at nucleotide positions 11778/ND4, 3460/ND1 and 14484/ND6 (Besch et al., 1999; Brown et al., 1992), all of which affect complex I (Beal, 1998). In addition, at least 14 different secondary mtDNA mutations have been found (Brown et al., 1992).

We previously reported the first animal model for optic neuropathy resulting from mitochondrial dysfunction caused by rotenone toxicity (Zhang et al., 2002). Rotenone was used because it is a specific and irreversible inhibitor of mitochondrial complex I and it binds strongly to the ND1 subunit of complex I (Ernster et al., 1963; Lindahl and Oberg, 1961; Singer and Ramsay, 1990). Rotenone was intravitreally microinjected into one eye of each mouse, while the other eye was injected with only the vehicle, dimethyl sulfoxide (DMSO). The thickness of the retinal ganglion cell layer (GCL) of the rotenone-treated eyes showed significant reductions in the 1 h and 24 h post-injection time groups, with the highest reduction of 41% at 24 h post-injection, as compared to the DMSO-treated eyes. The inner plexiform layer (IPL) also showed a significant reduction in thickness in the 24 h group (Zhang et al., 2002). The objective of the present study was to determine whether the reduction in GCL thickness after 24 h of rotenone microinjection was caused by cell loss or shrinkage, as determined by morphometric analyses including soma area, diameter, and perimeter measurements. In addition, in the current study, we verified whether the rotenone effect could be detected using routine Nissl staining instead of enzyme histochemistry.

The results showed a significant cell loss in the GCL following rotenone treatment, which resembles the degeneration of retinal ganglion cells in Leber's optic neuropathy. The results also revealed a significant reduction in the GCL thickness with Nissl staining.

4.3 MATERIALS AND METHODS

4.3.1 Subjects

Male CBA/J mice (N = 29, 25-44 g) (The Jackson Laboratory, Bar Harbor, ME) were used. Eighteen mice were studied after 24 h of intravitreal microinjection with one of four doses of rotenone (0.01, 0.3, 0.6, and 1.2 mM). The two lower doses showed no detectable effect, and all subsequent mice were therefore treated with the higher doses Two groups of mice given 1.2 mM microinjections of rotenone (0.2 mg/kg) or vehicle were studied in two different post-injection time intervals before euthanasia (0.5 h and 24 h). Seven mice were treated identically for the 0.5 h post-injection group. For the 24 h group, new tissue samples from 10 subjects included in a previous study (Zhang et al., 2002) were used. All experimental procedures were approved by the Institutional Animal Care and Use Committee (IACUE) of the University of Texas at Austin, and conformed to NIH Guidelines.

4.3.2 Intravitreal microinjection procedures

The mice were anesthetized by an intraperitoneal injection of a mixture of ketamine hydrochloride (45 mg/kg), xylazine hydrochloride (9 mg/kg), and acepromazine (1.5 mg/kg). One eye of each mouse was intravitreally microinjected

with 0.5 μl rotenone in DMSO. Intravitreal microinjections were performed by an experienced ophthalmologist using a stereomicroscope and microinjection system. A small sclerotomy was performed using a fine needle (30 gauge) inserted just behind the limbus of the cornea in the superior and temporal quadrant of the eye to give access to the vitreous body. The microinjection was done immediately underneath the corneoscleral junction with a blunt needle to avoid the lens and the retina. Microinjections were administered via 30-G blunt-ended dental injection needles (Monoject®, Sherwood Medical Company, Norfolk, NE) connected by polyethylene tubing to 10-μl Hamilton microsyringes (Hamilton Company, Reno, NV). The injections were delivered over 2 min using a CMA 100 microinjection pump (CMA microdialysis AB, North Chelmsford, MA), and the injection needles were left in place for an additional 40 s to allow for diffusion away from the needle tip and to avoid any efflux of fluid through the injection site (Salinas et al., 1997). The edges of the injection point were gripped with forceps while the microsyringe was slowly withdrawn. Then, a small amount of n-butyl cyanoacrylate monomer (Nexaband liquid tissue adhesive, Veterinary Products Laboratories, Phoenix) was applied on the surface of the injection point to form a sealed thin layer.

The estimated local concentration of rotenone in the eye was either 0.6 mM or 1.2 mM based on a measured eyeball volume averaging 13 μl in the mice. The other eye received the same volume and rate of the vehicle DMSO as a within-subject control. Following decapitation, the eyeballs and brains were rapidly removed, frozen in isopentane, and sectioned coronally at 20 μm in a cryostat (Reichert-Jung) at -18^{o}C. Four adjacent series were created for histochemical analysis.

4.3.3 Retinal laminar thickness measurement in sections stained for complex I

Mitochondrial complex I staining was used because rotenone is a selective complex I inhibitor. Complex I is sensitive to the effect of rotenone, and the histochemical reaction used can be partially inhibited by adding rotenone (Jung et al., 2002). Also, the neuropil surrounding the cell bodies in the GCL, including the optic nerve fibers at the inner surface of the GCL, is visible in complex I but not in cresyl violet stained tissues. Therefore, complex I staining was suitable for the retinal thickness measurement reflecting both cell bodies and neuropil, whereas cresyl violet staining delineated only cell bodies.

To determine whether the rotenone treatment reduces GCL thickness after a half hour of treatment, one series of sections from the 0.5 h group were stained for complex I activity following a well-documented method using tetrazolium salts (Barry et al., 1993; Sims et al., 1974). Tetrazolium salts are colorless or yellow and water-soluble; they can be reduced metabolically to the highly colored water-insoluble microcrystalline deposits called formazans by accepting hydrogen released from the substrate (NADH) through enzyme action which is, in this case, complex I. Slides with fresh-frozen 20 μm sections were put into three baths, 5 min each, of 0.1 M sodium phosphate buffer solution (PBS) with 10% (w/v) sucrose. The temperatures of the three baths were graded from about 4^{o}C to room temperature to bring the slides gradually to room temperature as a transition to the incubation temperature of 37^{o}C. After rinsing in 0.1 M PBS, slides were incubated at 37^{o}C in the dark for 15-20 min with agitation in phosphate buffer containing NADH (Sigma, 1 mg/ml), nitroblue

tetrazolium (Sigma, 1.33 mg/ml), and sodium azide (Sigma, 0.065 mg/ml). Sodium azide was used to inhibit cytochrome oxidase (complex IV) (Gonzalez-Lima and Cada, 1998).

Using a computerized microimaging system including an Olympus BX40 microscope with a 40x objective (Olympus America; Lake Success, NY), a CCD camera (Javelin Electronics; Torrance, CA), a Targa M8 image capture board and JAVA imaging software (Jandel Scientific; Corte Madera, CA), thickness was measured in the GCL, the IPL, and the whole retina, from eye sections stained for complex I activity. To avoid the effect of retinal thickness by location, data were taken from the center of the retina at a distance of approximately twice the diameter of the optic disc away from the center of the optic disc.

4.3.4 GCL thickness in cresyl violet stained sections and estimate of retinal nerve fiber layer (RNFL) thickness in the 24 h post-injection group

To determine if the reduction in GCL thickness by rotenone is caused by loss of cells or stain in the GCL, a series of sections was Nissl-stained with cresyl violet and used for GCL thickness, cell count, and morphometric analysis of cell bodies. The cresyl violet staining procedure consisted of dehydration of the fresh frozen tissue sections followed by staining (0.1% cresyl violet, 6-10 min) and rehydration in a series of graded ethanols (70-100%). Slides were then cleared in xylene and coverslipped with Permount. The same microscopic image-processing system and sampling procedure described for thickness measurement was used.

The RNFL at the inner surface of the GCL is mostly composed of axons of retinal ganglion cells. In the cresyl violet stained tissue the cell bodies are clearly

visible but the axons are not. To estimate the size of the thinning effect of rotenone in RNFL, GCL thickness was measured in cresyl violet-stained sections that do not show the retinal nerve fibers and only reveal the cell bodies in the GCL. Then the data were compared to the GCL thickness data taken from the complex I stained series of sections in which the RNFL contributed to the GCL thickness. A comparison of these two stains provided a reliable estimate of the RNFL thickness. A direct measurement using only one stain was unreliable because the RNFL of the treated eyes became too thin to be measured accurately.

4.3.5 Cell counts and morphometric analysis of somata of retinal GCL in cresyl violet-stained sections

Readings were taken from approximately the same length and location of the GCL in the retinal cross-sections in all eyes, and the sections with the largest diameter of the eye were chosen to control the variation of retinal thickness among sections. The profile cell counting was chosen because the number of the soma profiles in the GCL was counted only for the purpose of comparing rotenone-treated and non-treated eyes within each mouse. In addition, the sections examined were from every fourth consecutive 20 μm-thick section. Thus individual ganglion cells were unlikely to be counted more than once because soma diameters were smaller than 20 μm. In the mouse retina, most of the cells in GCL are retinal ganglion cells concentrated in the center. Other cells in GCL are small glial cells and displaced amacrine cells. The displaced amacrine cells are concentrated in the periphery of the mouse retina rather than the center (Drager and Olsen, 1981). The GCL cell counts were made at the center of the retina. Retinal ganglion cells were not distinguished from other cells in

the GCL because in the central retina, where the readings were taken, the ganglion cells are not displaced as in the periphery of the retina (Drager and Olsen, 1981).

To determine whether the reduction in GCL thickness by rotenone is caused by the shrinkage of the cells in the GCL, soma area, diameter (average of the long and short axis of each soma profile), and perimeter were measured from each soma profile in the GCL with the same image analysis system used for thickness measurement. About the same length of the GCL in the retinal cross sections from each eye was used for data collection.

4.3.6 Statistics

To analyze the effect of rotenone on soma size, we calculated the mean, mean +1 standard deviation (SD), and mean – 1 SD from the data of all the cells from both the DMSO control group and the rotenone treated group. The values were used for cut-off points to divide the total somata into four size categories for each morphometric measurement. This was done for both rotenone and DMSO treated groups.

Two-tailed t-tests at $p < 0.05$ were used with paired samples from both eyes in each subject, to test the significance of differences between the rotenone-treated eye of each subject and its vehicle DMSO-treated control eye. The “n” equals number of mice with pairs of treated and control eyes.

To compare the cell numbers in the largest cell size category in the GCL of rotenone-treated vs. DMSO-treated control eyes, a Chi-square test was used to analyze the difference in both the 0.5 h and 24 h groups.

4.4 RESULTS

The mice receiving rotenone and DMSO eye microinjections did not show evidence of malaise or behavioral alterations. The pupillary light reflex was tested immediately before decapitation and it was present in both eyes for all the subjects. No differences in histochemical staining could be seen in sections taken from the brains of these mice. The effects of the eye microinjection appeared limited to the retina.

4.4.1 Decreased somata and axons of GCL cells in the 24 h post-injection group

The GCL reduction can be detected by microscopic inspection after 24 h post-injection (Figure 4.1A and C). Using the cresyl violet staining technique, in which only somata can be observed, a significant 18% reduction of GCL thickness was measured ($n = 9$, $p = 0.038$). However, as early as 0.5 h post-injection, the results revealed no significant difference in the thickness of GCL (DMSO 21.43 ± 1.43 μm, rotenone 20.47 ± 1.19 μm) and the whole retina (DMSO 87.80 ± 5.57 μm, rotenone 95.78 ± 6.33 μm) in rotenone treated eyes as compared to that of the DMSO treated eyes.

Figure 4.1 Cross-section of the mouse retina with cresyl violet staining (A, C) and complex I staining (B, D) in rotenone treated (A, B) and DMSO treated control (C, D) of 24 h post-injection group. The thickness of the ganglion cell layer (GCL) and the retinal nerve fiber layer (RNFL) is clearly reduced in the rotenone treated eye as compared to the control eye. Color is needed to distinguish RNFL (blue) from the immediately adjacent GCL (red) in B and D. Digitized images set to 560x magnification. The unit bar at the bottom represents 50 microns.

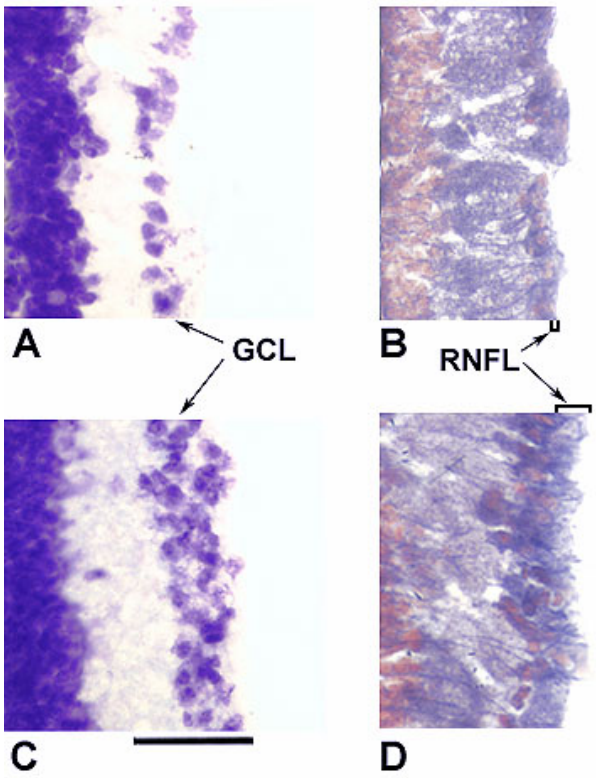

The RNFL reduction can also be observed by microscopic inspection (Figure 4.1B and D). The thicknesses of the GCL including RNFL from complex I staining are 23.82 ± 1.97 μm and 13.87 ± 1.16 μm for the DMSO and the rotenone treated groups respectively. The thicknesses of the GCL excluding the RNFL can be obtained from cresyl violet-stained sections, and they are 16.33 ± 1.52 μm and 13.07 ± 1.05 μm for the DMSO and the rotenone treated group, respectively. The combined information on GCL thickness reduction provided by the two different staining methods can provide an estimate of thickness reduction in the RNFL alone. The difference in GCL

thicknesses obtained from the two different staining methods are 7.49 ± 2.12 μm and 0.79 ± 1.16 μm for the DMSO and the rotenone treated groups, respectively. There was a large and significant reduction of 89% in RNFL thickness in the rotenone group ($n = 9$, $p = 0.009$).

The 1.2 mM rotenone microinjection was clearly effective in reducing retinal thickness as compared to 0.6 mM (Figure 4.2). Therefore, the 1.2 mM rotenone microinjection was chosen for the comparison of the 0.5 h and 24 h post-injection interval groups in this and our previous studies (Zhang et al., 2002).

Figure 4.2 Percent reduction in thickness of the ganglion cell layer as a function of rotenone concentration in the eye.

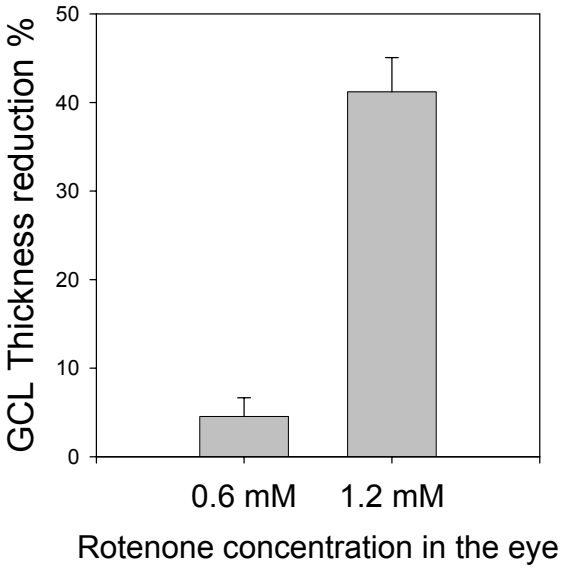

The effect of post-injection interval on retinal thickness is shown in Figure 4.3. Significant overall reductions in GCL (including RNFL = 41%, $n = 10$, $p < 0.001$) and IPL (13%, $n = 10$, $p < 0.05$) were found after 24 h post-injection, but no significant change was found in the thickness of the rest of the retina (Figure 4.3A). There were no differences in the 0.5 h post-injection group and the non-injected group (Figure 4.3B and C).

4.4.2 Increased thickness in the inner plexiform layer (IPL) of 0.5 h post-injection group

Thickness of the IPL in the rotenone treated eyes was significantly increased compared to that in the control eyes at 0.5 h post-injection time ($n = 7$, $p = 0.04$) (Figure 4.3B). The percent increase of the rotenone treated IPL is 11% as calculated from paired data of treated and control eyes. For testing the effect of rotenone on retinal layers other than the GCL and IPL, the thickness of the GCL and IPL was subtracted from that of the whole retina. No significant statistical differences were found in the rest of the retina.

Figure 4.3 Thickness of the ganglion cell layer, inner-plexiform layer and rest of the retina in complex I stained eyes with 24 h (A) and 0.5 h (B) post-injection time, and with no injection (C). Asterisks indicate statistically significant differences at the $p < 0.05$.

A

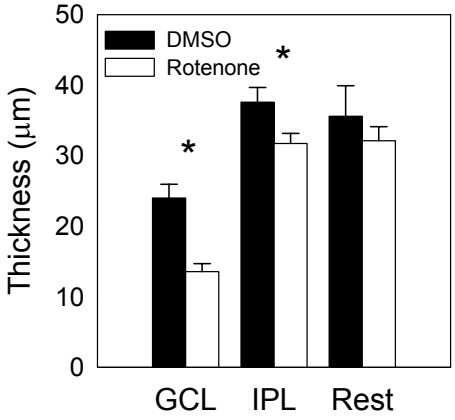
DMSO
Rotenone
Thickness (μm)
50
40
30
20
10
0
*
*
GCL
IPL
Rest

B

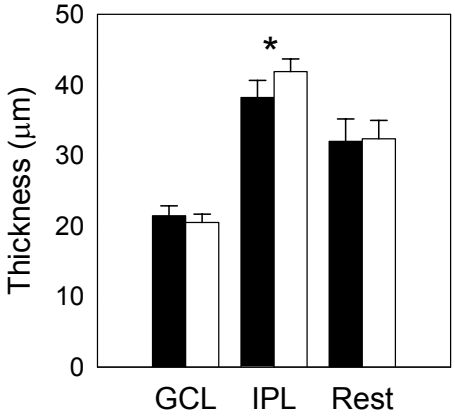
Thickness (μm)
50
40
30
20
10
0
*
GCL
IPL
Rest

C

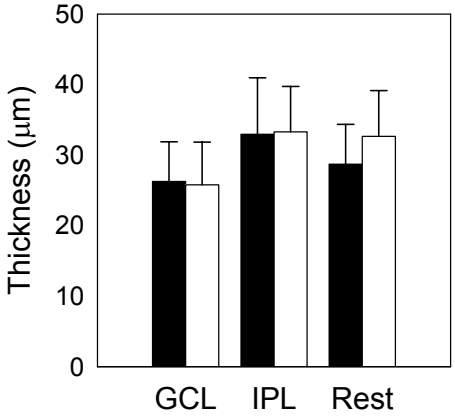
Thickness (μm)
50
40
30
20
10
0
GCL
IPL
Rest

4.4.3 Cell counts in the GCL of 0.5 h and 24 h post-injection groups

In the 0.5 h post-injection time group, there was a non-significant reduction in the number of the cells in the GCL between rotenone and DMSO treated eyes (Figure 4.4). This is consistent with the result that the GCL thickness in the 0.5 h group did not show a significant difference between the rotenone and DMSO treated eyes.

However, in the 24 h group, the number of the cells in GCL of rotenone treated eyes was significantly reduced (21% percent reduction) from that of the vehicle treated eyes ($n = 8$, $p = 0.02$), (Figure 4.4).

Figure 4.4 Percent of GCL cells in rotenone treated eyes as compared to DMSO with standard error bars in 0.5 h and 24 h groups, using Nissl staining.

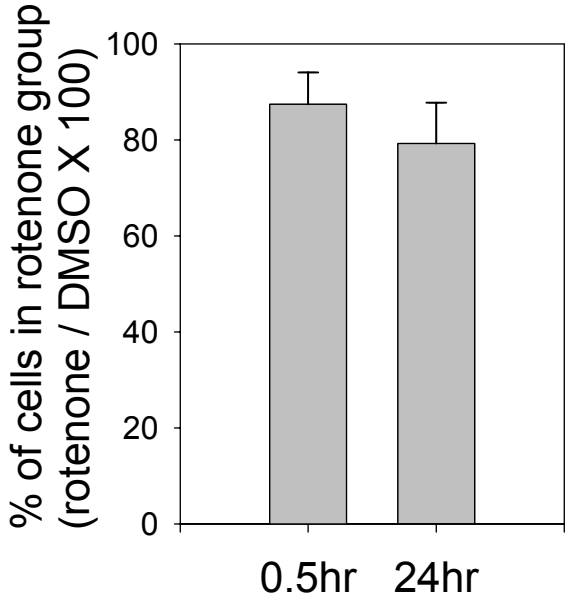

4.4.4 Soma morphometry and frequency distribution in cresyl violet-stained sections

No significant differences were found between DMSO and rotenone-treated eyes in measurements of soma area, diameter, or perimeter of the GCL cells in the 0.5- or 24 h groups. The soma area, diameter and perimeter were reduced by only about 2.5% in rotenone treated eyes of the 24 h group (Figure 4.5). This suggested that for the cells observed in the GCL, thinning of the GCL by rotenone injection could not be accounted for by overall cell shrinkage.

Figure 4.5 Soma morphometry in GCL of rotenone treated and control eyes in the 24 h group.

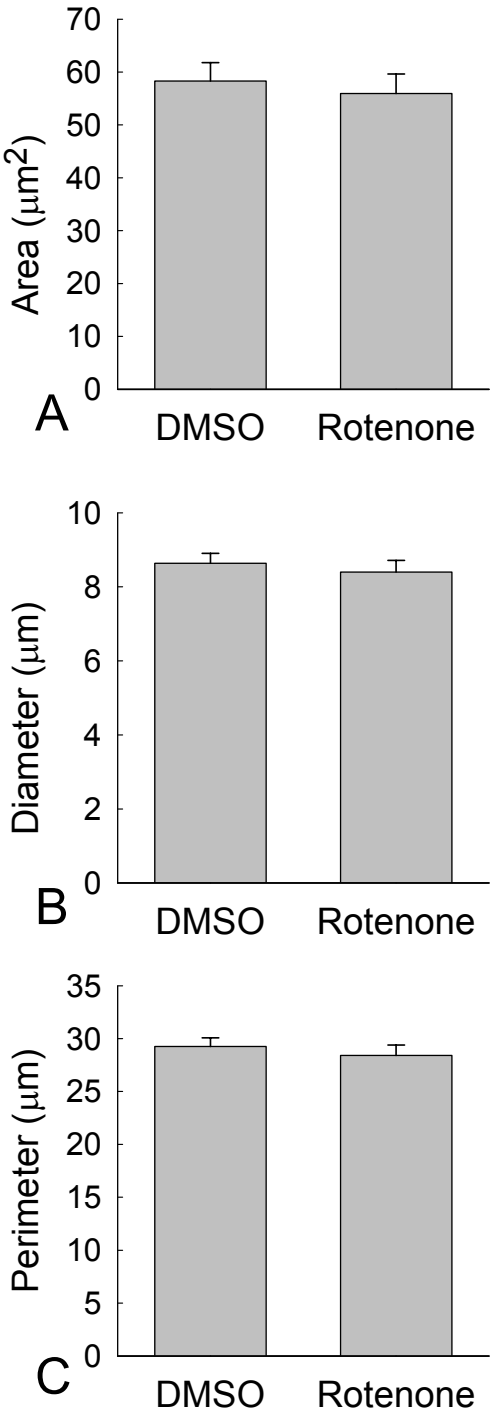
70
60
50
40
30
20
10
0
Area (μm2)
A
DMSO
Rotenone
10
8
6
4
2
0
Diameter (μm)
B
DMSO
Rotenone
35
30
25
20
15
10
5
0
Perimeter (μm)
C
DMSO
Rotenone

The morphometric analysis also revealed that the cell loss in the 24 h group was not uniform among cells of different sizes. There was a reduction in the proportion of larger cells in the 24 h post-injection group. In the largest cell category (soma diameter > 10 m), rotenone-treated GCL had fewer cells compared to DMSO-treated control eyes in the 24 h group (Figure 4.6). A Chi-square test showed this preferential loss of larger cells (larger than mean + 1 SD) in the rotenone-treated group in the 24 h group was significant and was consistent through all measures of area ($n = 108$, $p < 0.01$), diameter ($n = 140$, $p < 0.0001$), and perimeter ($n = 227$, $p < 0.001$) (Figure 4.7). However, this was the opposite pattern found in the 0.5 h group (Figure 4.7), but this trend did not reach the statistical significance (Chi-square test)

Figure 4.6 Frequency of cells in the GCL as a function of soma diameter in 24 h group. Cell counts were taken from the center of the retina about twice the diameter of the optic disc away from the center of the optic nerve for a GCL length about 155 μm. *$P < 0.0001$, when the cell number in the rotenone eyes was compared to that of the control eyes (the dashed line) using Chi-square test.

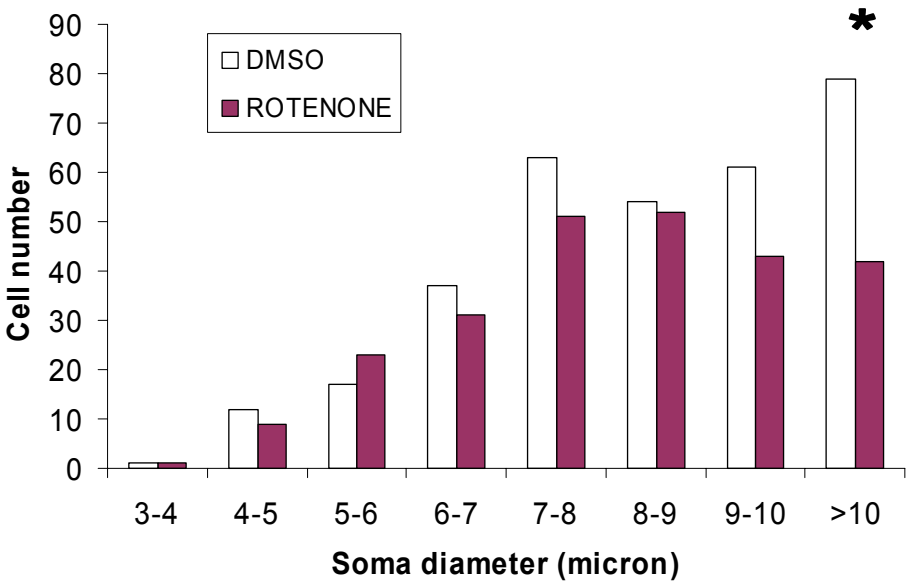

Figure 4.7 Percentage of GCL cells by soma area (A and B), diameter (C and D), and perimeter (E and F) in rotenone treated as compared to the DMSO treated eyes in 0.5 h (A, C, and E) and 24 h (B, D, and F) groups. Cells were divided into four size categories using the mean – 1 standard deviation, mean, and mean + 1 standard deviation of all the cells from both rotenone and DMSO treated eyes. *P < 0.01, when the cell number in the rotenone eyes was compared to that of the control eyes (the dashed line) using Chi-square test.

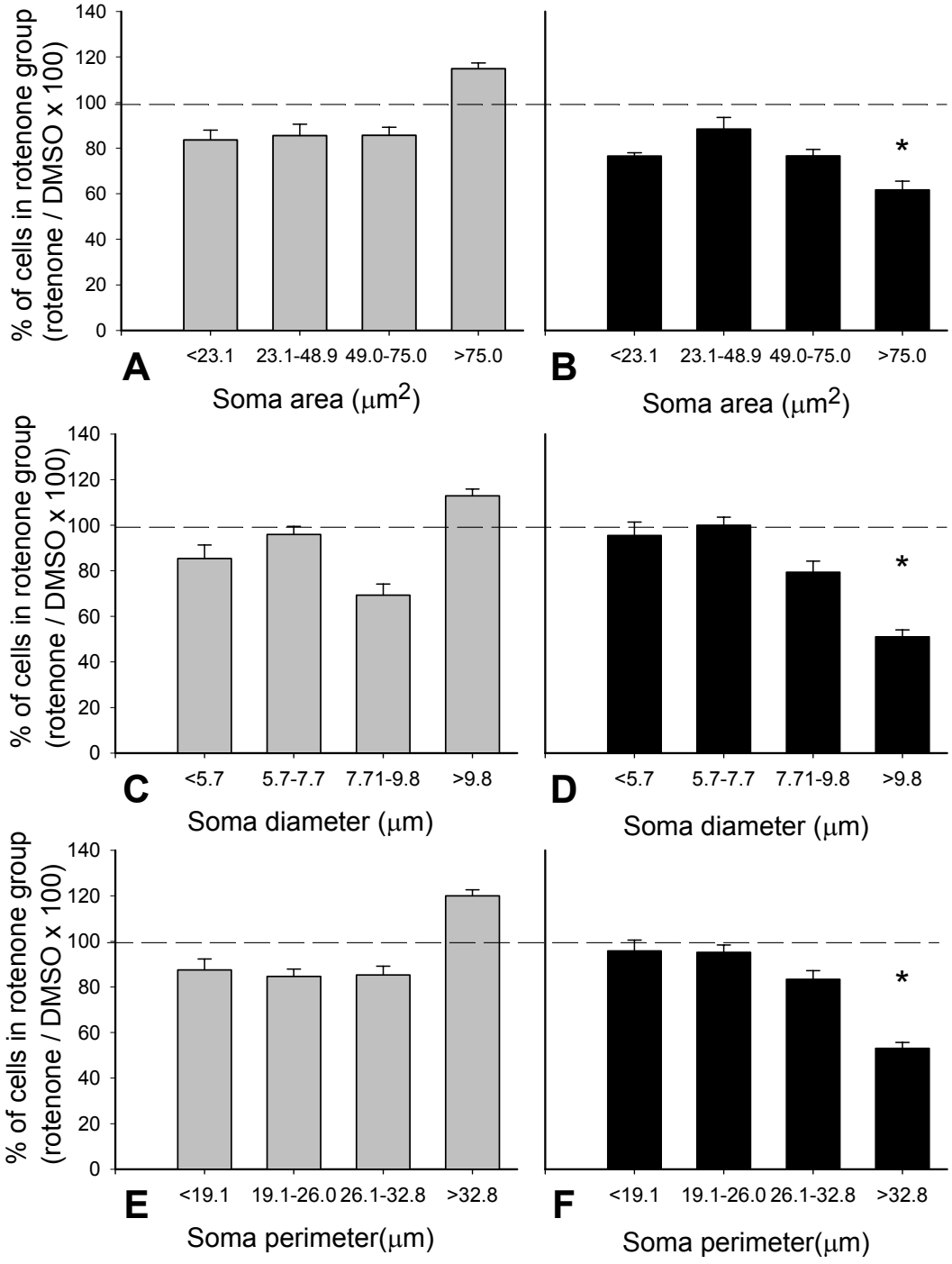
% of cells in rotenone group (rotenone / DMSO x 100)
140
120
100
80
60
40
20
0
<23.1
23.1-48.9
49.0-75.0
>75.0
A
Soma area (μm2)
B
Soma area (μm2)
*
<5.7
5.7-7.7
7.71-9.8
>9.8
C
Soma diameter (μm)
D
Soma diameter (μm)
<19.1
19.1-26.0
26.1-32.8
>32.8
E
Soma perimeter(μm)
F
Soma perimeter(μm)

4.5. DISCUSSION

The observed cell loss is consistent with GCL thickness reduction in rotenone treated eyes of the 24 h post-injection group (Zhang et al., 2002) and is also in line with the ganglion cell loss of LHON patients (Howell, 1998). A significant 18% reduction in GCL thickness was observed using the cresyl violet technique, in which only cell bodies are stained, suggesting that the effect of 1.2 mM rotenone on the GCL is not simply an artifact observed with complex I histochemical staining. This thinning of GCL by rotenone microinjection in the 24 h group (Zhang et al., 2002) could be accounted for by the observed 21% cell loss. The larger reduction (41%) of GCL thickness seen with complex I staining, which reflects ganglion cell bodies (GCL) and their axons (RNFL), could be accounted for by the additional 89% thinning of the RNFL.

However, the observed GCL decreases at 24 h post-injection do not appear to be caused by soma shrinkage. In addition, there was no significant change in the thickness or the cell number of GCL as early as 0.5 h after intravitreal treatment with 1.2 mM rotenone. We have previously observed that GCL thickness was significantly reduced by 28% one hour after a similar microinjection of rotenone (Zhang et al., 2002). This suggests that GCL thickness starts to decrease between 0.5 and one hour after 1.2 mM rotenone microinjection.

The method for quantifying the RNFL thickness reduction observed (Figure 4.1) was indirect because of the resulting negligible size of this layer in the rotenone-treated eyes. While this approach was not ideal, the pronounced thinning of the RNFL observed in the current study provided clear evidence that this layer was very susceptible to the inhibition of complex I activity by rotenone. The RNFL contains unmyelinated axons of the ganglion cells, and stained darkly for complex I, as opposed to the light staining of the optic nerve segment caudal to the lamina cribosa (a connective tissue consisting of holes through which axons cross into the myelinated optic nerve). The same pattern of staining has been reported in mitochondrial complex II and complex IV activity in monkeys and humans (Andrews et al., 1999; Kageyama and Wong-Riley, 1984). Myelinated segments of optic axons are energy and temporally efficient because ATPases on these fibers cluster only within the nodes of Ranvier and depolarization occurs in a “saltatory” fashion along successive nodes of Ranvier (Waxman and Ritchie, 1993). On the other hand, the unmyelinated segment of optic nerve axons (the prelaminar portion of the optic nerve, mostly RNFL) requires a much greater flow of current resulting in slow conduction velocity and high energy demand, because these axons are associated with a more uniform membrane distribution of ATPases (Waxman and Ritchie, 1993). Therefore, the unmyelinated RNFL has a higher demand for oxidative phosphorylation, making it a possible “choke-point” in LHON and other optic neuropathies (Carelli et al., 2002; Howell, 1998), and likewise this layer is more vulnerable to insult by rotenone.

The IPL contains ganglion cell dendrites and the processes of bipolar and amacrine cells. This layer stained darkly for complex I in our study. Kageyama and Wong-Riley (1984) also reported that the ganglion cell dendrites stained moderate to darkly and contributed to the overall intensity of cytochrome oxidase staining in the IPL. The above observations indicated a contribution of highly active mitochondrial enzymatic activity of ganglion cell dendrites in the IPL, which may be associated with the rich synaptic interactions in this layer. Our results of the thickness and cell number measurements from the 0.5 h group suggest that cell loss is not significantly involved during the early stage of the impairment of mitochondrial function caused by rotenone treatment. Rather than cell loss, there was evidence of enlargement of the retinal ganglion cell dendrites by 0.5 h, which may indicate initial swelling.

Rizzo (1995) and Sadun et. al. (2000) have reported that the papillomacular bundle formed by all macular area axons that are located centrally is selectively involved in a range of genetic or acquired optic neuropathies in humans. Sadun et. al. (2000) reported that smaller axons, presumably belonging to the P- (parvo-) ganglion cell pathway, were differentially affected in LHON. However, that conclusion might need further investigation because it was based on only two female cases with two normal males used as controls. Further, the spectra of the optic nerve fiber size showed an increased number of large axons, and the possibility of smaller axons swelling in response to the insult of the disease could not be excluded. Even though mouse retina does not contain a macula, its small and medium-sized retinal ganglion

cells distribute densely in the central retina, and large cells are mostly in the peripheral regions of the retina, as in primates and other rodents (Drager and Olsen, 1981; Kageyama and Wong-Riley, 1984). The somata that were measured in our studies presumably belong to a population of small-medium sized ganglion cells because data were taken from the center of the retina. However, our data showed that the larger ganglion cells among this population were the most vulnerable to rotenone. In the 24 h group, cells with larger somata were more reduced in numbers than smaller ones (Figure 4.6 and 4.7). The preferential loss of the larger cells may be caused by cell death and/or cell shrinkage, and may be associated with more mitochondria in the cell. It has been shown that in Alzheimer's disease, the large ganglion cells or M- (Magno-) cells were preferentially affected (Sadun and Bassi, 1990). It has also been reported that larger ganglion cells are more sensitive to intraocular injection of NMDA (Dreyer et al., 1994), more vulnerable to glaucomatous damage (Quigley et al., 1988), which are associated with ischemia and excitotoxicity (Osborne et al., 1999). The preferential loss of larger cells in our study may indicate that the mechanisms of rotenone toxicity may be similar to the effects of ischemia and excitotoxicity in these cells.

The 21% cell body loss in the GCL of rotenone-treated eyes is consistent with the neurodegeneration of the GCL in LHON. The neuronal toxicity of rotenone has been attributed to several aspects of defective cell metabolism. Rotenone blocks the oxidation of NADH to ubiquinone by binding to complex I, greatly reducing the mitochondrial proton motive force necessary to generate the mitochondrial

transmembrane potential, resulting in reduced production of ATP and increased production of reactive oxygen species. *In vitro* studies have shown that complex I inhibitors induce apoptosis. For example, apoptosis has been induced by rotenone after 12-18 h of administration (Wolvetang et al., 1994). Mitochondrial dysfunction triggers a cascade of apoptosis that continues after removal of rotenone, irreversibly leading to cell death (Barrientos and Moraes, 1999; Isenberg and Klaunig, 2000). The early steps of this pathway may involve mitochondrial swelling and release of cytochrome c, which triggers apoptosis (Howell, 1998); this was also suggested from our measurements of increased thickness and cell number in the 0.5 h post-injection time group (Figures 4.3B and 4.4).

The etiology of LHON is complex. For example, the penetrance of LHON is not complete. This means that not all individuals harboring a primary mutation express the disease at the phenotypic level (Howell, 1998). The primary mtDNA mutation is not sufficient for the manifestation of the optic neuropathy. The disparity between the phenotypic expression and the genotype suggests that the genetic factor is not the sole determinant; the etiology of mitochondrial neuropathies may not be simply one of genetic defects but may be exacerbated by or caused by environmental toxic agents inhibiting mitochondrial respiration (Berndt et al., 2001). It has been reported that exposure to tobacco, alcohol, and a variety of less common toxins including pesticides (Carelli et al., 2002) increased penetrance in LHON pedigrees. In fact, the clinical manifestation of toxic and nutritional optic neuropathies remarkably resemble that of

LHON (Carelli et al., 2002). Therefore, environmental factors are needed to express the neuropathy. This idea is also supported by toxicological studies of Parkinson's disease, which indicate links to rotenone, a commonly used pesticide and a mitochondrial complex I inhibitor (Betarbet et al., 2000). More attention should be brought to the contribution of exposure to environmental toxins, including pesticides, and the incidence of mitochondrial neurodegenerative diseases.

ACKNOWLEDGMENTS

We thank Ms. Alison Crane Tannenbaum for her technical advice. This work was supported by NIEHS grant ES07784 and NINDS grant NS37755.

ABBREVIATIONS:

DMSO: dimethyl sulfoxide

ETC: electron transport chain

GCL: ganglion cell layer

IPL: inner plexiform layer

LHON: Leber's hereditary optic neuropathy

MtDNA: mitochondrial DNA

RNFL: retinal nerve fiber layer

4.6. REFERENCES

Andrews RM, Griffiths PG, Johnson MA, Turnbull DM (1999) Histochemical localisation of mitochondrial enzyme activity in human optic nerve and retina. *Br J Ophthalmol* 83: 231-235.

Barrientos A, Moraes CT (1999) Titrating the effects of mitochondrial complex I impairment in the cell physiology. *J Biol Chem* 274: 16188-16197.

Barry MA, Halsell CB, Whitehead MC (1993) Organization of the nucleus of the solitary tract in the hamster: acetylcholinesterase, NADH dehydrogenase, and cytochrome oxidase histochemistry. *Microscopy research and technique* 26: 231-244.

Beal MF (1998) Mitochondrial dysfunction in neurodegenerative diseases. *Biochimi et Biophys Acta (BBA) - Bioenergetics* 1366: 211-223.

Berndt JD, Callaway NL, Gonzalez-Lima F (2001) Effects of chronic sodium azide on brain and muscle cytochrome oxidase activity: A potential model to investigate environmental contributions to neurodegenerative diseases. *Journal of Toxicology and Environmental Health - Part A* 63: 67-77.

Besch D, Leo-Kottler B, Zrenner E, Wissinger B (1999) Leber's hereditary optic neuropathy: Clinical and molecular genetic findings in a patient with a new mutation in the ND6 gene. *Graefe's Archive for Clinical and Experimental Ophthalmology* 237: 745-752.

Betarbet R, Sherer TB, MacKenzie G, Garcia-Osuna M, Panov AV, Greenamyre JT (2000) Chronic systemic pesticide exposure reproduces features of Parkinson's disease. *Nat Neurosci* 3: 1301-1306.

Brown MD, Voljavec AS, Lott MT, MacDonald I, Wallace DC (1992) Leber's hereditary optic neuropathy: A model for mitochondrial neurodegenerative diseases. *FASEB J* 6: 2791-2799.

Carelli V, Ross-Cisneros FN, Sadun AA (2002) Optic nerve degeneration and mitochondrial dysfunction: genetic and acquired optic neuropathies. *Neurochemistry International* 40: 573-584.

Drager UC, Olsen JF (1981) Ganglion cell distribution in the retina of the mouse. *Invest Ophthalmol Vis Sci* 20: 285-293.

Dreyer EB, Pan ZH, Storm S, Lipton SA (1994) Greater sensitivity of larger retinal ganglion cells to NMDA-mediated cell death. *NeuroReport* 5: 629-631.

Ernster L, Dallner G, Azzone GG (1963) Differential effects of rotenone and amytal on mitochondrial electron and energy transfer. *J Biol Chem* 238: 1124-1131.

Gonzalez-Lima F, Cada A (1998) Quantitative histochemistry of cytochrome oxidase activity. In: Cytochrome oxidase in neuronal metabolism and Alzheimer's disease (Gonzalez-Lima F, ed), pp 55-90. New York: Plenum Press.

Hatefi Y (1985) The mitochondrial electron transport and oxidative phosphorylation system. *Annual Review of Biochemistry* 54: 1015-1069.

Howell N (1998) Leber hereditary optic neuropathy: Respiratory chain dysfunction and degeneration of the optic nerve. *Vision Res* 38: 1495-1504.

Isenberg JS, Klaunig JE (2000) Role of the mitochondrial membrane permeability transition (MPT) in rotenone-induced apoptosis in liver cells. *Toxicol Sci* 53: 340-351.

Jung C, Higgins CMJ, Xu Z (2002) A quantitative histochemical assay for activities of mitochondrial electron transport chain complexes in mouse spinal cord sections. *J Neurosci Methods* 114: 165-172.

Kageyama GH, Wong-Riley MTT (1984) The histochemical localization of cytochrome oxidase in the retina and lateral geniculate nucleus of the ferret, cat, and monkey, with particular reference to retinal mosaics and on/off-center visual channels. *J Neurosci* 4: 2445-2459.

Lindahl PE, Oberg KE (1961) The effect of rotenone on respiration and its point of attack. *Exptl Cell Research* 23: 228.

Manfredi G, Beal MF (2005) Poison and antidote: A novel model to study pathogenesis and therapy of LHON. *Annals of Neurology* 56: 171-172.

Nagatsu T (2002) Amine-related neurotoxins in Parkinson's disease: Past, present, and future. *Neurotoxicol Teratol* 24: 565-569.

Osborne NN, Ugarte M, Chao M, Chidlow G, Bae JH, Wood JPM, Nash MS (1999) Neuroprotection in Relation to Retinal Ischemia and Relevance to Glaucoma. *Survey of Ophthalmology* 43: S102-S128.

Quigley HA, Dunkelberger GR, Green WR (1988) Chronic human glaucoma causing selectively greater loss of large optic nerve fibers. *Ophthalmology* 95: 357-363.

Rizzo J.F.3rd. (1995) Adenosine triphosphate deficiency: a genre of optic neuropathy. *Neurology* 45: 11-6.

Sadun AA, Bassi CJ (1990) Optic nerve damage in Alzheimer's disease. *Ophthalmology* 97: 9-17.

Sadun AA, Win PH, Ross-Cisneros FN, Walker SO, Carelli V (2000) Leber's hereditary optic neuropahty differentially affects smaller axons in the optic nerve. *Tr Am Opth Soc* 98: 223-235.

Salinas JA, Introini-Collison IB, Dalmaz C, McGaugh JL (1997) Posttraining intraamygdala infusions of oxotremorine and propranolol modulate storage of memory for reductions in reward magnitude. *Neurobiol Learn Mem* 68: 51-59.

Schapira AHV (1998) Human complex I defects in neurodegenerative diseases. *Biochimi et Biophys Acta (BBA) - Bioenergetics* 1364: 261-270.

Sherer TB, Kim JH, Betarbet R, Greenamyre JT (2003) Subcutaneous rotenone exposure causes highly selective dopaminergic degeneration and [alpha]-synuclein aggregation. *Exp Neurol* 179: 9-16.

Sims KL, Kauffman FC, Johnson EC, Pickel VM (1974) Cytochemical localization of brain nicotinamide adenine dinucleotide phosphate (oxidized)-dependent dehydrogenases qualitative and quantitative distributions. *The Journal of Histochemistry and Cytochemistry* 22: 7-19.

Singer TP, Ramsay RR (1990) Mechanism of the neurotoxicity of MPTP. An update. *FEBS Lett* 274: 1-8.

Valla J, Berndt JD, Gonzalez-Lima F (2001) Energy hypometabolism in posterior cingulate cortex of Alzheimer's patients: Superficial laminar cytochrome oxidase associated with disease duration. *J Neurosci* 21: 4923-4930.

Walker JE, Arizmendi JM, Dupuis A, Fearnley IM, Finel M, Medd SM, Pilkington SJ, Runswick MJ, Skehel JM (1992) Sequences of 20 subunits of NADH:ubiquinone oxidoreductase from bovine heart mitochondria. Application of a novel strategy for sequencing proteins using the polymerase chain reaction. *Journal of Molecular Biology* 226: 1051-1072.

Waxman SG, Ritchie JM (1993) Molecular dissection of the myelinated axon. *Ann of Neurol* 33: 121-136.

Wolvetang EJ, Johnson KL, Krauer K, Ralph SJ, Linnane AW (1994) Mitochondrial respiratory chain inhibitors induce apoptosis. *FEBS Letters* 339: 40-44.

Zhang X, Jones D, Gonzalez-Lima F (2002) Mouse model of optic neuropathy caused by mitochondrial complex I dysfunction. *Neurosci Lett* 326: 97-100.

Chapter 5: Methylene Blue Prevents Neurodegeneration Induced by Rotenone in Mouse Retinal Ganglion Cell Layer

5.1 ABSTRACT

An experimental optic neuropathy model was used to test the hypothesis that methylene blue, as an antioxidant, may protect the retinal ganglion cell layer from neurodegeneration caused by rotenone. Rotenone is a widely used pesticide that inhibits complex I, the first enzyme of the mitochondrial respiratory chain. Complex I dysfunction is linked to the degeneration of retinal ganglion cells in Leber's optic neuropathy. Methylene blue is a reduction–oxidation agent that can act as a powerful antioxidant, preventing formation of mitochondrial oxygen free radicals. The neurodegeneration of the retina was studied in mice with intravitreal microinjection of rotenone alone, or in combination with increasing doses of methylene blue, in one eye, and the vehicle in the contralateral control eye. Rotenone induced neurodegeneration in the retinal ganglion cell layer 24 h after injection, as indicated by significant reductions in both the thickness and cell numbers of the retinal ganglion cell layer of eyes microinjected with rotenone as compared to the control eyes. This neurodegeneration was completely prevented by the injection of methylene blue along with rotenone. The effect of rotenone and rotenone plus methylene blue was investigated using two histological stains, complex I and Nissl, and two measurements, morphometric layer thickness and non-biased stereological cell counts. The protective effect of methylene blue appeared to be related to its antioxidant action

because cytochrome oxidase activity was similarly activated in rotenone and rotenone plus methylene blue groups. It was concluded that rotenone-induced degeneration in the ganglion cell layer can be prevented by intravitreal injection of methylene blue. The findings suggest that methylene blue may be a promising therapeutic agent in optic neuropathy and perhaps other neurodegenerative diseases caused by mitochondrial dysfunction.

5.2 INTRODUCTION

Dysfunction of the mitochondrial electron transport chain has been implicated in the pathogenesis of neurodegenerative disorders such as Leber's optic neuropathy, Parkinson's disease, Huntington's disease, and Alzheimer's disease (Beal, 1998; Betarbet et al., 2000; Gonzalez-Lima and Cada, 1998; Howell, 1998; Valla et al., 2002). Leber's optic neuropathy, which classically manifests as bilateral central vision loss associated with degeneration of the retinal ganglion cell layer and the optic nerve (Howell, 1998), is linked to mitochondrial complex I dysfunction (Brown et al., 1992). Complex I, also known as nicotinamide adenine dinucleotide (NADH)-quinone oxidoreductase, is the first and the largest complex of the mitochondrial respiratory chain. It catalyzes the reduction of NADH to ubiquinone (coenzyme Q) (Schapira, 1998). Complex I is more susceptible to oxidative inactivation following exposure to free radicals than other mitochondrial enzymatic complexes such as cytochrome c oxidase (Zhang et al., 1990).

Rotenone is a naturally occurring and widely used pesticide that inhibits the ability of mitochondrial complex I to transfer electrons to coenzyme Q (Degli Esposti,

1998; Lindahl and Oberg, 1961; Singer and Ramsay, 1994). Thus, studies with rotenone may provide clues to the environmental role of pesticides in optic neuropathy and neurodegenerative diseases linked to mitochondrial dysfunction (Betarbet et al., 2000). A dysfunctional mitochondrial electron transport chain decreases ATP production and accelerates the generation of free radicals leading to cell death (Gonzalez-Lima et al., 1998; Beal, 1998)

Methylene blue (MB) is an oxidation-reduction (redox) agent previously used safely in humans as an antidote for certain metabolic poisons (Bradberry, 2003; Clifton and Leikin, 2003) as well as a neuroprotective agent for treatment of drug-induced encephalopathy, dementia and manic-depressive psychosis (Naylor et al., 1986; Kupfer et al., 1996; Wainwright and Crossley, 2002). MB can prevent the formation of superoxide (Kelner et al., 1988; Salaris et al., 1991) and nitric oxide (Mayer et al., 1993) in mitochondria. An early study by Lindahl and Oberg (1961) suggested that MB may be effective in reversing the effects of rotenone. They demonstrated that exposure of intact and excised gill filaments to rotenone induced a decreased oxygen consumption, and addition of MB reduced the inhibition of oxygen uptake caused by rotenone after excision (Lindahl and Oberg, 1961). Therefore, MB may act therapeutically as an antioxidant in experimental optic neuropathy and perhaps other forms of neurodegenerative diseases characterized by inhibition of mitochondrial complex I.

We previously investigated the neurodegenerative effects of rotenone on the retina of mice injected with rotenone in one eye and the vehicle dimethylsulfoxide (DMSO) in the contralateral eye as a within-subject control. We found that the retinal

ganglion cell layer of eyes injected with rotenone became significantly thinner than that of the control eyes after 24 h (Zhang et al., 2002). The objective of the present study was to test the hypothesis that the antioxidant MB may protect the retina from the neurodegeneration caused by rotenone in this experimental optic neuropathy model (Zhang et al., 2002).

5.3 MATERIALS AND METHODS

5.3.1 Subjects

Male CBA/J mice (average weight 29 g) (Jackson Laboratory, Bar Harbor, ME) were used. All experimental procedures were approved by the Institutional Animal Care and Use Committee of the University of Texas at Austin.

5.3.2 Surgery

The mice were anesthetized by an intraperitoneal injection of a mixture of ketamine hydrochloride (45 mg/kg), xylazine hydrochloride (9 mg/kg), and acepromazine (1.5 mg/kg). Intravitreal microinjections were performed by an experienced ophthalmologist (X. Zhang) using a stereomicroscope and microinjection system. A small sclerotomy was performed using a fine needle (30-G) inserted just behind the limbus of the cornea in the superior and temporal quadrant of the eye to give access to the vitreous body. The microinjection was done immediately underneath the corneoscleral junction with a blunt needle to avoid the lens and the retina. The 30-G blunt-ended dental injection needles (Monoject®, Sherwood Medical Company, Norfolk, NE) were connected by polyethylene tubing to 10-µl Hamilton

microsyringes (Hamilton Company, Reno, NV). The injections were delivered over 2 min using a microinjection pump (CMA microdialysis AB, North Chelmsford, MA), and the injection needles were left in place for an additional 40 sec to allow for diffusion away from the needle tip and to avoid any efflux of fluid through the injection site. The edges of the injection point were gripped with forceps while the microsyringe was slowly withdrawn. Then a small amount of n-butyl cyanoacrylate monomer (Nexaband liquid tissue adhesive, Veterinary Products Laboratories, Phoenix) was applied on the surface of the sclera at the injection point to form a sealed thin layer.

5.3.3 Drug treatments

Methylene blue was purchased from Faulding Pharmaceutical Co., Paramus, NJ. All other chemicals were purchased from Sigma-Aldrich, St. Louis, MO. One eye of each mouse was intravitreally microinjected with 0.5 μl of DMSO, rotenone, or with MB/rotenone. The 0.2 mg/kg rotenone dose we used was based on our previous study, in which we compared rotenone doses of 0.065, 0.1 and 0.2 mg/kg, and found that 0.2 mg/kg produced thickness reduction of the ganglion cell layer and the inner plexiform layer without nonspecific reduction of the rest of the retina (Zhang et al., 2002). The rotenone dose we used is low compared to doses used in another model of rotenone-induced neurodegeneration in the nigrostriatal pathway. Sherer et al. (Sherer et al., 2003) used rotenone doses of 2-3 mg/kg/day given subcutaneously for 28 or 56 days. The single intravitreal 0.2 mg/kg dose we used is unlikely to have nonspecific

systemic effects because it is ten times or more lower than the doses of rotenone used chronically by others to induce nigrostriatal neurodegeneration.

To the best of our knowledge, no reactions between rotenone and methylene blue have been reported based on a literature search in Chemical Abstracts Service and Medline database from 1907-2004. To rule out the possibility that rotenone and methylene blue might react, we mixed 100 µl methylene blue (0.406 mg/ml) with 100 µl rotenone (6.15 mg/ml), at half the concentrations used in the experiments, with acetonitrile and ethanol as the solvent. The mixture was allowed to sit at room temperature, and 10 µL of the mixture was taken out and injected in HPLC at 0, 10, 20, 30, and 60 min, respectively. The results showed clearly that no reactions occurred (spectra not shown). Therefore, tests using HPLC further ruled out the possibility that they might react.

The LD_{50} of MB for mice is 77 mg/kg i.v. (United States National Toxicology Program, 1990). The non-toxic MB doses chosen were approximately 1,000 times, 10,000 times and 100,000 times smaller than this LD_{50} dose. Hence, in the MB dose-response study, the three doses of MB added into rotenone were 0.07 mg/kg, 0.007 mg/kg, and 0.0007 mg/kg. The most effective neuroprotective MB dose of 0.07 mg/kg was used for the Nissl study to compare cell counts after rotenone alone or rotenone plus MB. The control eye received the same volume and rate of the vehicle DMSO as a within-subject control. Mice were decapitated 24 h after drug treatment. The eyeballs were rapidly removed, frozen in isopentane, and sectioned antero-posteriorly at 30 µm in a cryostat (Reichert-Jung, Germany) at -18^{o}C. Three adjacent series were created for histochemical analysis.

5.3.4 Histology

5.3.4.1 Complex I staining

To determine if the ganglion cell layer (GCL) thickness changed after the addition of MB to the rotenone, a series of sections was stained for complex I activity following a well-established histochemistry procedure using tetrazolium salts (Jung et al., 2002). By accepting hydrogen released from the substrate NADH through complex I enzymatic action, tetrazolium salts are reduced to highly colored water-insoluble microcrystalline deposits (see Chapter 2 for details). Briefly, fresh-frozen sections were incubated at 37^{o}C for 15-20 min with agitation in phosphate buffer containing NADH (Sigma, 1 mg/ml), nitroblue tetrazolium (Sigma, 1.33 mg/ml), and sodium azide (Sigma, 0.065 mg/ml) (Zhang et al., 2002).

5.3.4.2 Nissl staining

To confirm that the GCL thickness and cell number changed after the addition of MB to rotenone, and to verify that the thickness change was not simply due to the loss of the stain in complex I staining, another series of sections was stained with cresyl violet and used for thickness and cell count measures in the GCL. The cresyl violet staining procedure consisted of dehydration of the fresh-frozen tissue sections followed by staining (0.1% cresyl violet, 6-10 min) and dehydration in a series of ethanols (70-100%). Slides were then cleared in xylene and coverslipped with Permount.

5.3.4.3 Cytochrome oxidase (complex IV) staining

Cytochrome oxidase is the third and final proton-pumping protein of the electron transport chain in mitochondria. It plays a vital role in oxidative phosphorylation, in which electrons are accepted by oxygen to produce water, and the proton gradient is used by ATP synthase to produce ATP. Cytochrome oxidase activity is closely correlated to neuronal activity and oxygen consumption, and it is a reliable marker for long-term neuronal activity (Gonzalez-Lima and Cada, 1998; Nobrega et al., 1993; Wong-Riley, 1989).

Quantitative cytochrome oxidase histochemistry measurements were taken to determine the effect of rotenone and MB/rotenone on neuronal activity and oxygen consumption in the retina. Since the ganglion cell layer is difficult to define on the retina with cytochrome oxidase staining, samples were taken in the inner plexiform layer (IPL) and the optic nerve, which contain mostly the dendrites of ganglion cells, and the neurites of bipolar cells and amacrine cells. Using previously described procedures (Gonzalez-Lima and Cada, 1994; Gonzalez-Lima and Jones, 1994; Gonzalez-Lima et al., 1997; Gonzalez-Lima and Cada, 1998), a series of retinal fresh-frozen sections was treated in 10% sucrose phosphate buffer containing 0.5% glutaraldehyde for five min. After three changes at five min each of 10% phosphate buffer, the slides were preincubated for 10 min in Tris buffer (275 mg/l cobalt chloride, 10% sucrose, and 0.5% DMSO). After another rinse in phosphate buffer, the slides were then incubated at 37^{o}C for 90 min in 700 ml of an oxygen saturated solution containing 350 mg of diaminobenzidine tetrahydrochloride, 52.5 mg of cytochrome c, 35 g of sucrose, 14 mg of catalase, and 1.75 ml of DMSO in phosphate

buffer. The reaction was stopped and the tissue was fixed by immersing the slides in 10% glutaraldehyde for 30 min, before dehydrating gradually in ethanols, clearing in xylene, and coverslipping with Permount.

5.3.5 Measurements

Thickness was measured in the GCL using a computerized micro-imaging system consisting of an Olympus BX40 microscope with a 40x objective (Olympus America; Lake Success, NY), a CCD camera (Javelin Electronics; Torrance, CA), a Targa M8 image capture board and JAVA imaging software (Jandel Scientific; Corte Madera, CA). The Nissl stain revealed only somata of the GCL while the complex I stain also labeled the GCL neuropil. Therefore the nerve fiber layer on the inner side of the GCL was included in the complex I GCL thickness measurement.

Cell count in the GCL was measured with a 60x oil immersion objective at a final magnification of 1200, using the Neurolucida system (version 5 MicroBrightField, Williston, VT, USA). An unbiased optical dissector stereological method was applied; that is, any cells present on the top of the section were not counted. Because there was a decreased thickness of GCL in rotenone treated eyes (Zhang et al., 2002), cell number was counted in 3-dimensions as number of cells per length of the cross section of GCL and per thickness of the section on the slide, which is equal to cell counts per unit area of the retinal surface.

Quantitative cytochrome oxidase histochemistry measurements were taken using the same imaging setup as for the Nissl staining study (see above) to evaluate

the effects of rotenone and MB/rotenone on energy demand in the dendrites (IPL) and axons (optic nerve) of the ganglion cells.

To avoid the effect of retinal thickness by location, data were taken from the center of the retina at a distance of approximately twice the diameter of the optic disc away from its center. In the mouse retina, most of the cells in GCL are retinal ganglion cells concentrated in the center. Other cells in GCL are small glial cells and displaced amacrine cells. The displaced amacrine cells are concentrated in the periphery of the mouse retina rather than the center (Drager and Olsen, 1981). No effort was made to distinguish the retinal ganglion cells from other cells in the GCL. However, the purpose of taking the data from the center of the retina was to minimize the likelihood of counting the displaced amacrine cells and also to maintain the consistency of comparison throughout the subjects.

5.3.6. Statistical analysis

For the MB dose-response study, a between-groups one way ANOVA test with multiple comparisons and Bonferroni correction was used to evaluate GCL thickness in all groups, namely DMSO, rotenone alone, and rotenone plus three doses of MB. The “n” equals number of eyes.

To test the significance of within-subject differences in GCL thickness and cell counts between the experimental eye (treated with rotenone or rotenone plus MB 0.07 mg/kg) and the vehicle DMSO-treated control eye, paired t-tests were used with paired samples from both eyes of each subject. The “n” equals number of mice with pairs of treated and control eyes.

Repeated measures ANOVA were used to analyze cytochrome oxidase activity in the two groups. The "n" equals number of pairs of eyes. Mann-Whitney U-tests were used to test the percent differences from control in cytochrome oxidase activity of rotenone and MB/rotenone groups in IPL and optic nerve. All tests used a two-tailed $p < 0.05$ as criterion for significant differences.

5.4 RESULTS

Microscopic examination of the retina stained with complex I or cresyl violet indicated that MB treatment reduced the thinning and cell death in GCL caused by rotenone. Figure 5.1 provides examples of cresyl violet-stained sections, showing that eyes treated with MB plus rotenone did not have the same degree of thinning in the GCL seen in the eyes treated with rotenone alone.

Figure 5.1 Cross section of the retina with cresyl violet staining in DMSO (vehicle), rotenone (0.2 mg/kg), and MB (0.07 mg/kg) plus rotenone (0.2 mg/kg) treated eyes at 24 h post-injection time. The thickness of the ganglion cell layer (GCL) is shown in each group (arrows). The bar length equals 50 microns.

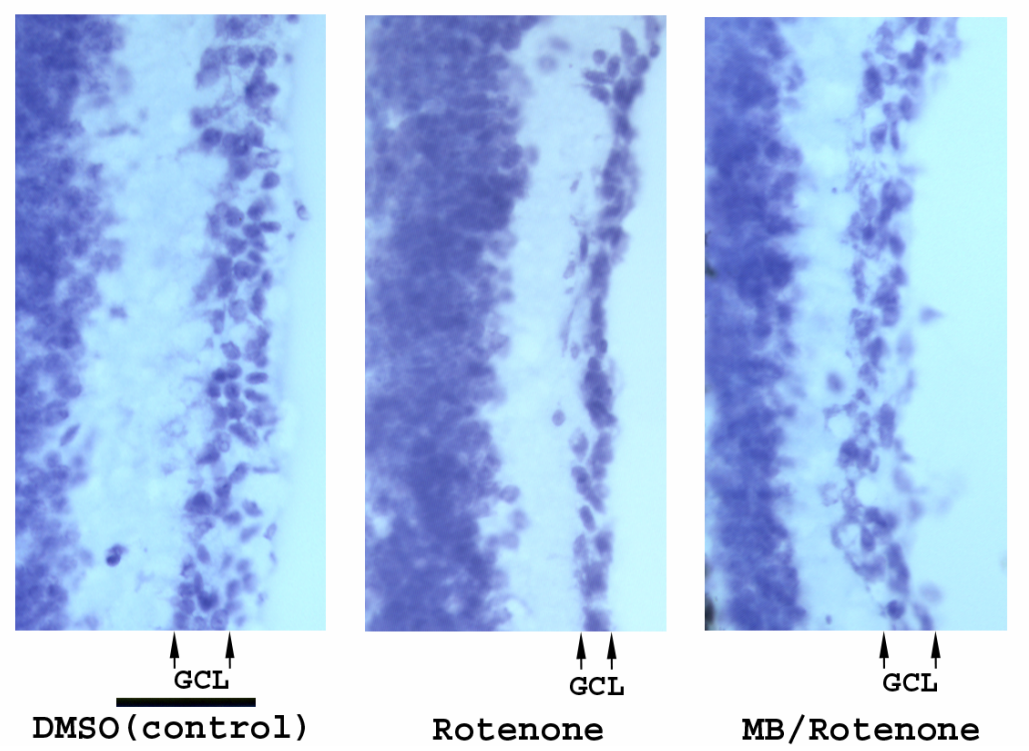

Figure 5.2 shows that rotenone-induced neurodegeneration was reduced in a dose-dependent manner by addition of MB as indicated by the GCL thickness. There was a highly significant group difference due to MB treatment ($F(4, 66) = 11.29$, $p = 6.05 \times 10^{-7}$). Individual group contrasts showed that the rotenone alone group had significant GCL reductions as compared to rotenone with the two higher MB doses ($p = 0.004$ and $p = 0.00008$, respectively). The lowest MB dose was ineffective because this group was not significantly different from the rotenone alone group ($p = 1$), and it still showed a significant GCL reduction as compared to the DMSO controls ($p = 0.014$). The GCL measures of GCL thickness of rotenone with the two higher MB doses, however, were not different from those in DMSO control eyes ($p = 1$). The

observations in each MB dose indicated that the higher doses of MB completely prevented the GCL reduction caused by rotenone.

Figure 5.2 Thickness (mean ± standard error bars) in the ganglion cell layer (GCL) of DMSO, rotenone (0.2 mg/kg) alone, and rotenone with three MB doses at 24 h post-injection time. * $p < 0.05$ compared to DMSO or MB/rotenone with MB at 0.007 mg/kg or 0.07 mg/kg. Sections stained for complex I.

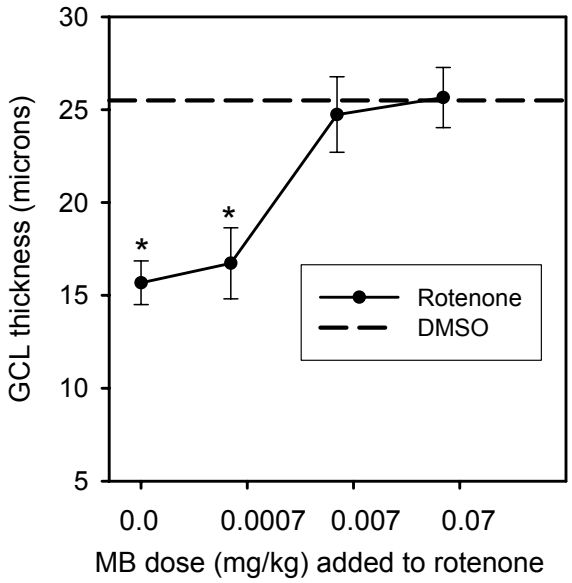

In addition to complex I staining, the neuroprotective action of the most effective MB dose was quantified using morphometric analysis of GCL thickness and stereological cell counts using routine cresyl violet staining. Figure 5.3A shows that

the thickness of the retinal GCL of the rotenone treated eyes was significantly reduced (paired t-test, n = 15, p = 0.01) compared to that of the DMSO control eyes. In contrast, in the eyes treated with rotenone plus MB 0.07 mg/kg there were no significant differences in GCL thickness as compared to the control eyes (paired t-test, n = 12, p = 0.21).

The number of cells in the GCL was also reduced by 23% in the rotenone treated eyes (paired t-test, n = 6, p = 0.03, Figure 5.3B). Cell numbers in the GCL were not different between the MB/rotenone and the DMSO treated eyes (paired t-test, n = 12, p = 0.85).

Figure 5.3 Thickness (A) and cell number (B) (mean ± standard error bars) in the ganglion cell layer (GCL) of DMSO (control), rotenone (0.2 mg/kg), and rotenone with MB (0.07 mg/kg) treated eyes at 24 h post-injection time. * $p < 0.05$ as compared to DMSO or MB/Rotenone groups. Sections stained with cresyl violet.

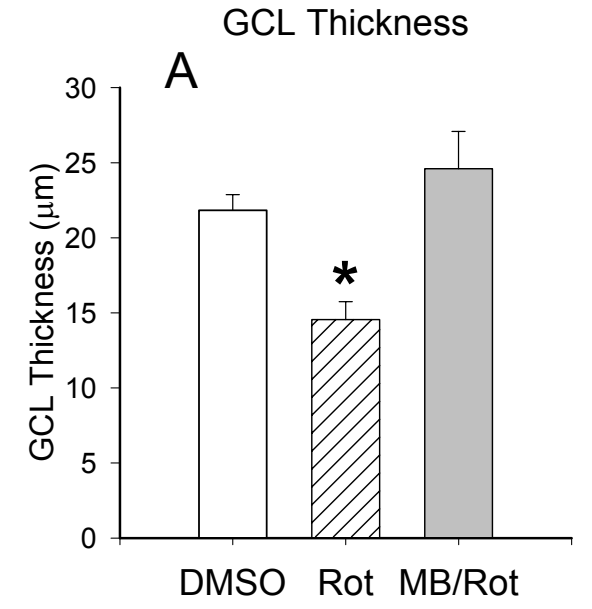
GCL Thickness
A
GCL Thickness (μm)
30
25
20
15
10
5
0
*
DMSO
Rot
MB/Rot

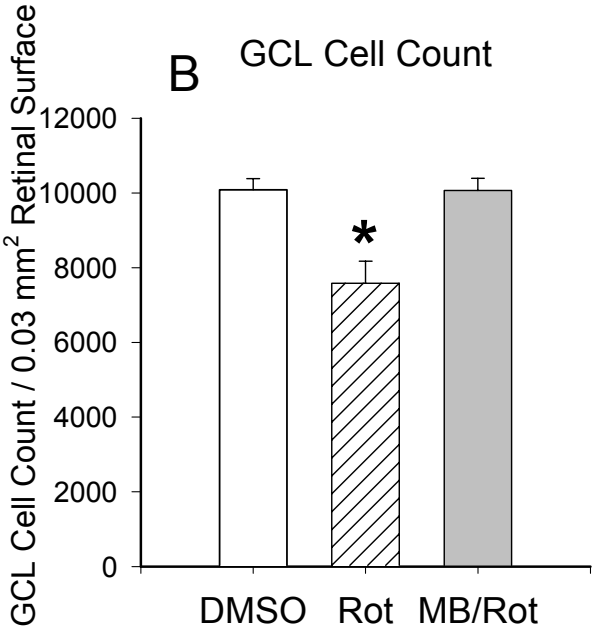
B
GCL Cell Count
GCL Cell Count / 0.03 mm2 Retinal Surface
12000
10000
8000
6000
4000
2000
0
*
DMSO
Rot
MB/Rot

Quantitative cytochrome oxidase histochemistry data in the IPL and the optic nerve showed that there was not a significant difference (rotenone or MB/rotenone) by group interaction in cellular oxygen consumption, but significantly higher cytochrome oxidase activity was detected in both the rotenone and MB/rotenone treated eyes as compared to their control eyes (repeated measures ANOVA, $n = 18$, $p = 0.036$ in the IPL; $n = 18$, $p = 0.01$ in the optic nerve). For the rotenone-treated eyes, cytochrome oxidase activity in the IPL showed an 18% increase, while the optic nerve showed a 51% increase. In the MB/rotenone treated eyes, the IPL showed a 22% increase and the optic nerve showed a 37% increase. Mann-Whitney U-tests showed that these percent increases in cytochrome oxidase activity in the experimental eyes were similar in rotenone and MB/rotenone groups in both the IPL ($n = 25$, $p = 0.8$) and optic nerve ($n = 25$, $p = 0.7$), indicating that both treatments produced similar increases in cytochrome oxidase activity.

5.5 DISCUSSION

The neurodegeneration caused by rotenone in the GCL has been shown previously in our model of optic neuropathy (Zhang et al., 2002), and it was confirmed in the present study by using two different stains (complex I and Nissl stains), and both layer thickness and stereological cell counts as measures. All eyes were microinjected with the same drug volume and thus the results produced by the different drug treatments are unlikely to be due to differences in compression of the GCL from intraocular injection. Thus, it is unlikely that the effects of rotenone on GCL are nonspecific or are due to a particular staining or measurement artifact.

Most importantly, the present study is the first to demonstrate that MB is effective in preventing GCL neurodegeneration (cell loss and layer thinning) following rotenone administration. The dose-response data indicated the potential of the higher MB dose to prevent ganglion cell degeneration, which was verified with cell counts using unbiased stereological methods. The highest MB dose we used (0.07 mg/kg) was 1,000 times lower than the LD_{50} of MB for mice (77 mg/kg i.v.), suggesting that we worked with non-toxic MB doses.

MB is an FDA-approved drug that has been used effectively as an antidote for certain metabolic poisons without significant side effects at doses of 1-2 mg/kg (Clifton and Leikin, 2003). MB has also been used as a neuroprotective agent in drug-induced encephalopathy, dementia and manic-depressive psychosis (Naylor et al., 1986; Kupfer et al., 1996; Wainwright and Crossley, 2002). Behaviorally, studies by Martinez et al. (1978) showed that MB (1 mg/kg, i.p.) given immediately after avoidance conditioning enhanced memory retention 24 h later. We have found that the same dose of MB reverses spatial memory deficits produced by sodium azide, an inhibitor of mitochondrial complex IV (Callaway et al., 2002). There is also enhanced memory retention in a food-search task in MB-treated rats relative to untreated controls 24 h after MB administration (Callaway et al., 2004).

MB's protective metabolic function has been documented to act through two main pharmacological mechanisms. One mechanism involves improving oxygen consumption and the other is related to its powerful antioxidant effects. MB acts as a redox agent that increases mitochondrial respiration by shuttling electrons to oxygen in the electron transport chain, resulting in elevated cellular oxygen consumption

(Callaway et al., 2004; Lindahl and Oberg, 1961; Visarius et al., 1997). MB has also been found to increase oxygen consumption on gill filaments pretreated with rotenone (Lindahl and Oberg, 1961).

One major antioxidant action of MB is that it inhibits superoxide, the most abundant oxygen radical generated *in vivo*, by accepting electrons from tissue oxidases (Kelner et al., 1988; Salaris et al., 1991). Another antioxidant action of MB is due to its inhibition of nitric oxide synthesis (Mayer et al., 1993). Nitric oxide can form the damaging peroxynitrite after reacting with superoxide. Therefore, MB administration could be very effective in preventing mitochondrial oxidative damage leading to neurodegeneration (Gonzalez-Lima et al., 1998).

In the current study and in our previous study (Zhang et al., 2002), rotenone stimulated cytochrome oxidase activity in the regions where the neuropil of the retinal ganglion cells reside (IPL and optic nerve), and rotenone induced neuronal death in the GCL after 24 h of administration (Zhang et al., 2002). The observed increase in cytochrome oxidase activity may be explained by a mechanism of excitotoxicity induced by rotenone in the retina. Excitotoxicity occurs when neurons are placed under adverse metabolic conditions such as exposure to certain toxins and increased levels of glutamate and oxidative stress (Coyle and Puttfarcken, 1993; Choi, 1988; Beal, 1998; Lafon-Cazal et al., 1993; Gunasekar et al., 1995; Lafon-Cazal et al., 1993).

An antioxidant interpretation of MB therapeutic action is consistent with other studies of toxin-induced inhibition of complex I. Inhibition of complex I by MPP^+ or rotenone produces neurodegeneration in the striatum (Sherer et al., 2003).

Interestingly, complex I inhibition caused by MPP^+ is blocked by antioxidants such as glutathione, catalase and ascorbate, implicating an antioxidant therapeutic mechanism (Cleeter et al., 1992). Further studies are needed to investigate the mechanisms of the neuroprotective action of MB on rotenone-induced neurodegeneration.

In summary, MB is remarkably effective in preventing ganglion cell neurodegeneration caused by rotenone. This protective effect may be mediated through the antioxidant action of MB to prevent mitochondrial oxidative damage and excitotoxic cell death. The present results suggest that MB should be further investigated as a potential therapeutic agent to prevent neurodegeneration caused by mitochondrial dysfunction in diseases such as Leber's optic neuropathy, Parkinson's disease, Huntington's disease, and Alzheimer's disease.

Acknowledgements

We thank Dr. Theresa A. Jones for her help with the stereological cell counts.

5.6. REFERENCES

Beal MF (1998) Mitochondrial dysfunction in neurodegenerative diseases. *Biochimi et Biophys Acta (BBA) - Bioenergetics* 1366: 211-223.

Betarbet R, Sherer TB, MacKenzie G, Garcia-Osuna M, Panov AV, Greenamyre JT (2000) Chronic systemic pesticide exposure reproduces features of Parkinson's disease. *Nat Neurosci* 3: 1301-1306.

Bradberry SM (2003) Occupational methaemoglobinaemia. Mechanisms of production, features, diagnosis and management including the use of methylene blue. *Toxicol Rev* 22: 13-27.

Brown MD, Voljavec AS, Lott MT, MacDonald I, Wallace DC (1992) Leber's hereditary optic neuropathy: A model for mitochondrial neurodegenerative diseases. *FASEB J* 6: 2791-2799.

Callaway NL, Riha PD, Bruchey AK, Munshi Z, Gonzalez-Lima F (2004) Methylene blue improves brain oxidative metabolism and memory retention in rats. *Pharmacol Biochem and Behav* 77: 175-181.

Callaway NL, Riha PD, Wrubel KM, McCollum D, Gonzalez-Lima F (2002) Methylene blue restores spatial memory retention impaired by an inhibitor of cytochrome oxidase in rats. *Neurosci Lett* 332: 83-86.

Choi DW (1988) Glutamate neurotoxicity and diseases of the nervous system. *Neuron* 1: 623-634.

Cleeter MW, Cooper JM, Schapira AH (1992) Irreversible inhibition of mitochondrial complex I by 1-methyl-4-phenylpyridinium: Evidence for free radical involvement. *J Neurochem* 58: 786-789.

Clifton J, Leikin JB (2003) Methylene blue. *Am J Ther* 10: 289-291.

Coyle JT, Puttfarcken P (1993) Oxidative stress, glutamate, and neurodegenerative disorders. *Science* 262: 689-695.

Degli Esposti M (1998) Inhibitors of NADH-ubiquinone reductase: an overview. *Biochimi et Biophys Acta (BBA) - Bioenergetics* 1364: 222-235.

Drager UC, Olsen JF (1981) Ganglion cell distribution in the retina of the mouse. *Invest Ophthalmol Vis Sci* 20: 285-293.

Gonzalez-Lima F, Cada A (1994) Cytochrome oxidase activity in the auditory system of the mouse: A qualitative and quantitative histochemical study. *Neuroscience* 63: 559-578.

Gonzalez-Lima F, Cada A (1998) Quantitative histochemistry of cytochrome oxidase activity. In: Cytochrome oxidase in neuronal metabolism and Alzheimer's disease (Gonzalez-Lima F, ed), pp 55-90. New York: Plenum Press.

Gonzalez-Lima F, Jones D (1994) Quantitative mapping of cytochrome oxidase activity in the central auditory system of the gerbil: a study with calibrated activity standards and metal-intensified histochemistry. *Brain Res* 660: 34-49.

Gonzalez-Lima F, Valla J, Jorandby L (1998) Cytochrome oxidase inhibition in Alzheimer's disease. In: Cytochrome oxidase in neuronal metabolism and Alzheimer's disease (Gonzalez-Lima F, ed), pp 171-200. New York: Plenum Press.

Gonzalez-Lima F, Valla J, Matos-Collazo S (1997) Quantitative cytochemistry of cytochrome oxidase and cellular morphometry of the human inferior colliculus in control and Alzheimer's patients. *Brain Res* 752: 117-126.

Gunasekar PG, Kanthasamy AG, Borowitz JL, Isom GE (1995) NMDA Receptor Activation Produces Concurrent Generation of Nitric Oxide and Reactive Oxygen Species: Implications for Cell Death. *J Neurochem* 65: 2016-2021.

Howell N (1998) Leber hereditary optic neuropathy: Respiratory chain dysfunction and degeneration of the optic nerve. *Vision Res* 38: 1495-1504.

Jung C, Higgins CMJ, Xu Z (2002) A quantitative histochemical assay for activities of mitochondrial electron transport chain complexes in mouse spinal cord sections. *J Neurosci Methods* 114: 165-172.

Kelner MJ, Bagnell R, Hale B, Alexander NM (1988) Potential of methylene blue to block oxygen radical generation in reperfusion injury. *Basic Life Sci* 49: 895-898.

Kupfer A, Aeschlimann C, Cerny T (1996) Methylene blue and the neurotoxic mechanisms of ifosfamide encephalopathy. *Eur J Clin Pharmacol* 50: 249-252.

Lafon-Cazal M, Pietri S, Culcasi M, Bockaert J (1993) NMDA-dependent superoxide production and neurotoxicity. *Nature* 364: 535-537.

Lindahl PE, Oberg KE (1961) The effect of rotenone on respiration and its point of attack. *Exptl Cell Research* 23: 228.

Martinez JLJr, Jensen RA, Vasquez BJ, McGuinness T, McGaugh JL (1978) Methylene blue alters retention of inhibitory avoidance responses. *Physiol Psychol* 6: 387-390.

Mayer B, Brunner F, Schmidt K (1993) Inhibition of nitric oxide synthesis by methylene blue. *Biochem Pharmacol* 45: 367-374.

Naylor GJ, Maton B, Hopwood SE, Watson Y (1986) A two-year double-blind crossover trial of the prophylactic effect of methylene blue in manic-depressive psychosis. *Biol Psychiatry* 21: 915-920.

Nobrega J, Raymond R, DiStefano L, Burnham WM (1993) Long-term changes in regional brain cytochrome oxidase activity induced by electroconvulsive treatment in rats. *Brain Res* 605: 1-8.

Salaris SC, Babbs CF, Voorhees III (1991) Methylene blue as an inhibitor of superoxide generation by xanthine oxidase: A potential new drug for the attenuation of ischemia/reperfusion injury. *Biochem Pharmacol* 42: 499-506.

Schapira AHV (1998) Human complex I defects in neurodegenerative diseases. *Biochimi et Biophys Acta (BBA) - Bioenergetics* 1364: 261-270.

Sherer TB, Kim JH, Betarbet R, Greenamyre JT (2003) Subcutaneous rotenone exposure causes highly selective dopaminergic degeneration and [alpha]-synuclein aggregation. *Exp Neurol* 179: 9-16.

Singer TP, Ramsay RR (1994) The reaction sites of rotenone and ubiquinone with mitochondrial NADH dehydrogenase. *Biochimi et Biophys Acta (BBA) - Bioenergetics* 1187: 198-202.

United States National Toxicology Program. (1990) Chemical Status Report. NTP Chemtrack System.

Valla J, Chen K, Berndt JD, Gonzalez-Lima F, Cherry SR, Games D, Reiman EM (2002) Effects of image resolution on autoradiographic measurements of posterior cingulate activity in PDAPP mice: implications for functional nrain

imaging studies of transgenic mouse models of Alzheimer's disease. *NeuroImage* 16: 1-6.

Visarius TM, Stucki JW, Bernhard H (1997) Stimulation of respiration by methylene blue in rat liver mitochondria. *FEBS Letters* 412: 157-160.

Wainwright M, Crossley KB (2002) Methylene Blue--a therapeutic dye for all seasons? *J Chemother* 14: 431-443.

Wong-Riley MT (1989) Cytochrome oxidase: an endogenous metabolic marker for neuronal activity. *Trends Neurosci* 12: 94-101.

Zhang X, Jones D, Gonzalez-Lima F (2002) Mouse model of optic neuropathy caused by mitochondrial complex I dysfunction. *Neurosci Lett* 326: 97-100.

Zhang Y, Marcillat O, Giulivi C, Ernster L, Davies KJ (1990) The oxidative inactivation of mitochondrial electron transport chain components and ATPase. *J Biol Chem* 265: 16330-16336.

Chapter 6: General Discussion and Future Directions

6.1 GENERAL DISCUSSION

Increasing evidence has suggested that the mitochondrion is a critical player in the life and death of neurons. Neurodegenerative diseases have been closely linked to the dysfunction of mitochondrial respiratory chain components, among which mitochondrial complex I (NADH dehydrogenase) is ranked first in many respects. It is the first enzyme of the respiratory chain, catalyzing the electron transfer from NADH to coenzyme Q and generating ubiquinol. It is the most complicated of the respiratory complexes, both in terms of protein structure and of genetics. It is the largest mitochondrial complex, consisting of 43 distinct protein subunits. It has the most (seven) mtDNA encoded subunits, while complex III, IV, and ATP synthase only have 1, 3, and 2 respectively (Genova et al., 2004). The daunting complexity of complex I suggests that complex I may be more susceptible to environmental or genetic insults than other mitochondrial complexes. This might explain the phenomenon that a wide variety of neurodegenerative diseases are associated with complex I dysfunction; these include Leber's hereditary optic neuropathy (LHON), Parkinson's disease, and dystonia (Schapira, 1998). Among them, LHON has been recognized as a model disease for mitochondrial neurodegenerative diseases (Brown et al., 1992).

A mouse model of optic neuropathy caused by mitochondrial complex I dysfunction was successfully created, as a part of this dissertation study, to help fulfill the need to develop effective *in vivo* animal models for exploring the underlying mechanisms and treatments for neurodegenerative diseases (Zhang et al., 2002). A

single intravitreal administration of rotenone, a complex I inhibitor, in mice started reducing the retinal ganglion cell layer (GCL) between 0.5-1 h without significantly affecting the rest of the retina. The maximum reduction in GCL thickness apparent in complex I staining was around 40% at 24 h following injection. The reduction was observed with both complex I histochemistry and with cresyl violet staining. The thickness of the retinal nerve fiber layer (RNFL) was reduced by 89% and the number of GCL cells was reduced by 21% (cell profile counts, experiment in Chapter 3) and 23% (unbiased stereological cell counts, experiment in Chapter 5) in rotenone-treated eyes. There was a relative reduction in the proportion of larger cells, while no overall cellular morphometric changes (soma area, perimeter, and diameter) were observed. Therefore, the reduction in GCL thickness 24 h after rotenone microinjection could be accounted for by cell loss and nerve fiber shrinkage, but not by overall soma size change. The preferential loss of the larger ganglion cells has been reported in Alzheimer's disease (Sadun and Bassi, 1990). It has also been seen in glaucoma (Quigley et al., 1988) and optic neuropathy induced by intravitreal injection of NMDA (N-methyl-D-aspartate) (Dreyer et al., 1994), both of which may be associated with ischemia and excitotoxicity. Excitotoxicity is a process of cell death in the nervous system due to overactivation of the glutamate receptors. The degeneration in the nerve fiber layer and the retinal ganglion cell layer in our model is consistent with the degeneration of retinal ganglion cells in Leber's hereditary optic neuropathy. This is the first animal model of optic neuropathy resulting from mitochondrial dysfunction, and it could be used as an efficient and convenient way to test new treatments for mitochondrial neurodegenerative diseases.

Our first therapeutic intervention in this optic neuropathy model was to test the hypothesis that methylene blue, as an antioxidant, may be protective against rotenone-induced neurodegeneration. Methylene blue is a reduction–oxidation agent that can act as a powerful antioxidant, preventing formation of mitochondrial oxygen free radicals by acting as an electron sink. The neurodegeneration in the retinal ganglion cell layer observed 24 h after rotenone injection was completely prevented by the injection of methylene blue along with rotenone, as indicated by both the thickness and cell numbers of the retinal ganglion cell layer. The effect of rotenone and rotenone plus methylene blue was investigated using two types of histological stains, complex I and Nissl, and two measurements, morphometric layer thickness and non-biased stereological cell counts. The protective effect of methylene blue appeared to be related to its antioxidant action because cytochrome oxidase activity was similarly elevated in both rotenone and rotenone plus methylene blue groups. It was concluded that methylene blue may be a promising therapeutic agent in optic neuropathy and perhaps other neurodegenerative diseases caused by mitochondrial dysfunction.

Rotenone and MB can act at two levels, within the cells and in the interaction between the cells. In the intracellular level, rotenone will decrease oxygen consumption by inhibiting the respiratory chain, resulting in increased free radicals mostly coming from superoxide generation. Administration of MB enhances oxygen consumption while at the same time act as an antioxidant, preventing oxidative damage and cell death.

In addition, rotenone may produce excitotoxicity through neuronal circuit mechanism, in which MB may also be protective as a powerful antioxidant. Figure 6.1

shows a schematic diagram of the proposed circuit mechanism of action of rotenone and MB in the retina. Visual information flow in the retina is through the neurotransmitter glutamate from the bipolar cells to the ganglion cells. Amacrine cells modulate this bipolar-ganglion cell pathway in the IPL. Rotenone has been shown to decrease the release of GABA in the striatum by intrastriatal injection (Brouillet et al., 1994). It is possible that the release of GABA also reduced in response to intravitreal rotenone injection, which results in relatively elevated excitatory input to the ganglion cell from the bipolar cell, leading to excitotoxic cell death of the ganglion cells. In addition, amacrine cells are particularly sensitive to excitotoxicity because they express receptors for glutamate released from bipolar cells (Duarte et al., 1998). Since the inhibitory neurotransmitter -aminobutyric acid (GABA) is the major transmitter released from amacrine cells, impairment of amacrine cells by excitotoxicity may reduce the inhibitory input from GABA on the ganglion cells. This will further decrease the release of GABA and form a feed-forward cycle to facilitate excitotoxicity. The resulting metabolic overactivation of ganglion cells, as indicated by cytochrome oxidase activity in the IPL and optic nerve, may lead to excitotoxic death of ganglion cells through apoptosis (Chen et al., 2001; Choi, 1995; Mattson, 2003). Excitotoxicity, triggered by excessive activation of glutamate receptors, has been postulated as a mechanism of neuronal death in a number of neurodegenerative disorders, such as Alzheimer’s, Parkinson’s, and Huntington's diseases (Choi, 1988; Coyle and Puttfarcken, 1993), as well as some eye diseases such as glaucoma and ischemic/hypoxic attack (Dreyer et al., 1996).

Figure 6.1 Proposed mechanism of the retinal ganglion cell death caused by rotenone and the protection by MB. Bipolar cells release glutamate to the amacrine and ganglion cells. Rotenone administration impairs amacrine cells which secrete the inhibitory neurotransmitter GABA. Without the modulation of GABA, the ganglion cells show glutamate-induced over-activity as reflected by increased cytochrome oxidase activity. The antioxidant action of MB may prevent the oxidative damage that leads to excitotoxic cell death. IPL: inner plexiform layer. ⟶: Excitatory output. ⟙: Inhibitory output.

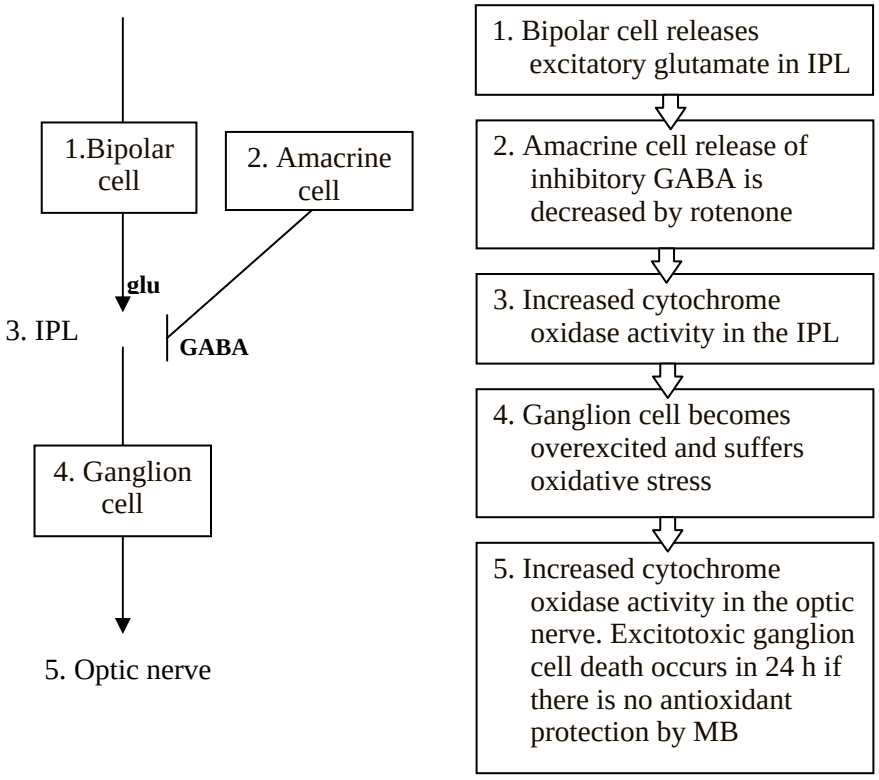

In our study, MB may have acted as an antioxidant to prevent oxidative damage because rotenone and MB/rotenone treated eyes showed similar enhancement of cytochrome oxidase activity. A similar level of cytochrome oxidase activity implies a similar level of mitochondrial respiration and oxidative stress (Gonzalez-Lima et al., 1998). MB effectively inhibits the production of superoxide, nitric oxide and hydroxyl radical (Kelner et al., 1988; Mayer et al., 1993). Complex I is particularly susceptible to inhibition by these free radicals (Zhang et al., 1990), which could aggravate the inhibition caused by rotenone. This suggests that in this rotenone-induced optic neuropathy, the neuroprotective action of MB may involve its antioxidant action to prevent oxidative damage and excitotoxic cell death.

6.2 FUTURE DIRECTIONS: MORE THERAPEUTIC INTERVENTIONS

6.2.1 Pharmacological approach: Anti-glutamatergic agent memantine

Excitotoxicity is implicated in the pathophysiology of a wide variety of neurodegenerative diseases (Lipton and Rosenberg, 1994). It is induced at least in part by excessive activation of glutamate receptors (presumably the NMDA subtype) (Waxman and Lynch, 2005). When stimulated, the channel in the receptor opens and a large amount of Ca^{2+} flows into the neurons resulting in Ca^{2+} overload in the mitochondria. This, in turn, triggers a cascade of processes that can lead to apoptosis, a type of programmed cell death. High concentration of intracellular Ca^{2+} may activate calcium-dependent proteases and phospholipases that can destroy protein and lipid components of the cell, and may produce reactive oxygen species that are toxic to the cell. For example, Ca^{2+}-dependent activation of nitric oxide synthase increases nitric

oxide production and the formation of toxic peroxynitrite; activation of certain protein kinases and transcription factors can further cause neuronal injury in the nucleus and eventually, cell death (Bonfoco et al., 1995; Budd et al., 2000; Dawson et al., 1993).

A large amount of work has indicated the therapeutic effects of anti-excitatory agents, which block the activation of the glutamate receptors, on neurodegenerative diseases (Le and Lipton, 2001; Hynd et al., 2004; Palmer, 2001). However, the side effects of traditional anti-excitatory drugs are usually severe, ranging from drowsiness to coma (Hickenbottom and Grotta, 1998; Le and Lipton, 2001). Glutamate is the most common excitatory neurotransmitter that is widely distributed in the nervous system. It is essential for normal neuronal activities, though it is also detrimental when it is present in excessive amounts. Traditional anti-glutamatergic drugs are competitive antagonists, competing one for one with the agonist of the receptor (glutamate or glycine). They actually block normal, lower activation of the receptors before they can block pathological state with high levels of the agonists. Therefore, ideal anti-excitotoxicity drugs should block only excessive activation of the glutamate receptors while sparing the normal neuronal transmission of the receptors.

Memantine (1-amino-3,5-dimethyladamantane) is a drug that has such features. It is a derivative of amantadine, which is used in treating influenza and sometimes, Parkinson's disease. It is a non-competitive open-channel (acts only when channel is open) NMDA receptor antagonist. Lipton (2003) reported that the degree of its blocking increases while the concentration of NMDA increases to pathological levels, which is the typical feature of a non-competitive antagonist. The binding site of memantine to the receptor is near the Mg^{2+} site, which, taken together with its non-

competitive antagonist behavior, suggests that it only blocks NMDA receptor activity when the channel is open long enough for it to enter the channel, and the agonist is present in excessive amounts; both occur at pathological levels. This is supported by its clinical safety profile (Lipton, 1993). Memantine has been shown to reduce neuronal cell death and to be protective for neurons, including retinal ganglion cells in many recent *in vitro* and *in vivo* studies (Osborne, 1999; Schuettauf et al., 2002; Tremblay et al., 2000; Lipton, 2003; Hare et al., 2001). For example, Hare et al. (2001) reported that memantine-treated glaucoma eyes suffered significantly less reduction of visually-evoked cortical potential (VECP) amplitude (at a dose of 4 mg/kg/day, orally, for 15 months in monkeys) and significant reduction in glaucoma-induced loss of retinal ganglion cells in rats (administered at 10 mg/kg/day, subcutaneous osmotic pump, for 3 weeks) when compared to control eyes.

Figure 6.2 Molecular structure of memantine (1-amino-3,5-dimethyladamantane).

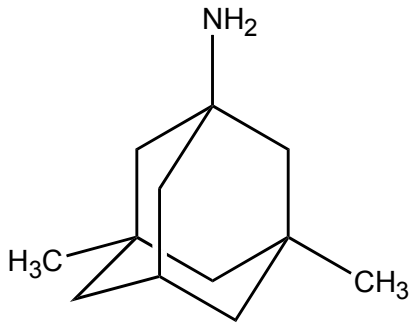

Because excitotoxicity is implicated in our animal model of neurodegeneration in the retina (see Chapter 5), anti-glutamatergic agents should also be of benefit to the treatment of neurodegeneration induced by rotenone in the GCL. We hypothesize that administration of memantine alone or in combination with methylene blue in the rotenone treated eye may prevent rotenone-generated retinal ganglion cell death.

6.2.2 Non-pharmacological approach: Near infrared light with light-emitting diode

Near infrared light (NIR) (wavelength range 630-900 nm) has been shown to promote wound healing in human and animal studies (Sommer et al., 2001; Yu et al., 1997; Conlan et al., 1996). Low intensity is the key to this therapy because the photochemical conversion prevails over the heat-generation of the energy absorbed by a photoacceptor. Light-emitting diodes (LED) and lasers are two types of devices producing near infrared light that have been used in therapeutic wound healing studies. However, the LED has more beneficial features compared to the laser. Unlike the laser, the LED generates light with longer wavelengths that can penetrate deeper into tissue; the LED does not generate significant heat, and therefore does not cause thermal injuries; also, the LED is more compact and more affordable. For these reasons, the LED has achieved FDA non-significant risk (NSR) status as a therapeutic device (Eells et al., 2004).

The mechanisms of the therapeutic action of NIR has been postulated to be associated with initial stimulation of cytochrome c oxidase activity (complex IV of mitochondrial respiratory chain) (Wong-Riley et al., 2004; Wong-Riley et al., 2001). The stimulation of cytochrome c oxidase triggers the activation of a signaling cascade

which promotes cellular proliferation and cytoprotection, including the activation of genes, transcription factors, elevated protein, growth factors and ATP synthesis (Wong-Riley et al., 2001; Karu, 1999; Eells et al., 2004; Mochizuki-Oda et al., 2002). Eells et al. (2004) reported that three brief (2 min 24 s) 670 nm LED treatments (4 J/cm^2) significantly reduced the retinal and optic nerve toxicities induced by methanol-derived formate using their rat model of methanol intoxication. We propose that the LED treatment may ameliorate compensatory effects to complex I dysfunction by promoting complex IV activity and the cascade of events that may protect against neurodegeneration induced by rotenone toxicity. Our optic neuropathy model using control and rotenone-treated eyes is ideally suited to test the efficacy of these potential therapeutic interventions.

6.3 REFERENCES

Bonfoco E, Krainc D, Ankarcrona M, et al. (1995) Apoptosis and necrosis: two distinct events induced respectively by mild and intense insults with NMDA or nitric oxide/superoxide in cortical cell cultures. *Proc Natl Acad Sci USA* 92: 7162-7166.

Brouillet E, Henshaw DR, Schulz JB, Beal MF (1994) Aminooxyacetic acid striatal lesions attenuated by 1,3-butanediol and coenzyme Q10. *Neurosci Lett* 177: 58-62.

Brown MD, Voljavec AS, Lott MT, MacDonald I, Wallace DC (1992) Leber's hereditary optic neuropathy: A model for mitochondrial neurodegenerative diseases. *FASEB J* 6: 2791-2799.

Budd SL, Tenneti L, Lishnak T, Lipton SA (2000) Mitochondrial and extramitochondrial apoptotic signaling pathways in cerebrocortical neurons. *Proc Natl Acad Sci USA* 97: 6161-6166.

Chen TA, Yang F, Cole GM, Chan SO (2001) Inhibition of caspase-3-like activity reduces glutamate induced cell death in adult rat retina1. *Brain Res* 904: 177-188.

Choi DW (1988) Glutamate neurotoxicity and diseases of the nervous system. *Neuron* 1: 623-634.

Choi DW (1995) Calcium: still center-stage in hypoxic-ischemic neuronal death. *Trend Neurosci* 18: 58-60.

Conlan MJ, Rapley JW, Cobb CM (1996) Biostimulation of Wound Healing by Low-Energy Laser Irradiation. *J Clin Periodont* 23: 492-496.

Coyle JT, Puttfarcken P (1993) Oxidative stress, glutamate, and neurodegenerative disorders. *Science* 262: 689-695.

Dawson VL, Dawson TM, Bartley DA (1993) Mechanisms of nitric oxide-mediated neurotoxicity in primary brain cultures. *J Neurosci* 13: 2651-2661.

Dreyer EB, Pan ZH, Storm S, Lipton SA (1994) Greater sensitivity of larger retinal ganglion cells to NMDA-mediated cell death. *NeuroReport* 5: 629-631.

Dreyer EB, Zurakowski D, Schumer RA, Podos SM, Lipton SA (1996) Elevated glutamate levels in the vitreous body of humans and monkeys with glaucoma. *Arch Ophthalmol* 114: 299-305.

Duarte CB, Ferreira IL, Santos PF, Carvalho AL, Agostinho PM, Carvalho AP (1998) Glutamate in Life and Death of Retinal Amacrine Cells. *Gen Pharmacol* 30: 289-295.

Eells JT, Wong-Riley MTT, VerHoeve J, Henry M, Buchman EV, Kane MP, Gould LJ, Das R, Jett M, Hodgson BD (2004) Mitochondrial signal transduction in accelerated wound and retinal healing by near-infrared light therapy. *Mitochondrion* 4: 559-567.

Genova ML, Pich MM, Bernacchia A, Bianchi C, Biondi A, Bovina C, Falasca AI, Formiggini G, Castelli GP, Lenaz G (2004) The Mitochondrial Production of Reactive Oxygen Species in Relation to Aging and Pathology. *Ann NY Acad Sci* 1011: 86-100.

Gonzalez-Lima F, Valla J, Jorandby L (1998) Cytochrome oxidase inhibition in Alzheimer's disease. In: Cytochrome oxidase in neuronal metabolism and

Alzheimer's disease (Gonzalez-Lima F, ed), pp 171-200. New York: Plenum Press.

Hare W, WoldeMussie E, Lai R, Ton H, Ruiz G, Feldmann B, Wijono M, Chun T, Wheeler L (2001) Efficacy and safety of Memantine, an NMDA-Type open-channel Blocker, for reduction of retinal injury associated with experimental glaucoma in rat and monkey. *Survey of Ophthalmology* 45: S284-S289.

Hickenbottom SL, Grotta J (1998) Neuroprotective therapy. *Semin Neurol* 18: 485-492.

Hynd MR, Scott HL, Dodd PR (2004) Glutamate-mediated excitotoxicity and neurodegeneration in Alzheimer's disease. *Neurochemistry International* 45: 583-595.

Karu T (1999) Primary and secondary mechanisms of action of visible to near-IR radiation on cells. *Journal of Photochemistry and Photobiology B: Biology* 49: 1-17.

Kelner MJ, Bagnell R, Hale B, Alexander NM (1988) Potential of methylene blue to block oxygen radical generation in reperfusion injury. *Basic Life Sci* 49: 895-898.

Le DA, Lipton SA (2001) Potential and current use of N-methyld-aspartate (NMDA) receptor antagonists in diseases of aging. *Drugs Aging* 18: 717-724.

Lipton SA (1993) Prospects for clinically tolerated NMDA antagonists: open-channel blockers and alternative redox states of nitric oxide. *Trends Neurosci* 16: 527-532.

Lipton SA (2003) Possible role for memantine in protecting retinal ganglion cells from glaucomatous damage. *Surv Ophthalmol* 48: S38-46.

Lipton SA, Rosenberg PA (1994) Excitatory Amino Acids as a Final Common Pathway for Neurologic Disorders. *N Engl J Med* 330: 613-622.

Mattson MP (2003) Excitotoxic and excitoprotective mechanisms: abundant targets for the prevention and treatment of neurodegenerative disorders. *Neuromolecular Med* 3: 65-94.

Mayer B, Brunner F, Schmidt K (1993) Inhibition of nitric oxide synthesis by methylene blue. *Biochem Pharmacol* 45: 367-374.

Mochizuki-Oda N, Kataoka Y, Cui Y, Yamada H, Heya M, Awazu K (2002) Effects of near-infra-red laser irradiation on adenosine triphosphate and adenosine diphosphate contents of rat brain tissue. *Neurosci Lett* 323: 207-210.

Osborne NN (1999) Memantine reduces alterations to the mammalian retina, *in situ*, induced by ischemia. *Vis Neurosci* 16: 45-52.

Palmer GC (2001) Neuroprotection by NMDA receptor antagonists in a variety of neuropathologies. *Curr Drug Targets* 2.

Quigley HA, Dunkelberger GR, Green WR (1988) Chronic human glaucoma causing selectively greater loss of large optic nerve fibers. *Ophthalmology* 95: 357-363.

Sadun AA, Bassi CJ (1990) Optic nerve damage in Alzheimer's disease. *Ophthalmology* 97: 9-17.

Schapira AHV (1998) Human complex I defects in neurodegenerative diseases. *Biochimi et Biophys Acta (BBA) - Bioenergetics* 1364: 261-270.

Schuettauf F, Quinto K, Naskar R, Zurakowski D (2002) Effects of anti-glaucoma medications on gangion cell survival: the DBA/2J mouse model. *Vision Res* 42: 2333-2337.

Sommer AP, Pinheiro ALB, Mester AR, Franke RP, Whelan HT (2001) Biostimulatory windows in low intensity laser activation: lasers, scanners and NASA's light emitting diode array system. *J Clin Laser Med Surg* 19: 29-33.

Tremblay R, Chakravarthy B, Hewitt K, Tauskela J, Morley P, Atkinson T, Durkin JP (2000) Transient NMDA Receptor Inactivation Provides Long-Term Protection to Cultured Cortical Neurons from a Variety of Death Signals. *The Journal of Neuroscience* 20: 7183-7192.

Waxman EA, Lynch DR (2005) N-methyl-D-aspartate Receptor Subtypes: Multiple Roles in Excitotoxicity and Neurological Disease. *Neuroscientist* 11: 37-49.

Wong-Riley MTT, Bai X, Buchmann E, Whelan HT (2001) Light-emitting diode treatment reverses the effect of TTX on cytochrome oxidase in neurons. *NeuroReport* 12: 3033-3037.

Wong-Riley MTT, Liang HL, Eells JT, Chance B, Henry MM, Buchmann E, Kane M, Whelan HT (2004) Photobiomodulation directly benefits primary neurons functionally inactivated by toxins: Role of cytochrome c oxidase. *J Biol Chem* M409650200.

Yu W, Naim JO, Lanzafame RJ (1997) Effects of Photostimulation on Wound Healing in Diabetic Mice. *Lasers Surg Med* 20: 56-63.

Zhang X, Jones D, Gonzalez-Lima F (2002) Mouse model of optic neuropathy caused by mitochondrial complex I dysfunction. *Neurosci Lett* 326: 97-100.

Zhang Y, Marcillat O, Giulivi C, Ernster L, Davies KJ (1990) The oxidative inactivation of mitochondrial electron transport chain components and ATPase. *J Biol Chem* 265: 16330-16336.

APPENDIX: Protocol of mitochondrial complex I histochemistry

Make (or check) the solutions the day before staining:

- 0.2 M phosphate buffer (PB), 3 L

  Add 3 L of ddH_2O to a 4 L flask,

  Add 56.8 g of anhydrous dibasic-sodium phosphate (fw = 141.96),

  Add 27.6 g of monobasic-sodium phosphate (fw = 137.99),

  Stir until dissolved and filter if necessary,

  Adjust pH to 7.6,

  Refrigerate

- 0.1 M phosphate buffer, 1.5 L

  Add 0.75 L 0.2 M PB to a 1.5 L flask,

  Add 0.75 L ddH_2O,

  Stir and refrigerate

- 10%w/v sucrose PB solution, 4 L

  Add 2 L of 0.2 M PB to a 6 L flask,

  Add 400 g of sucrose (fw = 342.31),

  Add 2 L ddH_2O,

  Stir until dissolved, and then keep refrigerated,

- 0.5% glutaraldehyde in 10% sucrose PB (The glutaraldehyde stock is 25%. Keep glutaraldehyde solution in the refrigerator until needed. Mix new solution for each batch.)

	0.5% glutaraldehyde (ml)	25% glutaraldehyde (ml)	10% Sucrose buffer (ml)
11 – 50 slides	700 =	14	686
10 slides	250 =	5	245
< 8 slides	100 =	2	98

- Ethanols (30%, 50%, 70%, 90%, 95%, 100%) and formalin (10%); Alcohols must made 24 h before use.

Procedure of the day of staining:

1. Prepare NBT solution (incubation solution):

   Set incubator temperature to 37°C and place glassware inside,

   Heat 0.1 M PB in the microwave to approximately 36°C (700 ml/ 1.5 min), then add below corresponding ingredients quickly as the NBT is light sensitive.

	Concentration (mg/ml)	700 ml/ <50 slices	250 ml/ 10 slices	70 ml/ 8 slices
PB(0.1M)		700 ml	250 ml	70 ml
NBT	1.33	933.33 mg	332.5 mg	93.33 mg
Sodium azide	0.065	45.5 mg	16.25 mg	4.55 mg
NADH (N8129, sigma, FW 709.4)	1 (=1.4mM)	700 mg	250 mg	70 mg

Cover to shield from light and stir slowly (at about 270 RPM) until reaching 36°C. Pour into glassware in oven (Make sure everything is dissolved!) after filter the solution.

2. Prepare fresh frozen tissue sections and place slides in racks.
3. Remove 0.5% glutaraldehyde in 10% sucrose PB from refrigerator, and lower slide racks in very slowly and gently, 5 min.
4. 10% sucrose PB, 3 changes, 5 min each: pour all just before step 3 ends so that each is subsequently warmer.
5. 0.1 M PB rinse, 5 min, at room temperature.
6. Incubate in NBT solution: Incubate with NBT solution at 37 °C in a dark oven, 25 min (30-60 min).
7. 0.1 M PB rinse, 5 min, at room temperature.
8. Fix tissue: Transfer slide rack to 10% formalin, 30 min.
9. Dehydrate: Dehydration bath of 30, 50, 70, 90, 95 (2 changes), 100% (2 changes) ethanol, 5 min each.

10. Clear and coverslip: Xylene (3 changes), 5 min each. Coverslip slides with Permount; dry for 24 h (keep from sunlight)

Bibliography

Andrews RM, Griffiths PG, Johnson MA, Turnbull DM (1999) Histochemical localisation of mitochondrial enzyme activity in human optic nerve and retina. *Br J Ophthalmol* 83: 231-235.

Bailey SM, Pietsch EC, Cunningham CC (1999) Ethanol stimulates the production of reactive oxygen species at mitochondrial complexes I and III. *Free Radical Biology and Medicine* 27: 891-900.

Barber DA, Rubin JW, Zumbro GL, and Tackett RL. (1995) The use of methylene blue as an extravascular surgical marker impairs vascular responses of human saphenous veins. *Journal of thoracic and cardiovascular surgery* 109: 21-29.

Barrientos A, Moraes CT (1999) Titrating the effects of mitochondrial complex I impairment in the cell physiology. *J Biol Chem* 274: 16188-16197.

Barry MA, Halsell CB, Whitehead MC (1993) Organization of the nucleus of the solitary tract in the hamster: acetylcholinesterase, NADH dehydrogenase, and cytochrome oxidase histochemistry. *Microscopy research and technique* 26: 231-244.

Beal MF, Brouillet E, Jenkins BG, Ferrante RJ, Kowall NQ, Miller JM, Storey E, Srivastava R, Rosen BR, and Hyman BT. (1993a) Neurochemical and histologic characterization of excitotoxic lesions produced by the mitochondrial toxin 3-nitropropionic acid. *J.Neurosci.* 13: 4192.

Beal MF, Brouillet E, Jenkins BG, Henshaw R, Rosen B, and Hyman BT. (1993b) Age-dependent striatal excitotoxic lesions produced by the endogenous mitochondrial inhibitor malonate. *J.Neurochem.* 61: 1147-1150.

Beal MF, Howell N, Bodis-Wollner I (1997) Mitochondria and free radicals in neurodegenerative diseases. New York: Wiley-Liss.

Beal MF (1998) Mitochondrial dysfunction in neurodegenerative diseases. *Biochimi et Biophys Acta (BBA) - Bioenergetics* 1366: 211-223.

Bear MF, Connors BW, Pardiso MA (2005) The eye. In: Neuroscience: Exploring the Brain, 2nd Edition pp 281-312. Lippincott Williams & Wilkins.

Bennett MC, Rose GM (1992) Chronic sodium azide treatment impairs learning of the Morris water maze task. *Behav Neural Biol* 58: 72-75.

Berndt JD, Callaway NL, Gonzalez-Lima F (2001) Effects of chronic sodium azide on brain and muscle cytochrome oxidase activity: A potential model to investigate environmental contributions to neurodegenerative diseases. *Journal of Toxicology and Environmental Health - Part A* 63: 67-77.

Besch D, Leo-Kottler B, Zrenner E, Wissinger B (1999) Leber's hereditary optic neuropathy: Clinical and molecular genetic findings in a patient with a new mutation in the ND6 gene. *Graefe's Archive for Clinical and Experimental Ophthalmology* 237: 745-752.

Betarbet R, Sherer TB, MacKenzie G, Garcia-Osuna M, Panov AV, Greenamyre JT (2000) Chronic systemic pesticide exposure reproduces features of Parkinson's disease. *Nat Neurosci* 3: 1301-1306.

Bodansky O, Gutmann H (1947) Treatment of methemoglobinemia. *J Pharmacol* 46-56.

Bonfoco E, Krainc D, Ankarcrona M, et al. (1995) Apoptosis and necrosis: two distinct events induced respectively by mild and intense insults with NMDA or nitric oxide/superoxide in cortical cell cultures. *Proc Natl Acad Sci USA* 92: 7162-7166.

Bradberry SM (2003) Occupational methaemoglobinaemia. Mechanisms of production, features, diagnosis and management including the use of methylene blue. *Toxicol Rev* 22: 13-27.

Brouillet E, Henshaw DR, Schulz JB, Beal MF (1994) Aminooxyacetic acid striatal lesions attenuated by 1,3-butanediol and coenzyme Q10. *Neurosci Lett* 177: 58-62.

Brown MD, Voljavec AS, Lott MT, MacDonald I, Wallace DC (1992) Leber's hereditary optic neuropathy: A model for mitochondrial neurodegenerative diseases. *FASEB J* 6: 2791-2799.

Brown MD, Wallace DC (1994) Spectrum of mitochondrial DNA mutations in Leber's hereditary optic neuropathy. *Clin Neurosci* 138-145.

Brown MD (1999) The enigmatic relationship between mitochondrial dysfunction and Leber's hereditary optic neuropathy. *Journal of the Neurological Sciences* 165: 1-5.

Budd SL, Tenneti L, Lishnak T, Lipton SA (2000) Mitochondrial and extramitochondrial apoptotic signaling pathways in cerebrocortical neurons. *Proc Natl Acad Sci USA* 97: 6161-6166.

Callaway NL, Riha PD, Bruchey AK, Munshi Z, Gonzalez-Lima F (2004) Methylene blue improves brain oxidative metabolism and memory retention in rats. *Pharmacol Biochem and Behav* 77: 175-181.

Callaway NL, Riha PD, Wrubel KM, McCollum D, Gonzalez-Lima F (2002) Methylene blue restores spatial memory retention impaired by an inhibitor of cytochrome oxidase in rats. *Neurosci Lett* 332: 83-86.

Carelli V, Ross-Cisneros FN, Sadun AA (2002) Optic nerve degeneration and mitochondrial dysfunction: genetic and acquired optic neuropathies. *Neurochemistry International* 40: 573-584.

Chen TA, Yang F, Cole GM, Chan SO (2001) Inhibition of caspase-3-like activity reduces glutamate induced cell death in adult rat retina1. *Brain Res* 904: 177-188.

Choi DW (1988) Glutamate neurotoxicity and diseases of the nervous system. *Neuron* 1: 623-634.

Choi DW (1995) Calcium: still center-stage in hypoxic-ischemic neuronal death. *Trend Neurosci* 18: 58-60.

Cleeter MW, Cooper JM, Schapira AH (1992) Irreversible inhibition of mitochondrial complex I by 1-methyl-4-phenylpyridinium: Evidence for free radical involvement. *J Neurochem* 58: 786-789.

Clifton J, Leikin JB (2003) Methylene blue. *Am J Ther* 10: 289-291.

Conlan MJ, Rapley JW, Cobb CM (1996) Biostimulation of Wound Healing by Low-Energy Laser Irradiation. *J Clin Periodont* 23: 492-496.

Coyle JT, Puttfarcken P (1993) Oxidative stress, glutamate, and neurodegenerative disorders. *Science* 262: 689-695.

Dawson VL, Dawson TM, Bartley DA (1993) Mechanisms of nitric oxide-mediated neurotoxicity in primary brain cultures. *J Neurosci* 13: 2651-2661.

Degli Esposti M (1998) Inhibitors of NADH-ubiquinone reductase: an overview. *Biochimi et Biophys Acta (BBA) - Bioenergetics* 1364: 222-235.

Derom AF, Wallaert PC, Janzing HM, Derom FE (1993) Intraoperative identification of parathyroid glands with methylene blue infusion. *Am J Surg* 165: 380-382.

DiMauro S. (2001) Lessons from mitochondrial DNA mutations. *Cell & Developmental Biology* 9: 397-405.

Dowling JE (1987) The retina: an approachable part of the brain. Belknap Press.

Drager UC, Olsen JF (1981) Ganglion cell distribution in the retina of the mouse. *Invest Ophthalmol Vis Sci* 20: 285-293.

Dreyer EB, Pan ZH, Storm S, Lipton SA (1994) Greater sensitivity of larger retinal ganglion cells to NMDA-mediated cell death. *NeuroReport* 5: 629-631.

Dreyer EB, Zurakowski D, Schumer RA, Podos SM, Lipton SA (1996) Elevated glutamate levels in the vitreous body of humans and monkeys with glaucoma. *Arch Ophthalmol* 114: 299-305.

Duarte CB, Ferreira IL, Santos PF, Carvalho AL, Agostinho PM, Carvalho AP (1998) Glutamate in Life and Death of Retinal Amacrine Cells. *Gen Pharmacol* 30: 289-295.

Eells JT, Wong-Riley MTT, VerHoeve J, Henry M, Buchman EV, Kane MP, Gould LJ, Das R, Jett M, Hodgson BD (2004) Mitochondrial signal transduction in accelerated wound and retinal healing by near-infrared light therapy. *Mitochondrion* 4: 559-567.

Ernster L, Dallner G, Azzone GG (1963) Differential effects of rotenone and amytal on mitochondrial electron and energy transfer. *J Biol Chem* 238: 1124-1131.

Ernster L, Jalling O, Low H, Lindberg O (1955) Alternative pathways of mitochondrial DPNH oxidation, studied with amytal. *Exptl Cell Res Suppl* 3: 124-132.

Etteldorf JN (1951) Methylene blue in the treatment of methemoglobinemia in premature infants caused by marking ink; a report of eight cases. *J Pediatr* 38: 24-27.

Ferrante RJ, Schulz JB, Kowall NW, Beal MF (1997) Systemic administration of rotenone produces selective damage in the striatum and globus pallidus, but not in the substantia nigra. *Brain Res* 753: 157-162.

Floyd RA, Schneider J, Dittmer DP (2004) Methylene blue photoinactivation of RNA viruses. *Antiviral Research* 61: 141-151.

Genova ML, Pich MM, Bernacchia A, Bianchi C, Biondi A, Bovina C, Falasca AI, Formiggini G, Castelli GP, Lenaz G (2004) The Mitochondrial Production of Reactive Oxygen Species in Relation to Aging and Pathology. *Ann NY Acad Sci* 1011: 86-100.

Gonzalez-Lima F, Cada A (1994) Cytochrome oxidase activity in the auditory system of the mouse: A qualitative and quantitative histochemical study. *Neuroscience* 63: 559-578.

Gonzalez-Lima F, Cada A (1998) Quantitative histochemistry of cytochrome oxidase activity. In: Cytochrome oxidase in neuronal metabolism and Alzheimer's disease (Gonzalez-Lima F, ed), pp 55-90. New York: Plenum Press.

Gonzalez-Lima F, Jones D (1994) Quantitative mapping of cytochrome oxidase activity in the central auditory system of the gerbil: a study with calibrated activity standards and metal-intensified histochemistry. *Brain Res* 660: 34-49.

Gonzalez-Lima F, Valla J, Jorandby L (1998) Cytochrome oxidase inhibition in Alzheimer's disease. In: Cytochrome oxidase in neuronal metabolism and Alzheimer's disease (Gonzalez-Lima F, ed), pp 171-200. New York: Plenum Press.

Gonzalez-Lima F, Valla J, Matos-Collazo S (1997) Quantitative cytochemistry of cytochrome oxidase and cellular morphometry of the human inferior colliculus in control and Alzheimer's patients. *Brain Res* 752: 117-126.

Greenamyre JT, Sherer TB, Betarbet R, Panov AV (2001) Complex I and Parkinson's disease. *IUBMB Life* 52: 135-141.

Gunasekar PG, Kanthasamy AG, Borowitz JL, Isom GE (1995) NMDA Receptor Activation Produces Concurrent Generation of Nitric Oxide and Reactive Oxygen Species: Implications for Cell Death. *J Neurochem* 65: 2016-2021.

Gyllensten U, Wharton D, Josefsson A, and Wilson AC. (1991) Paternal inheritance of mitochondrial DNA in mice. *Nature* 352: 255-257.

Hare W, WoldeMussie E, Lai R, Ton H, Ruiz G, Feldmann B, Wijono M, Chun T, Wheeler L (2001) Efficacy and safety of Memantine, an NMDA-Type open-channel Blocker, for reduction of retinal injury associated with experimental glaucoma in rat and monkey. *Survey of Ophthalmology* 45: S284-S289.

Hassan HM, Fridovich I (1979) Intracellular production of superoxide radical and of hydrogen peroxide by redox active compounds. *Archives of Biochemistry and Biophysics* 196: 385-395.

Hatefi Y (1985) The mitochondrial electron transport and oxidative phosphorylation system. *Annual Review of Biochemistry* 54: 1015-1069.

Heikkila RE, Nicklas WN, Vyas I, Duvoisin RC (1986) Dopaminergic toxicity of rotenone and the 1-methyl-4-phenylpyridinium ion after their stereotaxic administration to rats: implication for the mechanism of 1-methyl-4-phenyl-1,2,3,6,-tetrahydropyridine toxicity. *Neurosci Lett* **62**: 389-394.

Hickenbottom SL, Grotta J (1998) Neuroprotective therapy. *Semin Neurol* 18: 485-492.

Howell N, Mackey DA (1998) Low-penetrance branches in matrilineal pedigrees with leber hereditary optic neuropathy [2]. *American Journal of Human Genetics* 63: 1220-1224.

Howell N (1998) Leber hereditary optic neuropathy: Respiratory chain dysfunction and degeneration of the optic nerve. *Vision Res* 38: 1495-1504.

Hoyer PE, Lyon H (1991) Enzyme Histochemistry III: Oxidoreductases. In: Theory and Strategy in Histochemistry (Lyon H, ed), pp 337-364. Germany: Springer Verlag.

Hynd MR, Scott HL, Dodd PR (2004) Glutamate-mediated excitotoxicity and neurodegeneration in Alzheimer's disease. *Neurochemistry International* 45: 583-595.

Isenberg JS, Klaunig JE (2000) Role of the mitochondrial membrane permeability transition (MPT) in rotenone-induced apoptosis in liver cells. *Toxicol Sci* 53: 340-351.

Javitch JA, D'Amato RJ, Strittmatter SM, Snyder SH (1985) Parkinsonism-inducing neurotoxin, N-methyl-4-phenyl-1,2,3,6 -tetrahydropyridine: uptake of the metabolite N-methyl-4-phenylpyridine by dopamine neurons explains selective toxicity. *Proc Natl Acad Sci U S A* 82: 2173-2177.

Jeon C-J, Strettoi E, Masland RH (1998) The major cell populations of the mouse retina. *The Journal of Neuroscience* 18: 8936-8946.

Jung C, Higgins CMJ, Xu Z (2002) A quantitative histochemical assay for activities of mitochondrial electron transport chain complexes in mouse spinal cord sections. *J Neurosci Methods* 114: 165-172.

Kageyama GH, Wong-Riley MTT (1984) The histochemical localization of cytochrome oxidase in the retina and lateral geniculate nucleus of the ferret, cat, and monkey, with particular reference to retinal mosaics and on/off-center visual channels. *J Neurosci* 4: 2445-2459.

Karu T (1999) Primary and secondary mechanisms of action of visible to near-IR radiation on cells. *Journal of Photochemistry and Photobiology B: Biology* 49: 1-17.

Kelner MJ, Bagnell R, Hale B, Alexander NM (1988) Potential of methylene blue to block oxygen radical generation in reperfusion injury. *Basic Life Sci* 49: 895-898.

Kugler P (1982) Quantitative dehydrogenase histochemistry with exogenous electron carriers (PNS, MPMS, MB). *Histochemistry* 93: 537-540.

Kupfer A, Aeschlimann C, Cerny T (1996) Methylene blue and the neurotoxic mechanisms of ifosfamide encephalopathy. *Eur J Clin Pharmacol* 50: 249-252.

Kupfer A, Aeschlimann C, Wermuth B, Cerny T (1994) Prophylaxis and reversal of ifosfamide encephalopathy with methylene-blue. *Lancet* 343: 763-764.

Lafon-Cazal M, Pietri S, Culcasi M, Bockaert J (1993) NMDA-dependent superoxide production and neurotoxicity. *Nature* 364: 535-537.

Le DA, Lipton SA (2001) Potential and current use of N-methyld-aspartate (NMDA) receptor antagonists in diseases of aging. *Drugs Aging* 18: 717-724.

Lindahl PE, Oberg KE (1961) The effect of rotenone on respiration and its point of attack. *Exptl Cell Research* 23: 228.

Lipton SA (1993) Prospects for clinically tolerated NMDA antagonists: open-channel blockers and alternative redox states of nitric oxide. *Trends Neurosci* 16: 527-532.

Lipton SA (2003) Possible role for memantine in protecting retinal ganglion cells from glaucomatous damage. *Surv Ophthalmol* 48: S38-46.

Lipton SA, Rosenberg PA (1994) Excitatory Amino Acids as a Final Common Pathway for Neurologic Disorders. *N Engl J Med* 330: 613-622.

Luft R (1994) The development of mitochondrial medicine. *Proc Natl Acad Sci* 91: 8731-8738.

Luft R, Ikkos D, Paknueru G, Ernster L, Afzelius B (1962) A case of severe hypermetabolism of nonthyroid origin with a defect in the maintenance of mitochondrial respiratory control: a correlated clinical, biochemical, and morphological study. *J Clin Invest* 41: 1776--1804.

Manfredi G, Beal MF (2005) Poison and antidote: A novel model to study pathogenesis and therapy of LHON. *Annals of Neurology* 56: 171-172.

Manhes H, Shulman A, Haag T, Canis M, Demontmarin JL (2004) Infertility due to diseased pelvic peritoneum: laparoscopic treatment. *Gynecol Obstet Invest* 37: 191-195.

Martinez JLJr, Jensen RA, Vasquez BJ, McGuinness T, McGaugh JL (1978) Methylene blue alters retention of inhibitory avoidance responses. *Physiol Psychol* 6: 387-390.

Mattson MP (2003) Excitotoxic and excitoprotective mechanisms: abundant targets for the prevention and treatment of neurodegenerative disorders. *Neuromolecular Med* 3: 65-94.

Mayer B, Brunner F, Schmidt K (1993) Inhibition of nitric oxide synthesis by methylene blue. *Biochem Pharmacol* 45: 367-374.

Mochizuki-Oda N, Kataoka Y, Cui Y, Yamada H, Heya M, Awazu K (2002) Effects of near-infra-red laser irradiation on adenosine triphosphate and adenosine diphosphate contents of rat brain tissue. *Neurosci Lett* 323: 207-210.

Murray GI, Burke MD, Ewen SWB (1988) Enzyme histochemical demonstration of NADH dehydrogenase on resin-embedded tissue. *The Journal of Histochemistry and Cytochemistry* 36: 815-819.

Nagatsu T (2002) Amine-related neurotoxins in Parkinson's disease: Past, present, and future. *Neurotoxicol Teratol* 24: 565-569.

Naylor GJ, Maton B, Hopwood SE, Watson Y (1986) A two-year double-blind crossover trial of the prophylactic effect of methylene blue in manic-depressive psychosis. *Biol Psychiatry* 21: 915-920.

Nobrega J, Raymond R, DiStefano L, Burnham WM (1993) Long-term changes in regional brain cytochrome oxidase activity induced by electroconvulsive treatment in rats. *Brain Res* 605: 1-8.

O'Leary JL, Petty J, Harris AB, Inukai J (2005) Supravital staining of mammalian brain with intra-arterial methylene blue followed by pressurized oxygen. *Stain Technology* 43: 197-201.

Osborne NN (1999) Memantine reduces alterations to the mammalian retina, *in situ*, induced by ischemia. *Vis Neurosci* 16: 45-52.

Osborne NN, Ugarte M, Chao M, Chidlow G, Bae JH, Wood JPM, Nash MS (1999) Neuroprotection in Relation to Retinal Ischemia and Relevance to Glaucoma. *Survey of Ophthalmology* 43: S102-S128.

Palmer GC (2001) Neuroprotection by NMDA receptor antagonists in a variety of neuropathologies. *Curr Drug Targets* 2.

Pastorino JG, Snyder JW, Hoek JB, Farber JL (1995) Ca depletion prevents anoxic death of hepatocytes by inhibiting mitochondrial permeability transition. *American Journal of Physiology - Cell Physiology* 268: C676-C685.

Perry VH (1981) Evidence for an amacrine cell system in the ganglion cell layer of the rat retina. *Neuroscience* 6: 931-934.

Peter C, Hongwan D, Kupfer A, Lauterburg BH (2000) Pharmacokinetics and organ distribution of intravenous and oral methylene blue. *Eur J Clin Pharmacol* 56: 247-250.

Quigley HA, Dunkelberger GR, Green WR (1988) Chronic human glaucoma causing selectively greater loss of large optic nerve fibers. *Ophthalmology* 95: 357-363.

Raichle ME, Gusnard DA (2002) Appraising the brain's energy budget. *Proc Natl Acad Sci USA* 10237-10239.

Ramsay RR, Krueger MJ, Youngster SK, Gluck MR, Casida JE, Singer TP (1991) Interaction of 1-methyl-4-phenylpyridinium ion (MPP+) and its analogs with the rotenone/piericidin binding site of NADH dehydrogenase. *J Neurochem* 56: 1184-1190.

Reid CR (1999) Vision. In: Fundamental Neuroscience (Michael J.Zigmond, Floyd E.Bloom, Story C.Landis, James L.Roberts, Larry R.Squire, eds), pp 821-851. San Diego: Academic Press.

Richardson KC (2005) The fine structure of autonomic nerves after vital staining with methylene blue. *Anatomical Record* 164: 359-377.

Richter C (1992) Reactive oxygen and DNA damage in mitochondria. *Mutat Res* 249-255.

Riordan E, Harding A (1995) Leber's hereditary optic neuropathy: the clinical relevance of different mitochondrial DNA mutations. *J Med Genet* **32**: 81-87.

Rizzo J.F.3rd. (1995) Adenosine triphosphate deficiency: a genre of optic neuropathy. *Neurology* 45: 11-6.

Robinson BH (1998) Human Complex I deficiency: Clinical spectrum and involvement of oxygen free radicals in the pathogenicity of the defect. *Biochimi et Biophys Acta (BBA) - Bioenergetics* 1364: 271-286.

Sadun AA, Bassi CJ (1990) Optic nerve damage in Alzheimer's disease. *Ophthalmology* 97: 9-17.

Sadun AA, Win PH, Ross-Cisneros FN, Walker SO, Carelli V (2000) Leber's hereditary optic neuropahty differentially affects smaller axons in the optic nerve. *Tr Am Opth Soc* 98: 223-235.

Salaris SC, Babbs CF, Voorhees III (1991) Methylene blue as an inhibitor of superoxide generation by xanthine oxidase: A potential new drug for the attenuation of ischemia/reperfusion injury. *Biochem Pharmacol* 42: 499-506.

Salinas JA, Introini-Collison IB, Dalmaz C, McGaugh JL (1997) Posttraining intraamygdala infusions of oxotremorine and propranolol modulate storage of memory for reductions in reward magnitude. *Neurobiol Learn Mem* 68: 51-59.

Schapira AHV (1998) Human complex I defects in neurodegenerative diseases. *Biochimi et Biophys Acta (BBA) - Bioenergetics* 1364: 261-270.

Schuettauf F, Quinto K, Naskar R, Zurakowski D (2002) Effects of anti-glaucoma medications on gangion cell survival: the DBA/2J mouse model. *Vision Res* 42: 2333-2337.

Sherer TB, Kim JH, Betarbet R, Greenamyre JT (2003) Subcutaneous rotenone exposure causes highly selective dopaminergic degeneration and [alpha]-synuclein aggregation. *Exp Neurol* 179: 9-16.

Sherman J and Kleiner L. (1994) Visual system dysfunction in Leber's hereditary optic neuropathy. *Clinical Neuroscience* 2: 121-129.

Shulman RG, Hyder F, Rothman DL (2003) Cerebral metabolism and consciousness. *Crit Rev Biol* 326: 253-273.

Sims KL, Kauffman FC, Johnson EC, Pickel VM (1974) Cytochemical localization of brain nicotinamide adenine dinucleotide phosphate (oxidized)-dependent dehydrogenases qualitative and quantitative distributions. *The Journal of Histochemistry and Cytochemistry* 22: 7-19.

Singer TP, Ramsay RR (1990) Mechanism of the neurotoxicity of MPTP. An update. *FEBS Lett* 274: 1-8.

Singer TP, Ramsay RR (1994a) The reaction sites of rotenone and ubiquinone with mitochondrial NADH dehydrogenase. *Biochimica et Biophysica Acta - Bioenergetics* 1187: 198-202.

Singer TP, Ramsay RR (1994b) The reaction sites of rotenone and ubiquinone with mitochondrial NADH dehydrogenase. *Biochimi et Biophys Acta (BBA) - Bioenergetics* 1187: 198-202.

So K-F, Aguayo AJ (1985) Lengthy regrowth of cut axons from ganglion cells after peripheral nerve transplantation into the retina of adult rats. *Brain Res* 328: 349-354.

Sommer AP, Pinheiro ALB, Mester AR, Franke RP, Whelan HT (2001) Biostimulatory windows in low intensity laser activation: lasers, scanners and NASA's light emitting diode array system. *J Clin Laser Med Surg* 19: 29-33.

Storey BT. (1980) Inhibitors of energy-coupling site 1 of the mitochondrial respiratory chain. *Pharmac.Ther.* 10: 399-406.

Storey E, Hyman BT, Jenkins BT, Brouillet E, Miller JM, Rosen BR, and Beal MF. (1992) MPP produces excitotoxic lesions in rat striatum due to impairment of oxidative metabolism. *J.Neurochem.* 58: 1975-1978.

Stryer L (1999) Biochemistry. New York: W. H. Freeman and Company.

Takano M, Horie H, Iijima Y, Dezawa M, Sawada H, Ishikawa Y (2002) Brain-derived Neurotrophic Factor Enhances Neurite Regeneration from Retinal Ganglion Cells in Aged Human Retina in vitro. *Experimental Eye Research* 74: 319-323.

Talpade DJ, Greene JG, Higgins DSJr, Greenamyre JT (2000) In vivo labeling of mitochondrial complex I (NADH:ubiquinone oxidoreductase) in rat brain using [3H] dihydrorotenone. *J Neurochem* 75: 2611-2621.

Thanos S, Thiel HJ (1990) Regenerative and proliferative capacity of adult human retinal cells in vitro. *Graefes Arch Clin Exp Ophthalmol* 228: 369-376.

Tremblay R, Chakravarthy B, Hewitt K, Tauskela J, Morley P, Atkinson T, Durkin JP (2000) Transient NMDA Receptor Inactivation Provides Long-Term Protection to Cultured Cortical Neurons from a Variety of Death Signals. *The Journal of Neuroscience* 20: 7183-7192.

United States National Toxicology Program. (1990) Chemical Status Report. NTP Chemtrack System.

Valla J, Berndt JD, Gonzalez-Lima F (2001) Energy hypometabolism in posterior cingulate cortex of Alzheimer's patients: Superficial laminar cytochrome oxidase associated with disease duration. *J Neurosci* 21: 4923-4930.

Valla J, Chen K, Berndt JD, Gonzalez-Lima F, Cherry SR, Games D, Reiman EM (2002) Effects of image resolution on autoradiographic measurements of posterior cingulate activity in PDAPP mice: implications for functional nrain imaging studies of transgenic mouse models of Alzheimer's disease. *NeuroImage* 16: 1-6.

Van Noorden CJF, Frederiks WM (1992) Microscopy handbooks 26. New York: Oxford University Press.

Visarius TM, Stucki JW, Bernhard H (1997) Stimulation of respiration by methylene blue in rat liver mitochondria. *FEBS Letters* 412: 157-160.

Voet D, Voet JG (1995) Biochemistry. John Wiley & Sons, Inc.

Wainwright M, Crossley KB (2002) Methylene Blue--a therapeutic dye for all seasons? *J Chemother* 14: 431-443.

Walker JE, Arizmendi JM, Dupuis A, Fearnley IM, Finel M, Medd SM, Pilkington SJ, Runswick MJ, Skehel JM (1992) Sequences of 20 subunits of

NADH:ubiquinone oxidoreductase from bovine heart mitochondria. Application of a novel strategy for sequencing proteins using the polymerase chain reaction. *Journal of Molecular Biology* 226: 1051-1072.

Wallace DC, Brown MD, and Lott MT. (1999) Mitochondrial DNA variation in human evolution and disease. *Gene* 238: 211-230.

Wassle H, Boycott BB (1991) Functional architecture of the mammalian retina. *Physiol Rev* 71: 447-480.

Waxman EA, Lynch DR (2005) N-methyl-D-aspartate Receptor Subtypes: Multiple Roles in Excitotoxicity and Neurological Disease. *Neuroscientist* 11: 37-49.

Waxman SG, Ritchie JM (1993) Molecular dissection of the myelinated axon. *Ann of Neurol* 33: 121-136.

Wieding JU, Hellstern P, and Kohler M. (1993) Inactivation of viruses in fresh-frozen plasma. *Ann Hematol* 67: 259-266.

Wolvetang EJ, Johnson KL, Krauer K, Ralph SJ, Linnane AW (1994) Mitochondrial respiratory chain inhibitors induce apoptosis. *FEBS Letters* 339: 40-44.

Wong-Riley MT (1989) Cytochrome oxidase: an endogenous metabolic marker for neuronal activity. *Trends Neurosci* 12: 94-101.

Wong-Riley MTT, Bai X, Buchmann E, Whelan HT (2001) Light-emitting diode treatment reverses the effect of TTX on cytochrome oxidase in neurons. *NeuroReport* 12: 3033-3037.

Wong-Riley MTT, Liang HL, Eells JT, Chance B, Henry MM, Buchmann E, Kane M, Whelan HT (2004) Photobiomodulation directly benefits primary neurons functionally inactivated by toxins: Role of cytochrome c oxidase. *J Biol Chem* M409650200.

Yu W, Naim JO, Lanzafame RJ (1997) Effects of Photostimulation on Wound Healing in Diabetic Mice. *Lasers Surg Med* 20: 56-63.

Zhang X, Jones D, Gonzalez-Lima F (2002) Mouse model of optic neuropathy caused by mitochondrial complex I dysfunction. *Neurosci Lett* 326: 97-100.

Zhang Y, Marcillat O, Giulivi C, Ernster L, Davies KJ (1990) The oxidative inactivation of mitochondrial electron transport chain components and ATPase. *J Biol Chem* 265: 16330-16336.

Vita

Xian Zhang was born in Hefei, Anhui, China on October 28, 1969, the second daughter of Renmin Zhang and Pei Shen. In 1987, she entered Anhui Medical University in Hefei, China. She graduated as the top student of the class and Honor Graduate from the Province and received the Doctor of Medicine Degree in May of 1992. After entering the Affiliated Hospital of Anhui Medical University, she was trained as an ophthalmologist for five years and was promoted to attending doctor in the department of Opthalmology in 1997. In 1998, she entered the Graduate School of the University of Texas at Austin and joined Professor Francisco Gonzalez-Lima's research group in 2000.

Permanent address: 7201 Wood Hollow Dr. APT 230, Austin, TX 78731

This dissertation was typed by Xian Zhang.